1970

Photochemical studies of some 2-cyclohexenones

Gene LeRoy Wampfler
Iowa State University

Recommended Citation

Wampfler, Gene LeRoy, "Photochemical studies of some 2-cyclohexenones " (1970). *Retrospective Theses and Dissertations*. 4370.
https://lib.dr.iastate.edu/rtd/4370

71-14,271

WAMPFLER, Gene LeRoy, 1945-
PHOTOCHEMICAL STUDIES OF SOME 2-CYCLOHEXENONES.

Iowa State University, Ph.D., 1970
Chemistry, organic

University Microfilms, A XEROX Company, Ann Arbor, Michigan

PHOTOCHEMICAL STUDIES OF SOME 2-CYCLOHEXENONES

by

Gene LeRoy Wampfler

A Dissertation Submitted to the
Graduate Faculty in Partial Fulfillment of
The Requirements for the Degree of
DOCTOR OF PHILOSOPHY

Major Subject: Organic Chemistry

Approved:

In Charge of Major Work

Head of Major Department

Dean of Graduate College

Iowa State University
Of Science and Technology
Ames, Iowa

1970

TABLE OF CONTENTS

Page

INTRODUCTION 1

REVIEW OF LITERATURE 3

- Spectroscopic Studies of 2-Cyclohexenones 3
- Pertinent Photochemical Reactions of Some 2-Cyclohexenones 10
  - Olefin cycloaddition 10
  - Rearrangement and reduction 18

RESULTS AND DISCUSSION 37

- The Photocycloaddition of Isophorone and 1,1-Diphenylethylene 37
- The Photorearrangement and Photoreduction of 4,4-Dimethyl-2-Cyclohexenone 59

EXPERIMENTAL 141

- The Photocycloaddition of Isophorone and 1,1-Diphenylethylene 141
  - Instruments and methods 141
  - Purification of reagents 141
  - Preparative photocycloaddition in *t*-butyl alcohol 142
  - Preparative photocycloaddition in benzene 144
  - Isomerization of 3,3,4a-trimethyl-9-phenyl-1,2,3,4,4a,9,10,10a-octahydro-1-phenanthrone 144
  - Deuteration of 3,3,4a-trimethyl-9-phenyl-1,2,3,-4,4a,9,10,10a-octahydro-1-phenanthrone 145
  - Deuteration of 2,2,10a-trimethyl-9-phenyl-1,2,-3,4,4a,9,10,10a-octahydro-4-phenanthrone 146
  - Attempted isomerization of 2,2,10a-trimethyl-9-phenyl-1,2,3,4,4a,9,10,10a-octahydro-4-phenanthrone 146
  - Attempted Baeyer-Villiger oxidation of 3,3,4a-trimethyl-9-phenyl-1,2,3,4,4a,9,10,10a-octahydro-1-phenanthrone 147
- Instruments and Methods for the Measurement of Quantum Yields 148

Page

Rotating photochemical apparatus 148
Linear quantum yield apparatus 149
Cells used for quantum yield measurements 150
Actinometry 150
Preparation and irradiation of samples 151
Analytical procedure 152
Correction of data 153
Plots of quantum yield data 154
Phosphorescence equipment 154
Format and symbols used in the tables of data 155
Preparation and purification of reagents 155

The Photorearrangement of 4,4-Dimethyl-2-Cyclohexenone 157

Absolute quantum yield of rearrangement 157
Effect of cyclohexenone concentration on the quantum yield of rearrangement 158
Quenching rearrangement by di-*t*-butyl nitroxide 159
Quenching rearrangement by naphthalene 159
Sensitization of rearrangement by acetophenone 160
Sensitization of rearrangement by benzophenone 161
Sensitization of rearrangement by thioxanthone 161
Sensitization of rearrangement by 9-fluorenone and 2-acetonaphthone 162
Sensitization of rearrangement by *m*-methoxyacetophenone, *p*-methoxyacetophenone, and 3,4-methylenedioxyacetophenone 162
Quantum yield for photoreduction of thioxanthone in isopropyl alcohol 164

Photoisomerization Studies of *trans*-β-Methylstyrene 165

Determination of the sensitized photostationary state of β-methylstyrene 165
Sensitization of the isomerization of *trans*-β-methylstyrene 165

Page

Effect of olefin concentration on the quantum yield of isomerization of *trans*-β-methylstyrene 169
Effect of impure olefin on the quantum yield of isomerization of *trans*-β-methylstyrene 170

Photoisomerization Studies of *trans*-α-Methylstilbene 171

The Photoreduction and Photorearrangement of 4,4-Dimethyl-2-Cyclohexenone in Isopropyl Alcohol 172

Absolute quantum yield of reduction and rearrangement 172
Preparative photoreduction in isopropyl alcohol 173
Quenching reduction and rearrangement by di-*t*-butyl nitroxide 174
Irradiation in the presence of di-*t*-butyl nitroxide at 446 nm 175
Determination of the photostability of di-*t*-butyl nitroxide in isopropyl alcohol 175
Quenching reduction and rearrangement by naphthalene 175
Quenching reduction and rearrangement by dienes 176
Effect of thiophenol on reduction and rearrangement 177
Sensitization of reduction and rearrangement 178
Effect of hydroquinone on reduction and rearrangement 179
Effect of hydroquinone dimethyl ether on reduction and rearrangement 180
Effect of biphenyl on reduction and rearrangement 180

SUMMARY 181

BIBLIOGRAPHY 184

ACKNOWLEDGEMENTS 192

LIST OF FIGURES

Page

Figure 1. Energy level diagrams
Top: steroidal ketones 5-10
Bottom: santonins 12-14 7

Figure 2. A three triplet mechanism for the photocycloaddition and photorearrangement reactions of 4,4-dimethyl-2-cyclohexenone 17

Figure 3. Energy level diagrams
Top: phenanthrone 11 and naphthalene
Bottom: photochemical reactions of 10-methyl-$\Delta^{1,9}$-2-octalone 28

Figure 4. An energy level diagram for the photochemical reactions of 2,4,6-tri-t-butyl-3-methoxy-2,5-cyclohexadienone 34

Figure 5. Infrared spectra
Top: 3,3,4a-trimethyl-9-phenyl-1,2,-3,4,4a,9,10,10a-octahydro-1-phenanthrone
Middle: 2,2,10a-trimethyl-9-phenyl-1,2,3,4,4a,9,10,10a-octahydro-4-phenanthrone
Bottom: 4,4,6-trimethyl-8,8-diphenylbicyclo[4.2.0]octan-2-one 40

Figure 6. Nuclear magnetic resonance spectra
Top: 3,3,4a-trimethyl-9-phenyl-1,2,-3,4,4a,9,10,10a-octahydro-1-phenanthrone
Middle: base isomerized 3,3,4a-trimethyl-9-phenyl-1,2,3,4,4a,9,10,10a-octahydro-1-phenanthrone
Bottom: 3,3,4a-trimethyl-9-phenyl-1,2,3,4,4a,9,10,10a-octahydro-1-phenanthrone-2,2,10-d_3 42

Page

Figure 7. Nuclear magnetic resonance spectra
Top: 2,2,10a-trimethyl-9-phenyl-1,2,3,4,4a,9,10,10a-octahydro-4-phenanthrone
Middle: 2,2,10a-trimethyl-9-phenyl-1,2,3,4,4a,9,10,10a-octahydro-4-phenanthrone-3,3,4a-d_3
Bottom: 4,4,6-trimethyl-8,8-diphenylbicyclo[4.2.0]octan-2-one 44

Figure 8. Stern-Volmer plot for quenching rearrangement by di-*t*-butyl nitroxide and naphthalene in *t*-butyl alcohol 63

Figure 9. A triplet mechanism for the rearrangement of 4,4-dimethyl-2-cyclohexenone 64

Figure 10. Phosphorescence emission spectra of *m*-methoxyacetophenone as a function of concentration 80

Figure 11. Plot of ϕ_o/ϕ_{sens} versus sensitizer concentration for thioxanthone, 3,4-methylenedioxyacetophenone, *m*-methoxyacetophenone, and *p*-methoxyacetophenone sensitization of rearrangement 82

Figure 12. A mechanism for the sensitized *cis*-*trans* isomerization of olefins 92

Figure 13. Plot of reciprocal of quantum yield of isomerization of *trans*-β-methylstyrene versus sensitizer concentration for acetophenone and *m*-methoxyacetophenone 99

Figure 14. Plot of logarithm of reciprocal of quantum yield of isomerization of *trans*-β-methylstyrene versus logarithm of sensitizer concentration for Michler's Ketone 100

Figure 15. Plot of reciprocal of quantum yield of isomerization of *trans*-β-methylstyrene versus sensitizer concentration for benzophenone at low concentrations 101

Page

Figure 16. Plot of reciprocal of quantum yield of isomerization of *trans*-β-methylstyrene versus sensitizer concentration for benzophenone at high concentrations 103

Figure 17. Plot of reciprocal of quantum yield of isomerization of *trans*-β-methylstyrene versus reciprocal of olefin concentration 116

Figure 18. Plot of quantum yield of isomerization of *trans*-β-methylstyrene versus square of the concentration of impure olefin 117

Figure 19. Plot of reciprocal of quantum yield of isomerization of *trans*-α-methylstilbene versus reciprocal of concentration of 4,4-dimethyl-2-cyclohexenone 119

Figure 20. Stern-Volmer plot for quenching reduction and rearrangement by di-*t*-butyl nitroxide in isopropyl alcohol 128

Figure 21. Stern-Volmer plot for quenching reduction and rearrangement by naphthalene in isopropyl alcohol 130

Figure 22. Stern-Volmer plot for quenching reduction and rearrangement by hydroquinone in isopropyl alcohol 132

LIST OF TABLES

Page

Table 1. Photolysis products of 10-methyl-$\Delta^{1,9}$-2-octalone in various solvents 25

Table 2. Mass spectra of adducts 74, 75, and 76 45

Table 3. Photoreactivity of substituted acetophenones 71

Table 4. Approximate values of k_t 84

Table 5. Intersystem crossing efficiencies 95

Table 6. Values of $\mathcal{J}$, k_r, and k_d' for reduction and rearrangement in isopropyl alcohol 136

Table 7. Absolute quantum yield of rearrangement 158

Table 8. Effect of cyclohexenone concentration on the quantum yield of rearrangement 158

Table 9. Quenching rearrangement by di-*t*-butyl nitroxide 159

Table 10. Quenching rearrangement by naphthalene 160

Table 11. Sensitization of rearrangement by acetophenone 160

Table 12. Sensitization of rearrangement by benzophenone 161

Table 13. Sensitization of rearrangement by thioxanthone 161

Table 14. Sensitization of rearrangement by 9-fluorenone and 2-acetonaphthone 162

Table 15. Sensitization of rearrangement by *m*-methoxyacetophenone 163

Table 16. Sensitization of rearrangement by *p*-methoxyacetophenone 163

Page

Table 17. Sensitization of rearrangement by 3,4-methylenedioxyacetophenone 164

Table 18. Sensitization of β-methylstyrene to the photostationary state 165

Table 19. Sensitization of _trans_-β-methylstyrene isomerization by acetophenone 166

Table 20. Sensitization of _trans_-β-methylstyrene isomerization by naphthalene 166

Table 21. Sensitization of _trans_-β-methylstyrene isomerization by Michler's Ketone 167

Table 22. Sensitization of _trans_-β-methylstyrene isomerization by _m_-methoxyacetophenone 167

Table 23. Sensitization of _trans_-β-methylstyrene isomerization by 3,4-methylenedioxyacetophenone 168

Table 24. Sensitization of _trans_-β-methylstyrene isomerization by thioxanthone 168

Table 25. Sensitization of _trans_-β-methylstyrene isomerization by benzophenone 169

Table 26. Effect of olefin concentration on the quantum yield of isomerization of _trans_-β-methylstyrene 170

Table 27. Effect of impure olefin on the quantum yield of isomerization of _trans_-β-methylstyrene 171

Table 28. Sensitization of the isomerization of _trans_-α-methylstilbene 172

Table 29. Quenching reduction and rearrangement by di-_t_-butyl nitroxide 174

Table 30. Quenching reduction and rearrangement by naphthalene 176

Page

Table 31. Quenching reduction and rearrangement by dienes 177

Table 32. Sensitization of reduction and rearrangement 178

Table 33. Effect of hydroquinone on reduction and rearrangement 179

Table 34. Effect of biphenyl on reduction and rearrangement 180

INTRODUCTION

As the field of organic photochemistry has developed, photochemical studies that go beyond determining just the structural changes that result from irradiation of a molecule have increased. This increased interest in the more physical and mechanistic aspects of organic photochemistry has concentrated on questions such as the number and nature of the excited states involved in photochemical reactions, their energies and lifetimes, and the sequence and rates of the photophysical and photochemical steps involved between excitation of the molecule and formation of the products.

In recent years, there has been an interest in photochemical reactions of molecules which proceed through more than one excited state to give a product or products derived from these multiple states. A rich source of reactions of this type has been found in the photochemical transformations of α,β-unsaturated ketones, because of the variety and number of excited states which are available upon excitation with ultraviolet light. The variety of the reactions of 2-cyclohexenones (dimerization, photorearrangement, photoreduction, and photocycloaddition) make these molecules prime candidates for studies designed to detect reactions from multiple excited states (see Review of Literature).

The molecule chosen for the present study, 4,4-dimethyl-2-cyclohexenone (<u>1</u>), undergoes three of these four reactions:

photocycloaddition (equation 1), photorearrangement (equation 2), and photoreduction (equation 3). The photocycloaddition reactions of 1 have been studied in detail (1, 2). This thesis describes the photorearrangement to products 2 and 3 and the photoreduction to product 4. This study is of interest in that it illustrates a photochemical system in which the several excited states which are available upon excitation are distinctive in their chemistry.

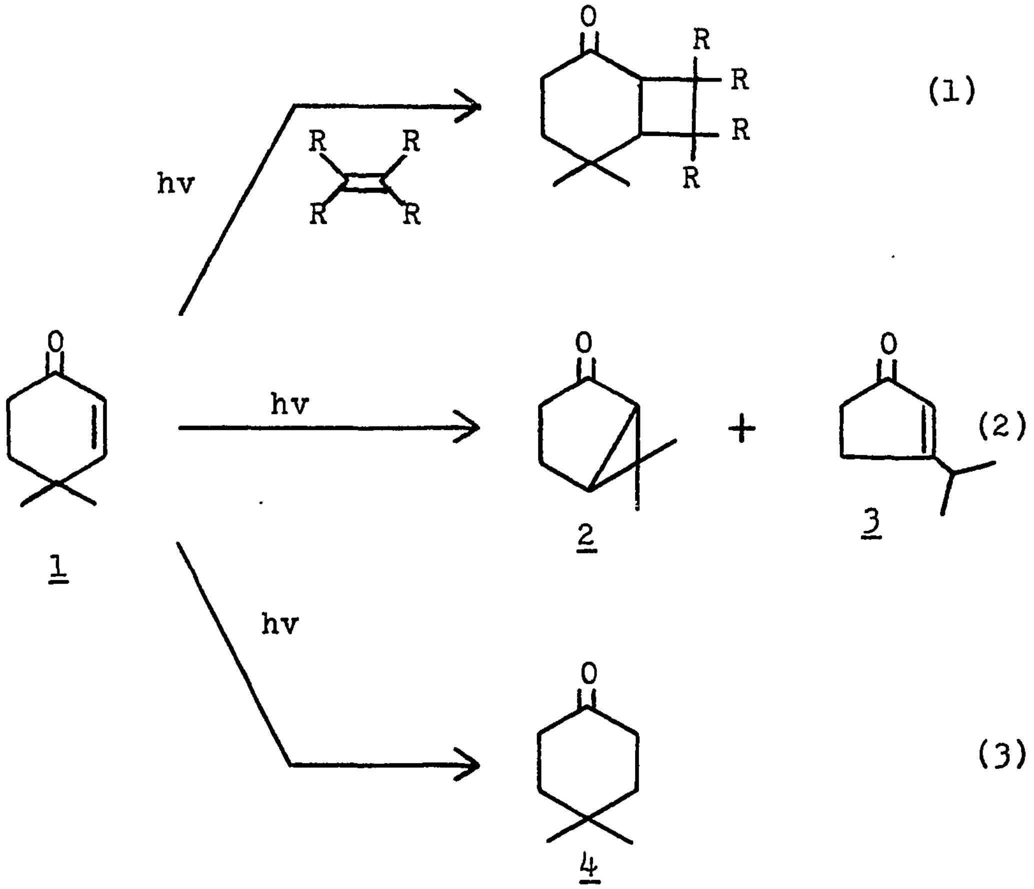

REVIEW OF LITERATURE

The photochemical reactions of 2-cyclohexenones have been studied for a number of years. The reactions are numerous, and only those which are pertinent to the present work will be discussed. Like many photochemical studies, the reactions of these molecules are best understood by an awareness of the excited states available and their relative energies. Accordingly, the spectroscopic investigation of 2-cyclohexenones has received recent attention in the prospect of characterizing and understanding more completely the photochemical reactions of these molecules.

Spectroscopic Studies of 2-Cyclohexenones

The spectroscopic investigation of six steroidal ketones (5-10) by phosphorescence excitation and emission methods was carried out by Kearns and coworkers in 1968 (3, 4). Direct absorption and phosphorescence excitation techniques allowed location of the $^3(n,\pi^*)$ states. These states were found to be the second excited triplet states and not the states responsible for emission. The emitting states were found to be the $^3(\pi,\pi^*)$ states, which exhibited very diffuse phosphorescence spectra. The diffuseness of this emission was attributed to a large change in the molecular geometry upon excitation, probably to a non-planar configuration. The $S \rightarrow T_{n,\pi^*}$ absorption spectra were also

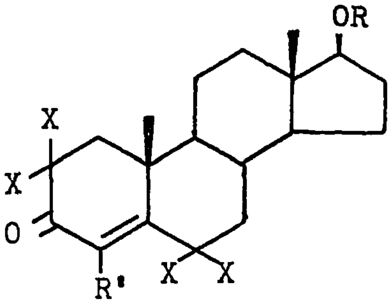

5. R = Ac, R' = X = H
6. R = Ac, R' = CH_3, X = H
7. R = Ac, R' = Cl, X = H
8. R = Ac, R' = OAc, X = H
9. R = H, R' = X = D
10. R = Ac, R' = Br, X = H

diffuse, and this was attributed to interactions between the $^3(n,\pi^*)$ and $^3(\pi,\pi^*)$ states, which varies with substitution, as shown in Figure 1. Substitution has very little effect on the relative energy levels of the S_{n,π^*} and T_{n,π^*} states, but causes large changes in the energy of the T_{π,π^*} states. The investigators concluded that the identification of the reactive triplet states in the room temperature photochemistry of 2-cyclohexenones may be complicated by such rapidly equilibrating configurations, the lowest of which is dependent on substitution and solvent effects.

In the course of some studies of the photochemical rearrangements of 2-cyclohexenones (vide infra), Zimmerman, et al. (5) have observed the phosphorescence emission spectrum of 4a-methyl-4,4a,9,10-tetrahydro-2(3H)-phenanthrone (11). From the 0-0 band in the emission spectrum, a triplet energy of 71 kcal/mole was determined, and fine structure characteristic of an n,π^* triplet was observed. Studies of this same compound by flash photolysis (6) led to the detection of two transient species differing in spectral and decay characteristics. While the longer-lived intermediate is believed to be a ketyl radical, the shorter-lived of the two is a triplet excited state with no observable fine structure.

The spectroscopic investigation of the santonin molecules, 12, 13, and 14 has led to conclusions similar to those in studies of cyclohexenones (7). The lowest excited triplet state in each case is identified as the $^3(\pi,\pi^*)$ state, with the $^3(n,\pi^*)$ state lying just above it (3.5-4.5 kcal/mole). The relative locations and assignments of the excited states are shown in Figure 1.

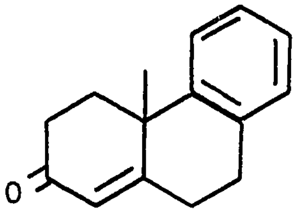

11

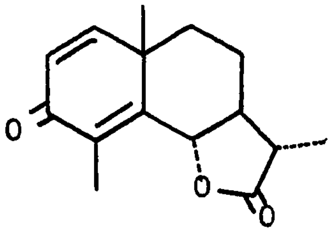

12

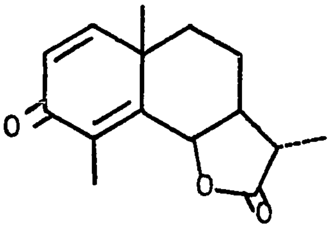

13

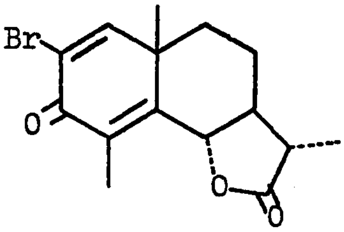

14

Figure 1. Energy level diagrams

Top: steroidal ketones 5-10

Bottom: santonins 12-14

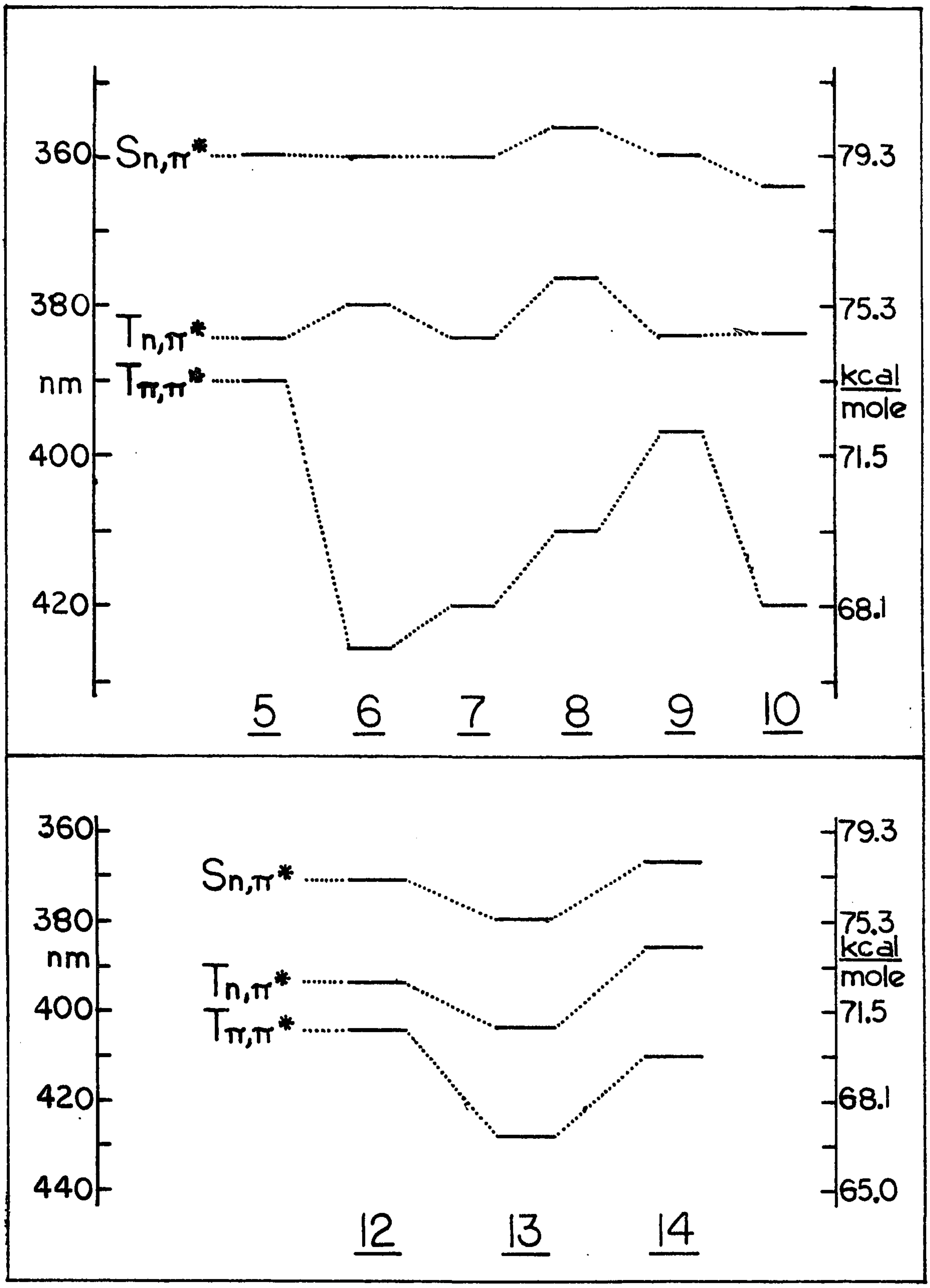
360
380
nm
400
420
S_{n,π^*}
T_{n,π^*}
T_{π,π^*}
79.3
75.3
kcal/mole
71.5
68.1
5
6
7
8
9
10
360
380
nm
400
420
440
S_{n,π^*}
T_{n,π^*}
T_{π,π^*}
79.3
75.3
kcal/mole
71.5
68.1
65.0
12
13
14

Fisch and Richards (8) have investigated the triplet state of lumisantonin (15) by phosphorescence techniques. The molecule exhibits a weak structureless emission with the 0-0 band at 64 ± kcal/mole. Solvent shifts were not measurable and the nature of the triplet state could not be determined.

Spectroscopic investigations of various cyclopentenones have also contributed information about the excited states of enone systems. The phosphorescence spectrum of compound 16 indicates a low-lying (n,π^*) triplet of energy 71.6 kcal/mole in EPA and 70.8 kcal/mole in MCIP (9). Compound 17 shows a structureless emission, characteristic of a $^3(\pi,\pi^*)$ state with an energy of about 75 kcal/mole in both EPA and MCIP (9). The phosphorescence emission spectrum of

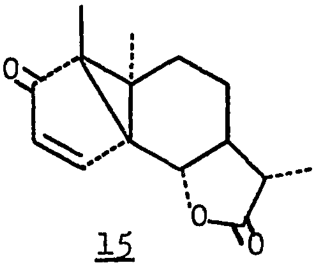

15

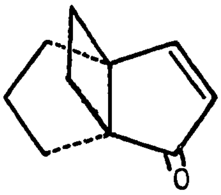

16

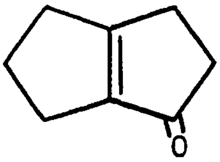

17

18a is structured and indicates a triplet energy of 74.5 kcal/mole in EPA (10). The emission from 18b, on the other hand, is structureless, and the molecule has a triplet energy of 74 kcal/mole in EPA.

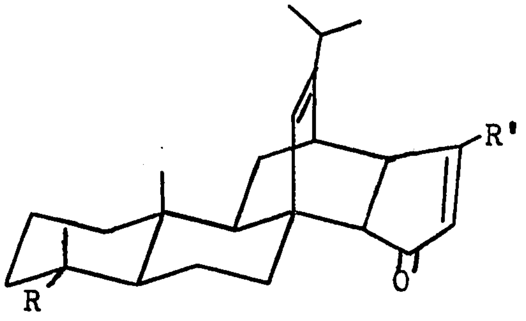

18a: R=CH_2OH, R'=H

18b: R=CO_2CH_3, R'=OCH_3

Santry and coworkers (11) have carried out molecular orbital calculations on the enone moiety to determine the geometry and relative energies of the triplet states. Acrolein was chosen as the model and calculations were carried out using Complete Neglect of Differential Overlap techniques. The calculations indicate that the lowest triplet state is n,π^* in character, and planar with respect to rotation about the β-methylene group. The next highest triplet is π,π^* in character and the most stable configuration is non-planar with an equilibrium angle of rotation for the β-methylene group of approximately 72°. This result is in qualitative agreement with molecular orbital calculations on ethylene by Baird (12) which indicate that the 90° twisted conformations of both the excited singlet and triplet states are substantially more stable than the planar forms.

Pertinent Photochemical Reactions of Some 2-Cyclohexenones

Olefin cycloaddition

Corey, et al. (13) provided in 1964 a qualitative picture of the cycloaddition reactions of 2-cyclohexenones and substituted olefins to form bicyclo[4.2.0]octan-2-ones. A mechanism provided to explain orientation and reactivity involved formation of an oriented π-complex which then gave a diradical. Closure of the diradical to the cyclobutane determined the stereochemistry of the product. The significant features of Corey's results are (1) trans-fused cyclobutane adducts are usually obtained, often as the major product; (2) the orientation of the π-complex is determined by the electron demands of the olefin substituents; and (3) the relative rate of addition of various olefins are dependent on the electron donating ability of its substituents.

In an attempt to determine the steric and electronic effects of substituents on the enone moiety, Cantrell et al. (14) have studied the photocycloaddition reactions of 3-methyl-, 3-phenyl-, and 3-acetoxy-2-cyclohexenone with a variety of substituted olefins. The photocycloaddition of 3-methyl-2-cyclohexenone to 1,1-dimethoxyethylene is a typical reaction in that it results in both cis- and trans-6-methyl-7,7-dimethoxybicyclo[4.2.0]octan-2-ones (19 and 20) in 38 and 26% yields, respectively. Cyclopentene also adds

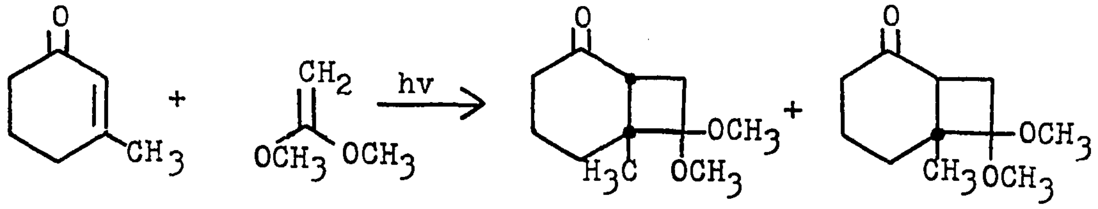

19 20

to excited 3-methyl-2-cyclohexenone to give cis and trans adducts. The addition of ethoxyethylene, acrylonitrile, and 1,2-dichloroethylene to 3-methyl-2-cyclohexenone, and the addition of 1,1-dimethoxyethylene, isobutene, cyclopentene, and ethoxyethylene to 3-phenyl-2-cyclohexenone results in only adducts with a cis-fused ring junction.

The nature of the substituent on the cyclohexenone seems to have little effect on the orientation of the addition, with one exception. Irradiation of 3-acetoxy- and 3-methyl-2-cyclohexenone with isobutylene yields significant quantities of the 8,8-dimethylbicyclo[4.2.0]octan-2-one products, while addition to 3-phenyl-2-cyclohexenone gives only the 7,7-dimethylbicyclo adduct. The phenyl ring can achieve coplanarity with the enone system and does not exert a significant blocking effect, as do the other two substituents. Since isobutylene has relatively little charge separation, the steric effect in this case is able to overcome any electronic effects influencing orientation.

The orientation of the addition and the order of reactivities are, in most cases, predicted by the Corey rule of the oriented π-complex. The most electron rich atom of the olefin becomes aligned adjacent to the α-carbon of the enone, which is in an n,π* excited state (equation 4). The relative rates of addition of the various olefins to each enone vary over about one order of magnitude and support the low degree of charge separation in the intermediates. The mild electronic effects of the substituents R thus exert no dramatic effect on the course and nature of the reaction.

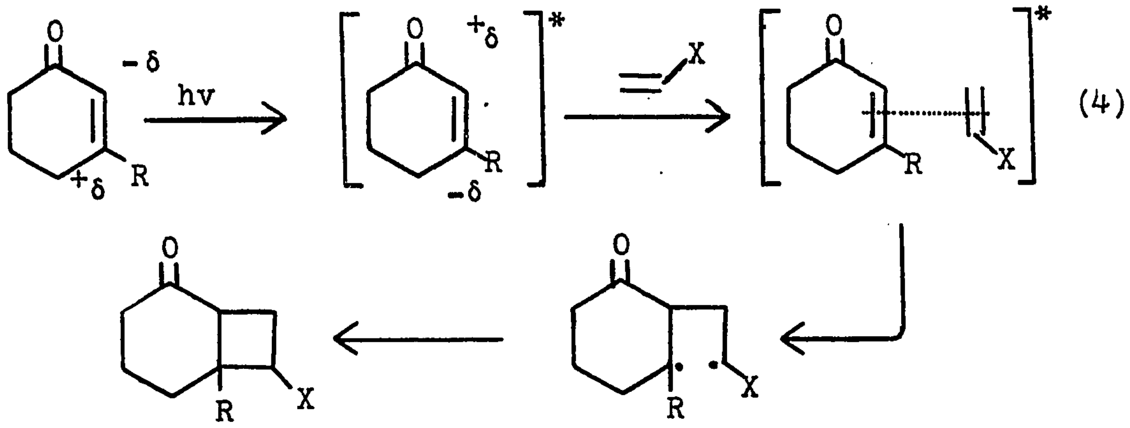

Cycloaddition of substituted olefins to isophorone gives exclusively 7,7-disubstituted bicyclooctanes (15). Isophorone adds to 1,1-dimethoxyethylene to give cis- and trans-7,7-dimethoxy-4,4,6-trimethylbicyclo[4.2.0]octan-2-ones (21 and 22) in a ratio of 1.92:1 (85% yield). The addition of 1,1-dichloroethylene leads to only one adduct, cis-7,7-dichloro-4,4,6-trimethylbicyclo[4.2.0]octan-2-one (23) in 44% yield, and the addition of vinyl acetate leads to the

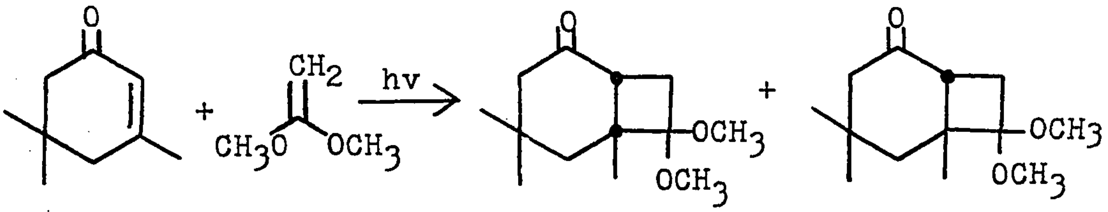

21 22

corresponding 7-acetoxy adduct (24) which is a mixture of isomers formed in 54% total yield. In contrast, addition of isophorone and tetrachloroethylene produces two unusual adducts (25 and 26) which appear to be derived from the tetrachloro adduct.

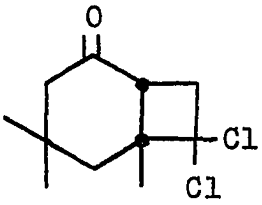

23

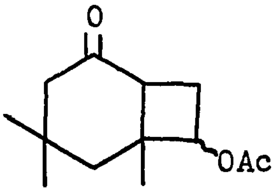

24

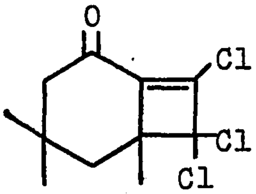

25

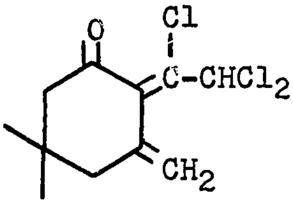

26

1,1-diphenylethylene reacts with 4,4-dimethyl-2-cyclohexenone to give a trans-cyclobutane adduct (27) as the major product (1), and a minor product of either structure 28a or 28b (16). The nmr spectrum strongly favors structure 28a. Tetramethylethylene adds to give a trans-cyclobutane adduct (29) and an oxetane (30) (17).

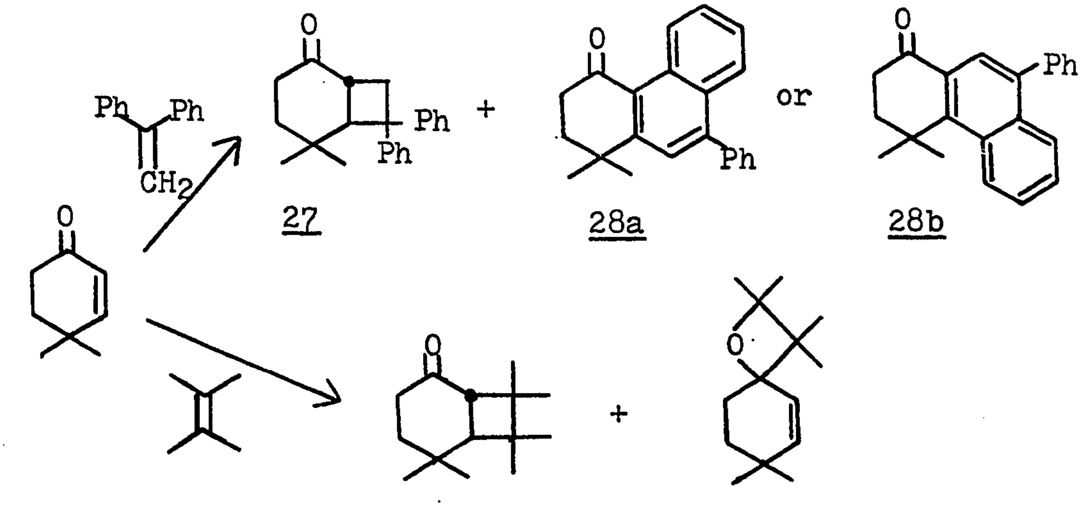

27 28a 28b

29 30

Chapman *et al.* (2, 18, 19) have quantitatively studied the cycloaddition reactions of 1,1-dimethoxyethylene with 4,4-dimethyl-2-cyclohexenone, isophorone, and 2-cyclohexenone. Irradiation of 4,4-dimethyl-2-cyclohexenone and 1,1-dimethoxyethylene in hexane results in an oxetane (31, 20%), a *trans*-adduct (32,46%), and a *cis*-adduct (33, 29%). The photoreaction is sensitive to solvent; in *t*-butyl alcohol, rearrangement (*vide infra*) competes with cycloaddition and oxetane formation is not observed, while in hexane and benzene only cycloaddition occurs.

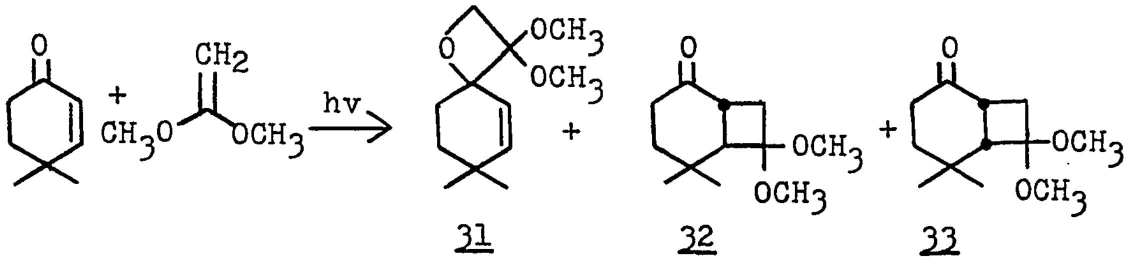

The cycloaddition reaction can be sensitized $(\phi_{sens}/\phi_o = 1)$ with triphenylamine and triphenylene under conditions in which the sensitizer absorbs most of the light. Naphthalene is inefficient in quenching the reaction, but quenching studies with di-*t*-butylnitroxide yield linear Stern-Volmer plots for all three adducts indicating reaction *via* triplet excited states. The slopes of the quenching lines for each adduct in hexane are different (oxetane, 81.0 ± 2.1 l./mole; *cis*-adduct, 157 ± 2.4 l./mole; *trans*-adduct, 90.2 ± 2.0 l./mole and indicate that the *cis*-adduct is derived from a different triplet excited state than the oxetane and the *trans*-adduct, whose quenching slopes are within experimental error of each other. While the nature of the two chemically distinct triplets cannot be inferred from the available data, the nature of the observed quenching suggests that the two triplets have a common excited state precursor and are not formed sequentially. A possible mechanism, consistent with these facts, involves the formation of two daughter triplets which give rise to the chemically different products (2)

(Figure 2). Further discussion of this mechanism as well as its relationship to the present work will be taken up in the Results and Discussion section.

In similar fashion, the cycloaddition of isophorone and 1,1-dimethoxyethylene in benzene to produce the cis- and trans- adducts 21 and 22 was found to be an excited triplet state reaction (18). Sensitization with triphenylene and triphenylamine gave ϕ_{sens}/ϕ_o ratios of 0.91 and 0.88, respectively. Quenching studies with di-t-butyl nitroxide led to linear Stern-Volmer plots with different slopes for cis- and trans-adduct formation. As before, the cis-adduct is quenched more efficiently than the trans-adduct. When naphthalene (E_t = 60.9 kcal/mole) was used as a quencher, no differential quenching was observed, although overall quenching was more efficient. These results were again explained on the basis of a two-triplet mechanism.

Irradiation of 2-cyclohexenone and 1,1-dimethoxyethylene in benzene produces the cis- and trans-adducts 34 and 35 (18). The results of quenching and sensitization experiments

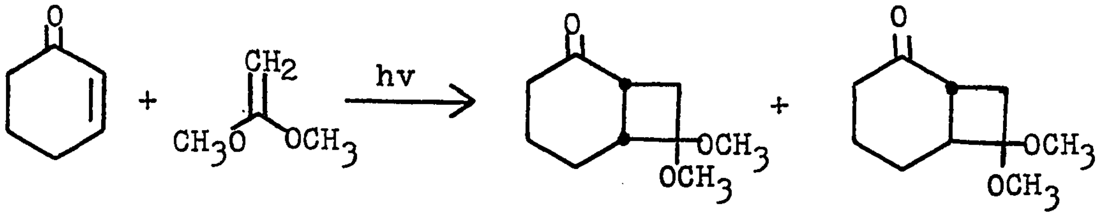

34 35

$$K + hv \longrightarrow {}^1K^*$$

$${}^1K^* \xrightarrow{k_d} K$$

$${}^1K^* \xrightarrow{k_{ic}} {}^3K^*$$

$${}^3K^* \xrightarrow{k_d'} K$$

$$\begin{tikzcd}{}^3K^* \arrow[r, "k_{it}"] \arrow[dr, "k_{it}'"'] & {}^3K \\ & {}^3K'\end{tikzcd}$$

K = 4,4-dimethyl-2-cyclohexenone

O = 1,1-dimethoxyethylene

Q = quencher

S = sensitizer

$${}^3K + O \xrightarrow{k_c} \underline{cis}\text{-adduct}$$

$${}^3K \xrightarrow{k_d''} K$$

$${}^3K + Q \xrightarrow{k_q} K + Q^*$$

$${}^3K' + O \xrightarrow{k_o} \text{oxetane}$$

$${}^3K' + O \xrightarrow{k_t} \underline{trans}\text{-adduct}$$

$${}^3K' \xrightarrow{k_r} \text{rearrangement products}$$

$${}^3K' \xrightarrow{k_d'''} K$$

$${}^3K' + Q \xrightarrow{k_q'} K + Q^*$$

$${}^3S^* + K \longrightarrow {}^3K^* + S$$

Figure 2. A three triplet mechanism for the photocycloaddition and photorearrangement reactions of 4,4-dimethyl-2-cyclohexenone

parallel those obtained in cycloaddition reactions of isophorone and 4,4-dimethyl-2-cyclohexenone. Di-t-butyl nitroxide quenches cis-adduct formation more efficiently than trans-adduct formation indicating the intermediacy of different triplet precursors for these products.

Rearrangement and reduction

The photolysis of 4,4-dimethyl-2-cyclohexenone in t-butyl alcohol results in rearrangement (equation 2) to 6,6-dimethylbicyclo[3.1.0]hexan-2-one (2) and 3-isopropyl-2-cyclopentenone (3) (20). The cyclopentenone was found to be a reaction product of 2 as well as a primary product of the reaction (1). The rearrangement was subsequently shown to be a triplet reaction by sensitization and quenching studies (1, 2). The quantum yields for formation of 2 and 3 are 5.3×10^{-3} and 6.4×10^{-3}, respectively at 52°.

When the rearrangement is carried out in the presence of 1,1-dimethoxyethylene in t-butyl alcohol, trans- and cis-adducts, 32 and 33 are also formed (2). Di-t-butyl nitroxide differentially quenches the formation of cis-adduct, trans-adduct and rearrangement products. The slopes of the quenching lines for each product in this case are: photorearrangement products, 17.5 ± 2.0 l./mole; trans-adduct, 34.9 ± 4.2 l/mole; and cis-adduct, 75.6 ± l./mole. Despite the difference in the quenching slopes for formation of rearrangement products and trans-adduct, these two reactions are postulated to occur from the same daughter triplet (see Figure 2).

An alternate mechanism proposed by Koch involves the formation of separate triplet complexes for all three cycloaddition products and for rearrangement products. If separate exciplexes are formed for each product, the quenching efficiency of each exciplex can be different. This mechanism requires that each exciplex results in predominantly one product, and that the rate of exciplex formation competes efficiently with quenching rates, since otherwise the quencher should quench the uncomplexed triplet before it forms the exciplex.

In isopropyl alcohol, 4,4-dimethyl-2-cyclohexenone photoreduces to give 4,4-dimethylcyclohexanone (4, equation 3), as well as rearranging (2). Prolonged irradiation results in photoreduction of the cyclopentenone to 3-isopropylcyclopentanone (36).

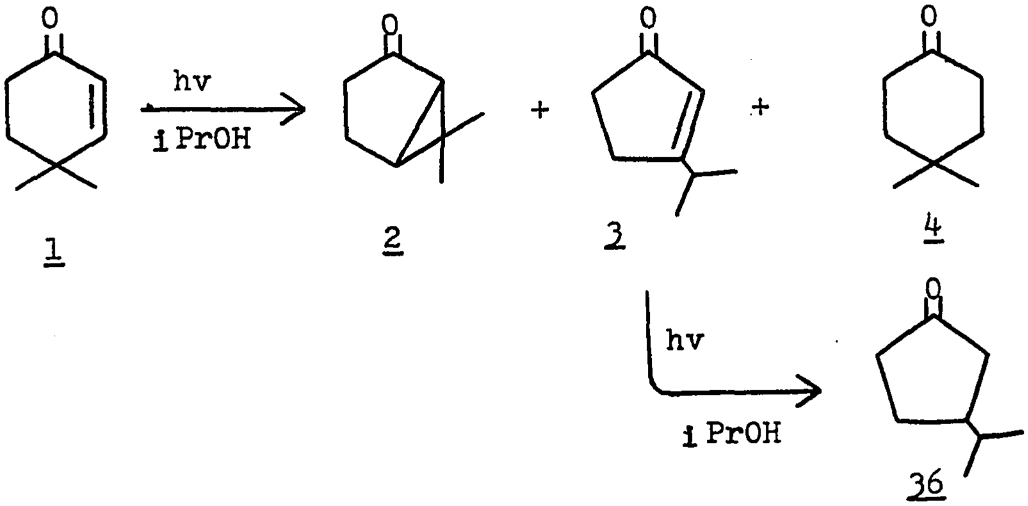

Pinacol formation from 4,4-dimethyl-2-cyclohexenone is also known (2). When the photocycloaddition reaction of 4,4-dimethyl-2-cyclohexenone and 1,1-dimethoxyethylene in benzene is sensitized with Michler's Ketone, two new products are formed in addition to the usual cycloadducts. These new products have been identified as the dl and meso pinacols of structure 37.

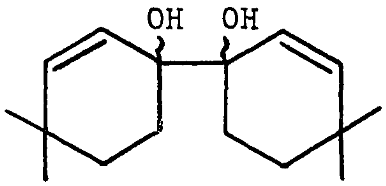

37

A similar rearrangement is that of 4a-methyl-4,4a,9,10-tetrahydro-2(3H)phenanthrone (11) to the lumiproduct 38 (5, 21). The rearrangement proceeds with low quantum efficiency

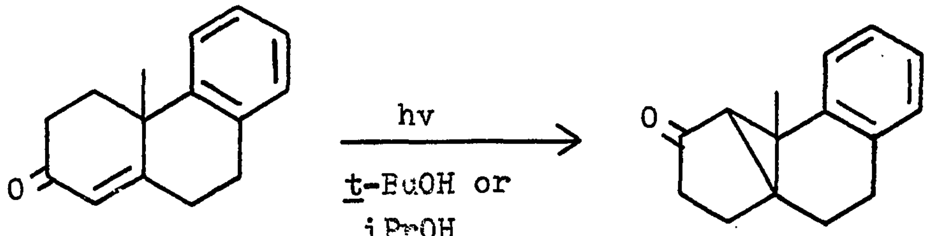

11

38

(8.4 x 10^{-3}) and is a triplet state reaction as shown by quenching and sensitization studies. Chapman _et_ _al_. (22) have shown that optically active phenanthrone _11_ rearranges to lumiproduct _38_ with at least 95% retention of optical activity, indicating that the rearrangement must involve stereospecific 4-4a bond migration. Zimmerman concludes that the rearrangement probably results from the n,π^* triplet state that has recently been observed spectroscopically (6).

Zimmerman also reports the photoreduction in isopropyl alcohol of phenanthrone _11_ to a pinacol (_39_) which accompanies rearrangement in a ratio of 1:5 (5). The formation of both products is quenched equally by naphthalene indicating that both are formed from triplet species. Zimmerman concludes that either the two products are formed from one triplet, or that two triplets are involved, in exceedingly rapid equilibrium, with one responsible for each reaction.

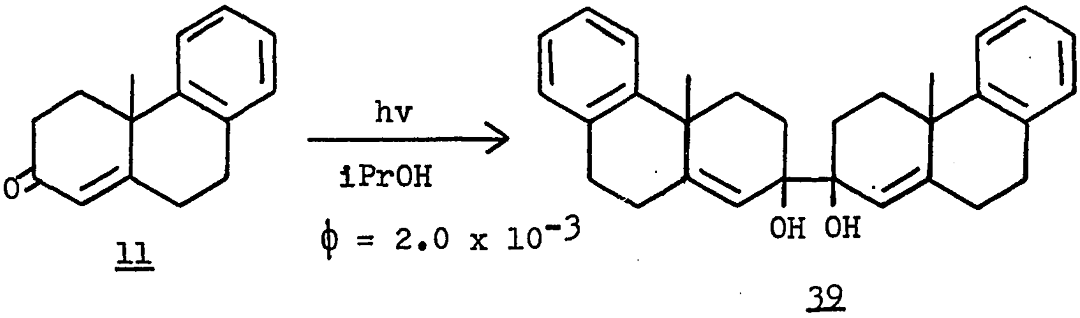

The rearrangement of phenanthrone 11 has also been studied by the flash spectropolarimetric technique (6, 23). Since the reaction proceeds with retention of stereochemistry, there is a strong possibility that it proceeds through an optically active triplet, which is amenable to study by this method. Flash excitation of 11 led to the two transients noted previously. The assignment of the longer-lived component as the ketyl radical 40 accords with the formation of the pinacol 39. The ketyl radical is presumably a precursor of this product. The shorter-lived transient is a triplet state consisting of a broad, structureless band, which is produced independently of the longer-lived component. While oxygen quenches this species at a diffusion controlled rate, naphthalene has no effect on the lifetime of the species, but results in an increase in its concentration. The lifetime of the naphthalene triplet is decreased with increasing concentration of the ketone. The results are explained by the formation of at least two triplets upon photoexcitation, and a possible energy scheme is shown in Figure 3. An undetected triplet, T_1, sensitizes the $^3(\pi,\pi^*)$ state of

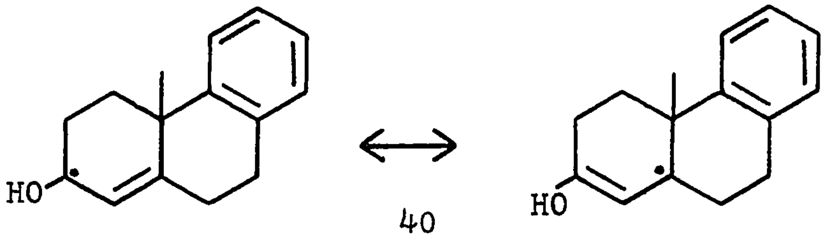

40

naphthalene. Since naphthalene quenches reduction and rearrangement, T_1 must be the intermediate for these products. Naphthalene, in turn, increases the concentration of T_1', the observed triplet, by energy transfer. This analysis implies that T_1 and T_1' are formed by independent paths and that T_1 decays directly to S_o and not to T_1'. The investigators conclude that T_1 may be the $^3(n,\pi^*)$ state with either a very short lifetime or a very inefficient intersystem crossing efficiency from S_1, to account for the low quantum yield for photoreduction. T_1' is believed to be either the π,π^* triplet state of the aromatic moiety of 11, or a charge-transfer triplet state. All attempts to observe optical rotation in the transient were unsuccessful within the limits of accuracy and detection of the flash spectropolarimeter.

The photochemical rearrangements of O-acetyl testosterone (41) (20, 24) and 10-methyl-$\Delta^{1,9}$-octalone (42) (5, 21) have been known for a number of years, and are similar to the rearrangements of other 2-cyclohexenones. Recently, the mechanistic photochemistry of these two compounds in a variety of solvents has been investigated (25). The choice of reaction products of 41 depends strongly on solvent. In t-butyl alcohol, 41 rearranges stereospecifically to products 43 and 44. Product 43 is not photostable, and prolonged irradiation results in its conversion to 44 and a small amount of starting ketone 41. In benzene, irradiation of 41 produces only one product, a double-bond shifted isomer 45. This reaction was determined kinetically to be bimolecular and is pictured as hydrogen abstraction from a ground-state ketone by the oxygen of an excited ketone. In toluene, the major reaction of 41 is solvent incorporation through hydrogen addition to the β-carbon of the enone to produce product 46. This reaction is accompanied by minor reactions to produce 45 and another new product, 47, in which the double bond has been reduced.

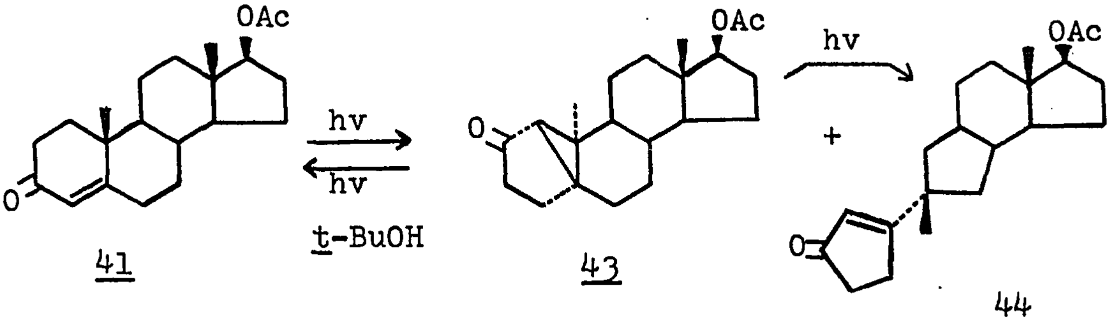

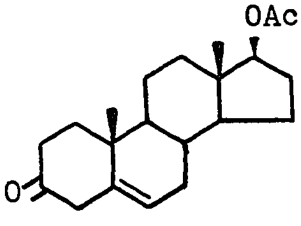
45

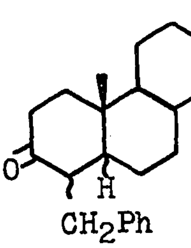

46

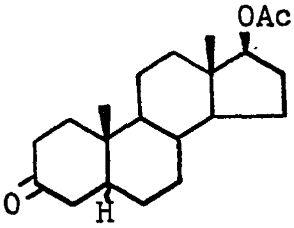

47

The photochemical transformations of 10-methyl-$\Delta^{1,9}$-2-octalone (42) are analogous to those of the testosterone, and have a complex solvent dependence. The products of the photolysis for various solvents are summarized in Table 1.

Table 1. Photolysis products of 10-methyl-$\Delta^{1,9}$-2-octalone in various solvents

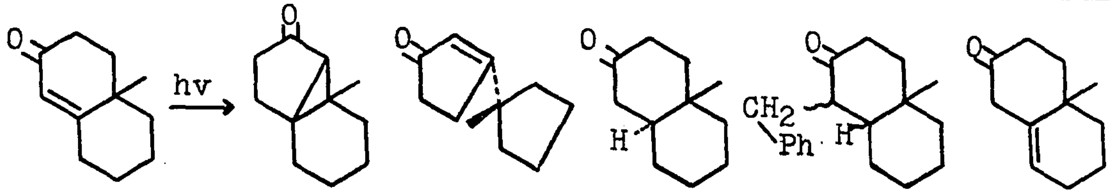

42	48	49	50	51	52
solvent	percentage of products				
t-butyl alcohol	80	5	3	--	11
isopropyl alcohol	31	2	35	--	6
toluene	3	trace	19	40	2
pyridine	41	trace	10	--	25
benzonitrile	37	trace	5	--	18
benzene	14	trace	6	--	45
trifluoro-toluene	24	trace	7	--	28

Sensitization and quenching experiments confirmed the triplet nature of the above reactions of 41 and 42, as previously determined. Differential quenching of the photoproducts of 42 was observed with a variety of quenchers in the various solvents. The slopes of the Stern-Volmer quenching plots for products 48, 50, and 51 are similar (~10 l./mole) in all solvents, and clearly differentiated from that for 52, which is about 2 l./mole in these same solvents. On the basis of this differential quenching, the investigators con- conclude that rearrangement, double bond reduction, and toluene addition arise from one triplet state of the enone, tentatively assigned as the $^3(\pi,\pi^*)$ state, and the double bond shift arises from another triplet, assigned as the $^3(n,\pi^*)$ state. These conclusions, and the relative ordering of the states in the various types of solvents, are shown schematically in Figure 3.

A definite contrast in the mechanistic interpretation of some similar transformations of a 2-octalone has been provided by Schuster and Brizzolara (26). Irradiation through Pyrex in t-butyl alcohol of 10-hydroxymethyl-$\Delta^{1,9}$-2-octalone (53) gives lumiketone 54 in low efficiency. In chloroform, toluene, cumene, and benzene, a fragmentation reaction also occurs to give $\Delta^{9,10}$-2-octalone (55) and $\Delta^{1,9}$-2-octalone (56) as well as several minor products derived from them.

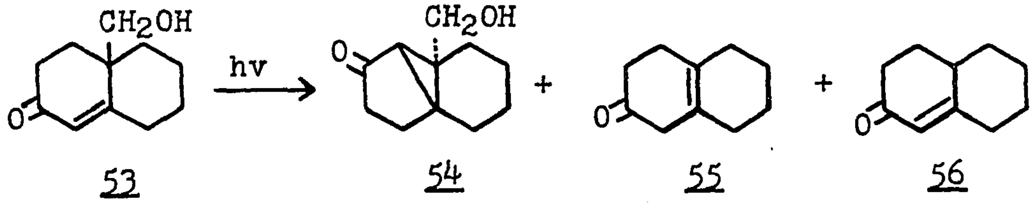

Quenching and sensitization experiments indicate that all products are derived from the same radical-like triplet excited state and not from two triplet states, as is believed

Figure 3. Energy level diagrams

Top: phenanthrone <u>11</u> and naphthalene

Bottom: photochemical reactions of 10-methyl-$\Delta^{1,9}$-2-octalone (<u>42</u>)

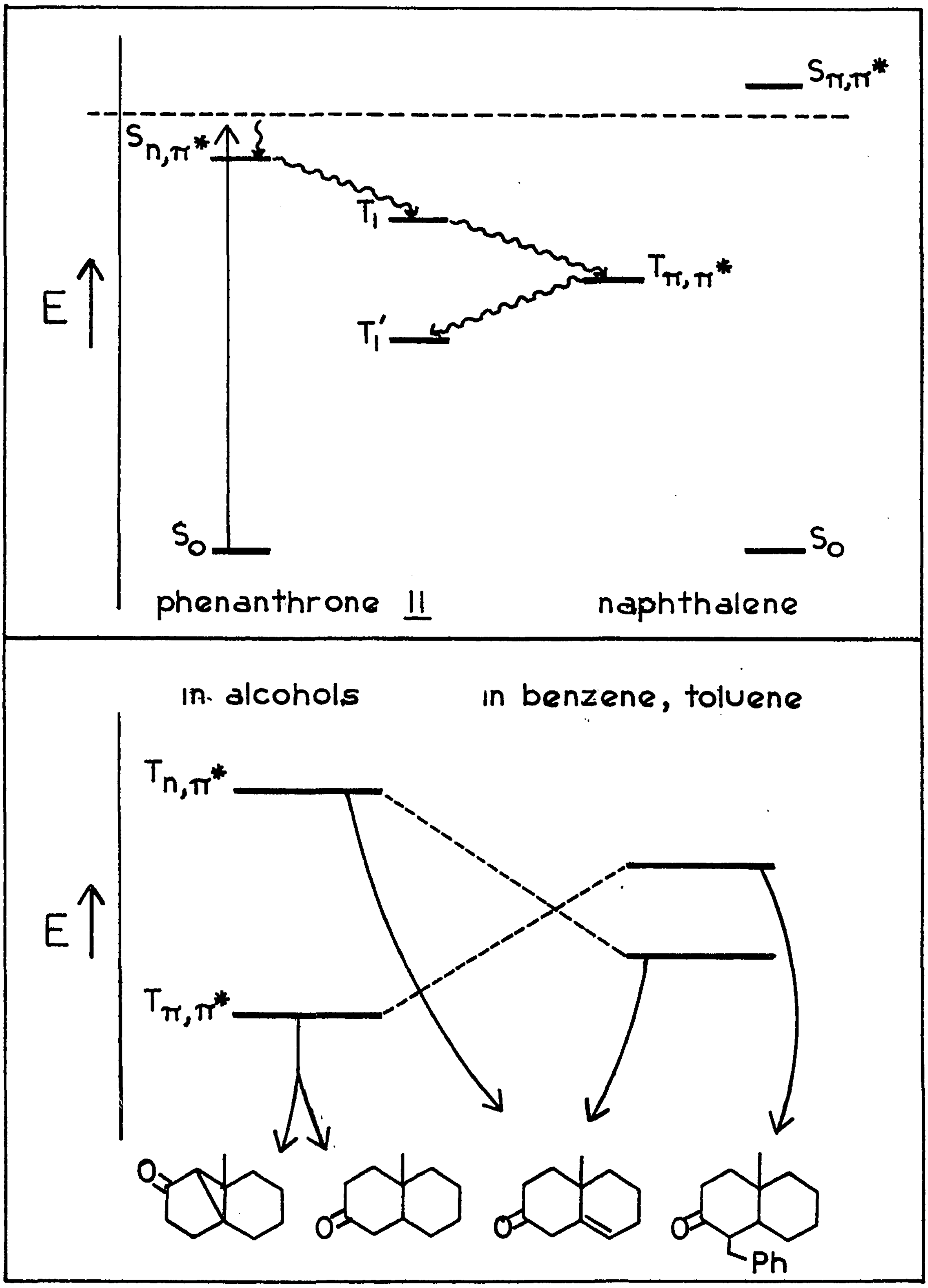
S_{π,π^*}
S_{n,π^*}
T_1
T_{π,π^*}
T_1'
E
S_0
S_0
phenanthrone II
naphthalene
in alcohols
in benzene, toluene
T_{n,π^*}
E
T_{π,π^*}
O
O
O
O
Ph

to be the case with 10-methyl-$\Delta^{1,9}$-2-octalone. The formation of products 55 and 56 are envisaged to proceed through a hydrogen abstraction process from the solvent, leading to a radical intermediate which can fragment to give the observed

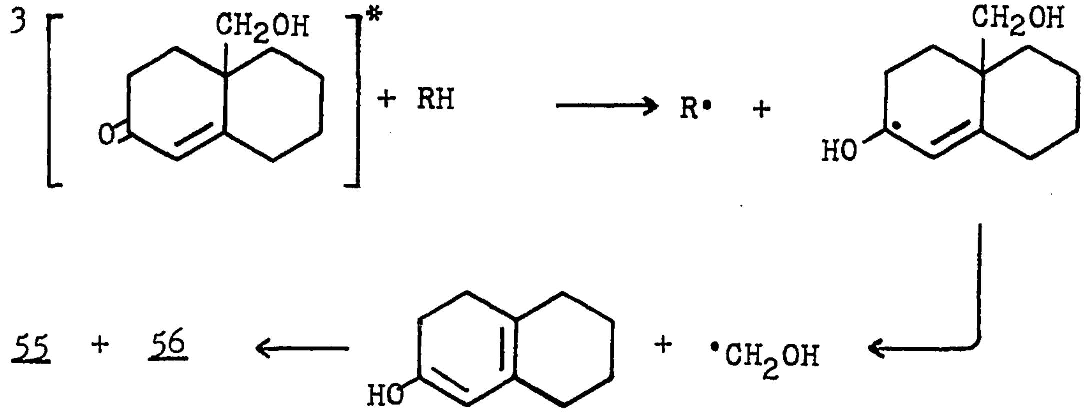

products.

On the basis of the hydrogen abstraction mechanism, the triplet state is assigned the n,π^* configuration. The investigators believe that the rapid rate constant for triplet state deactivation in this case ($\sim 10^9$ sec^{-1}) and in cyclohexenone systems in general is due to the formation of a diradical intermediate (*i.e.*, 57) which preferentially recyclizes to give 53 in its ground state rather than following the alternate mode of cyclization to give 54. The observed specificity of 2-cyclohexenone rearrangements which would argue against such an intermediate is accounted for by steric interactions of the angular methyl or hydroxymethyl substituents which inhibit rotation that would give products with a new stereochemistry.

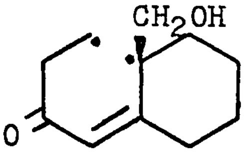

57

Zimmerman and coworkers have studied extensively the mechanistic details of the rearrangements of 4,4-diphenylcyclohexadienones 58 → 59 (27, 28), 4,4-diaryl-2-cyclohexenones 60 → 61 (29, 30, 31, 32), 4,4-dialkyl-2-cyclohexenones 62 → 63 (5, 21), and the relationships between the three. These reactions become progressively less efficient (*e.g.*, equation 5 > equation 6 > equation 7) in terms of quantum yield and reaction rate, due to enhancement of the necessary 3,5-bonding in the rearrangement (equation 8). This enhancement occurs when aryl groups are substituted at the 4-position and when a $\Delta^{5,6}$ double bond is also present.

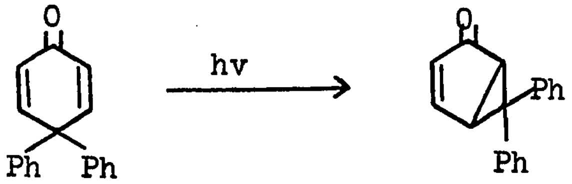

(5)

58 59

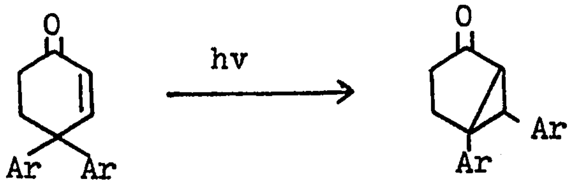

(6)

60 61

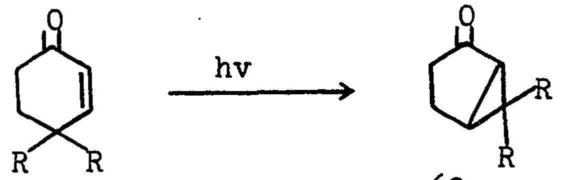

62 63 (7)

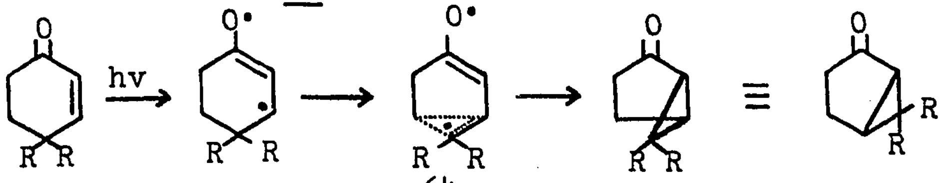

64 (8)

The support for an intermediate of type 64 has come recently with the trapping of a 3,5-bonded intermediate (33). Irradiation of the diene 65 in methanol resulted in a 3,5-bonded product 67 which is probably derived from the zwitterionic intermediate 66.

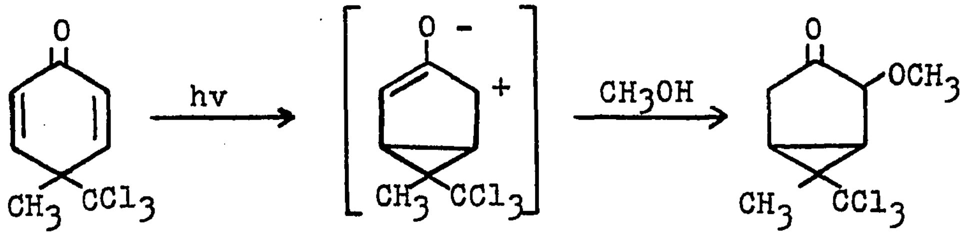

65 66 67

In a study of the photochemistry of 4,4-diphenyl-2-cyclohexenone (60, Ar = Ph), an unusually large energy gap in the triplet manifold was detected (31). The sensitization and quenching experiments indicated that at least 90% of the reaction proceeds through a triplet state. The phosphorescence emission spectrum indicated an n,π^* triplet of energy 69 kcal/mole (34). Sensitization became efficient only in the 74 kcal/mole range (*i.e.*, propiophenone), however, quenching was efficient (as indicated by the slopes of Stern-Volmer plots) only when quenchers below 58 kcal/mole (*i.e.*, 1,3-cyclohexadiene and 2,5-dimethyl-2,4-hexadiene) were used. This large energy gap (16 kcal/mole) between efficient sensitization and quenching may be indicative of the involvement of two cyclohexenone triplet states. The higher triplet, at about 70 kcal/mole, which is sensitized by high energy sensitizers, would be the one responsible for the weak emission noted in the phosphorescence spectrum (5). A lower triplet state, in the 61 kcal/mole range as noted by Hammond (35) would be quenched only by low energy quenchers and responsible for the products of the reaction. Zimmerman believes that the two triplets may be of different geometry, the upper triplet planar, and the lower triplet twisted at the β-carbon (36). Attempts to intercept a higher energy triplet state in 2-cyclohexenone by using very high concentrations of 2,3-diphenyl-2-butene in sensitized isomerization experiments were unsuccessful (35).

A recent report of the photochemistry of 2,4,6-tri-*t*-butyl-3-methoxy-2,5-cyclohexadiene (68) postulates reaction from two triplet states (37). Photolysis of 68 in benzene proceeds through several isolable intermediates (38) which are not photostable but react further to give 69 and 68 in 25% and 7% yields. The molecule also undergoes an internal Norrish Type II reaction to form a cyclobutanol which loses water under the reaction conditions to give product 70 in 38% yield. The photolysis of 68 is wavelength dependent and the

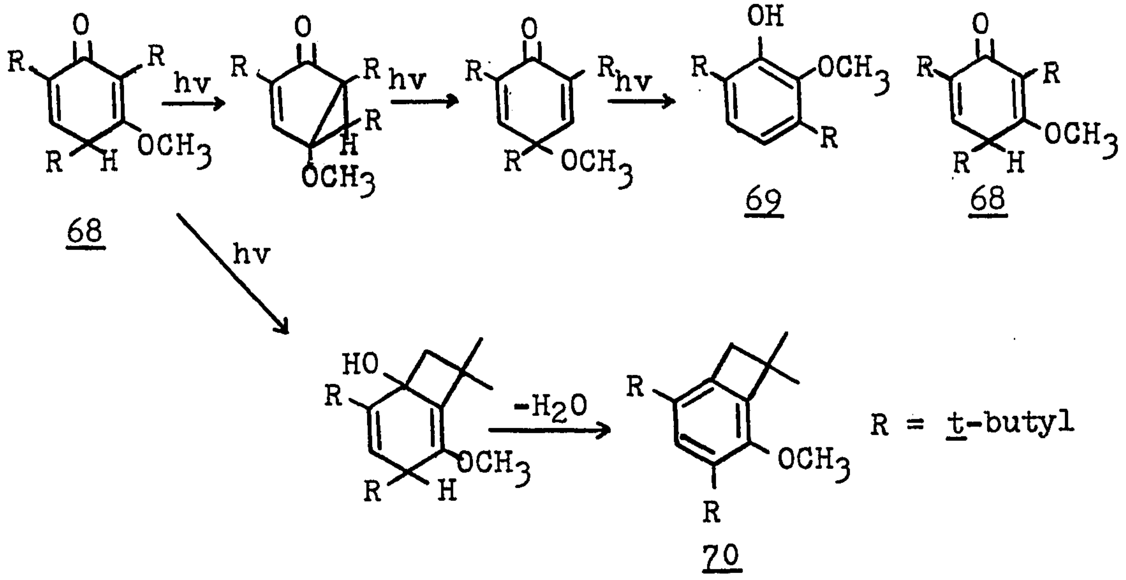

ratio of 70 to 69 increases with shorter wavelength irradiation. The wavelength dependence is explained on the basis of excitation of 68 to two excited singlet states with the relative population of these two states dependent on the wavelength of irradiation used. Sensitization and quenching of the reactions have shown that all products arise from the triplet state. Therefore, intersystem crossing from the singlet states to two different triplet states must occur. The energy scheme shown in Figure 4 is used to explain the reaction. Excitation to the $^1(\pi,\pi^*)$ state using shorter

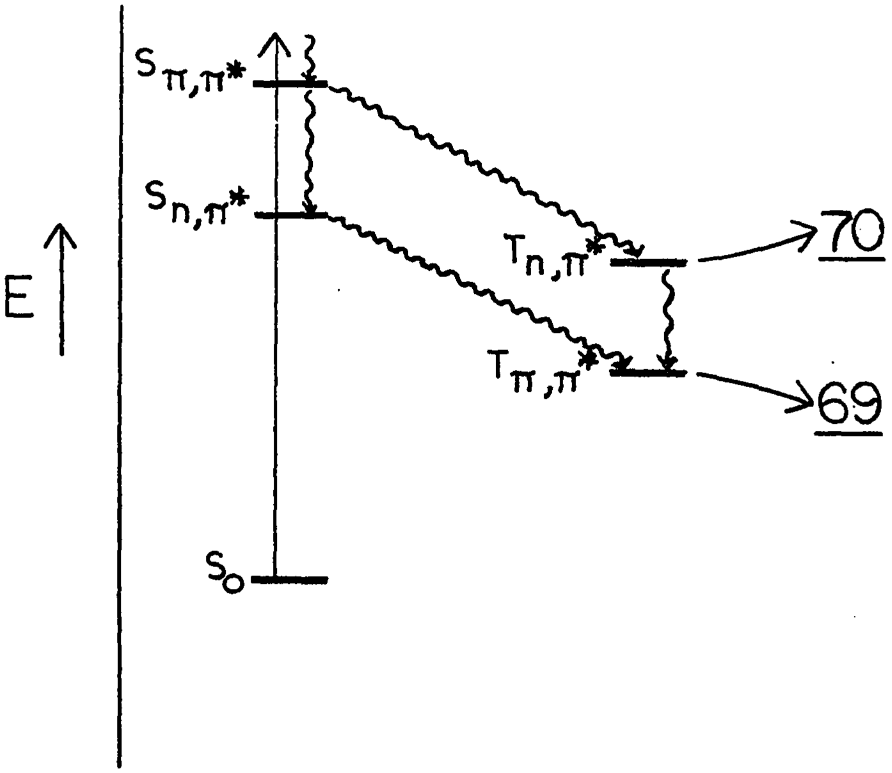

Figure 4. An energy level diagram for the photochemical reactions of 2,4,6-tri-t-butyl-3-methoxy-2,5-cyclohexadienone (68)

wavelength irradiation is followed by both intersystem crossing to the $^3(n,\pi^*)$ state and internal conversion to the lower $^1(n,\pi^*)$ state. This lower singlet state is exclusively populated using higher wavelength irradiation, and it can intersystem cross to the $^3(\pi,\pi^*)$ state. Product 70 is formed from the upper triplet state. Internal conversion to the lower $^3(\pi,\pi^*)$ state can also occur with production of 68 and 69 from this triplet state.

The photochemistry of eucarvone (71) is also believed to involve more than one triplet state (39). Photolysis of eucarvone results in the formation of 72 with a quantum yield of 2.5×10^{-3}. The reaction can be sensitized with triplet sensitizers of energy greater than 62 kcal/mole. Linear Stern-Volmer plots (slope ~ 110 l./mole) are obtained out to quencher concentrations of about 0.01 M, at which point the plots level off. This effect indicates reaction from two excited states, only one of which is quenchable. Quenching with 1,3-cyclohexadiene (CHD) gives CHD dimers (a result of triplet energy transfer from eucarvone) and an adduct of structure 73. When eucarvone is photolyzed with increasing concentrations of CHD, the ratio of adduct 73 to dimers increases, implying that the adduct arises from an intermediate which is a precursor to the triplet state of eucarvone that transfers energy to CHD. The intermediate must be an upper triplet state. If it were an excited singlet state, the

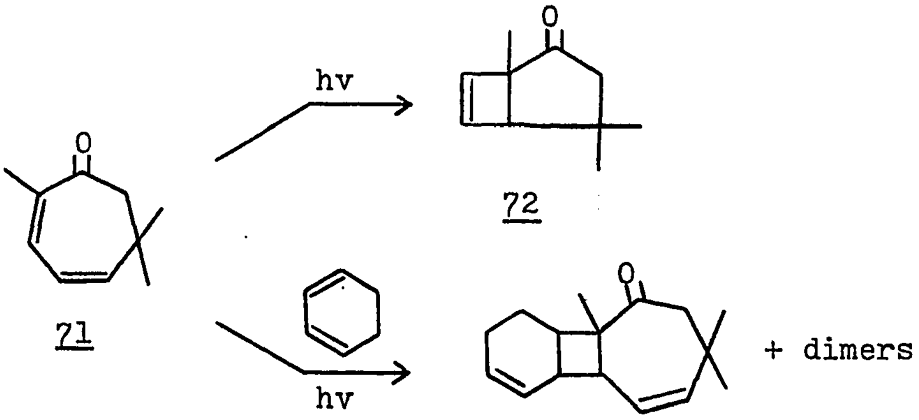

71 72 73

Stern-Volmer plot would rise more sharply instead of leveling off at high quencher concentration. The investigators tentatively conclude that product 72 comes from a lower triplet state and that adduct 73 comes from an upper triplet state.

There have been several additional cases of multiple or upper excited states being invoked in photochemical reactions. The reactions, which will not be discussed here, include the photocycloaddition of 2-cyclopentenone to olefins (40, 41), the photocycloaddition of 9-anthraldehyde to olefins (42, 43), energy transfer from upper triplet states of anthracenes (44, 45, 46), the dye-sensitized photooxygenation of cholest-4-en-3-ol (47, 48), the dimerization of isophorone (49), and the photochemical electrocyclic reaction of 6b,10b-dihydrobenzo-[1,2]-cyclobut[3,4-a]acenaphthylene to pleiadene (50).

RESULTS AND DISCUSSION

The Photocycloaddition of Isophorone and 1,1-Diphenylethylene

The study by Corey et al. (13) of the photocycloaddition reactions of olefins with 2-cyclohexenones provided a basic mechanism that rationalized orientation and stereochemistry in the products for most cases studied. The extended study of cycloaddition reactions by Cantrell et al. (14) involving 3-substituted 2-cyclohexenones revealed that substituents on the enone system often have unusual effects on orientation and stereochemistry that can not be fully explained by Corey's rule. Cycloaddition reactions of isophorone (15) have disclosed a preference for formation of bicyclooctanones substituted in the 7-positions. The present work, involving isophorone and 1,1-diphenylethylene, was part of a continuing study of cycloaddition reactions aimed at revealing more precisely the factors affecting product formation, and locating a reaction amenable to mechanistic study.

Irradiation of isophorone and 1,1-diphenylethylene in t-butyl alcohol with a Pyrex filter results in three products. The major adduct was identified as 3,3,4a-trimethyl-9-phenyl-1,2,3,4,4a,9,10,10a-octahydro-1-phenanthrone (74), the minor adduct as 2,2,10a-trimethyl-9-phenyl-1,2,3,4,4a,9,10,10a-octahydro-4-phenanthrone (75), and the small amount of third adduct as 4,4,6-trimethyl-8,8-diphenylbicyclo[4.2.0]octan-2-one (76). Formation of 74 (76.7%), 75 (21.9%), and 76 (1.4%) accounts for 25% of the reaction.

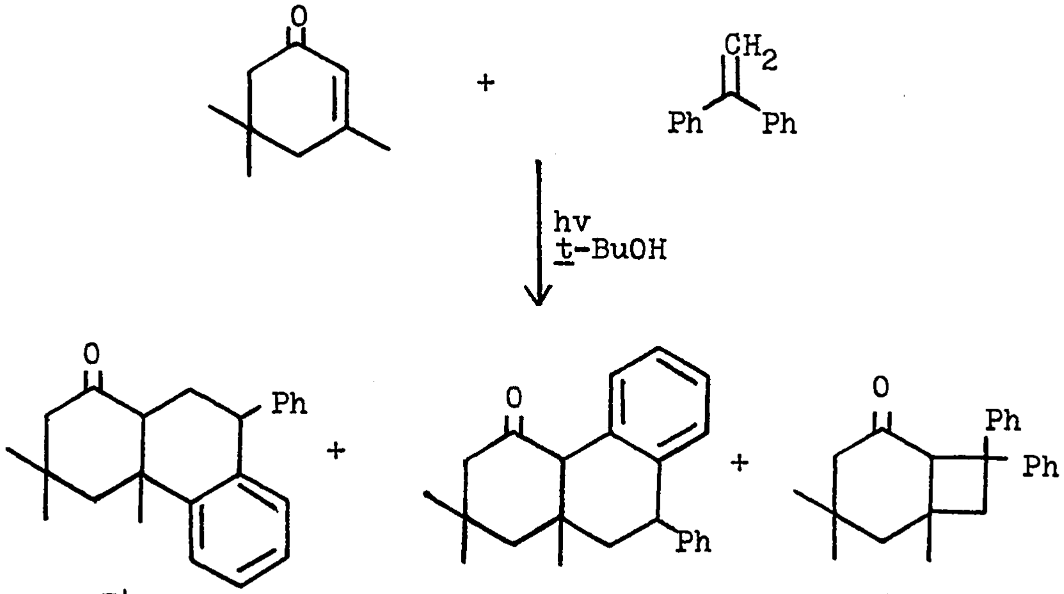

74 75 76

In benzene, irradiation of isophorone and 1,1-diphenylethylene yields only 74 and 75 in a combined yield of 28%. The reaction results mainly in oils from which the products separate as crystals.

Structures 74 and 75 were assigned on the basis of spectral evidence from the parent compounds and the isomerized and deuterated analogs. The infrared spectrum of the major adduct (74, Figure 5) shows a carbonyl absorption of 5.83 μ and peaks at 6.26 μ (w), 6.70 μ (m), and 6.89 μ (m), characteristic of aromatic structure. An infrared spectrum in KBr shows medium strong absorptions at 13.10, 13.21, and 14.32 μ.

Figure 5. Infrared spectra (CCl_4)

Top: 3,3,4a-trimethyl-9-phenyl-1,2,3,4,4a,9,10-10a-octahydro-1-phenanthrone (74)

Middle: 2,2,10a-trimethyl-9-phenyl-1,2,3,4,4a-9,10,10a-octahydro-4-phenanthrone (75)

Bottom: 4,4,6-trimethyl-8,8-diphenylbicyclo-[4.2.0] ootan-2-one (76)

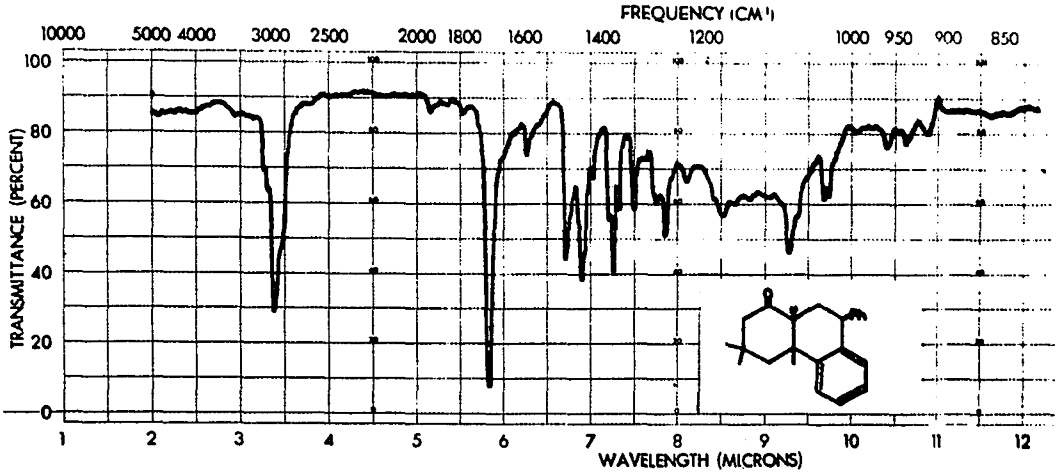
FREQUENCY (CM⁻¹)
10000
5000 4000
3000
2500
2000
1800
1600
1400
1200
1000
950
900
850
TRANSMITTANCE (PERCENT)
100
80
60
40
20
0
1
2
3
4
5
6
7
8
9
10
11
12
WAVELENGTH (MICRONS)

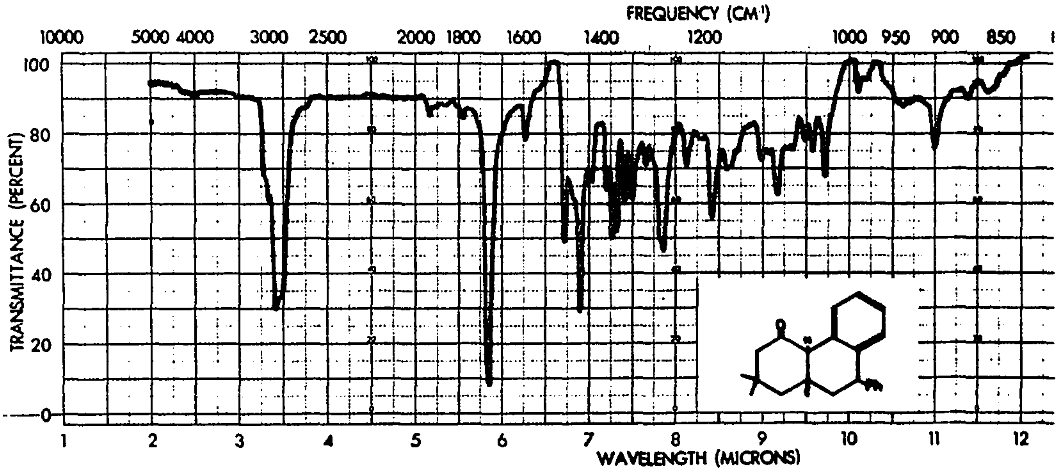
FREQUENCY (CM⁻¹)
10000
5000 4000
3000
2500
2000
1800
1600
1400
1200
1000
950
900
850
TRANSMITTANCE (PERCENT)
100
80
60
40
20
0
1
2
3
4
5
6
7
8
9
10
11
12
WAVELENGTH (MICRONS)

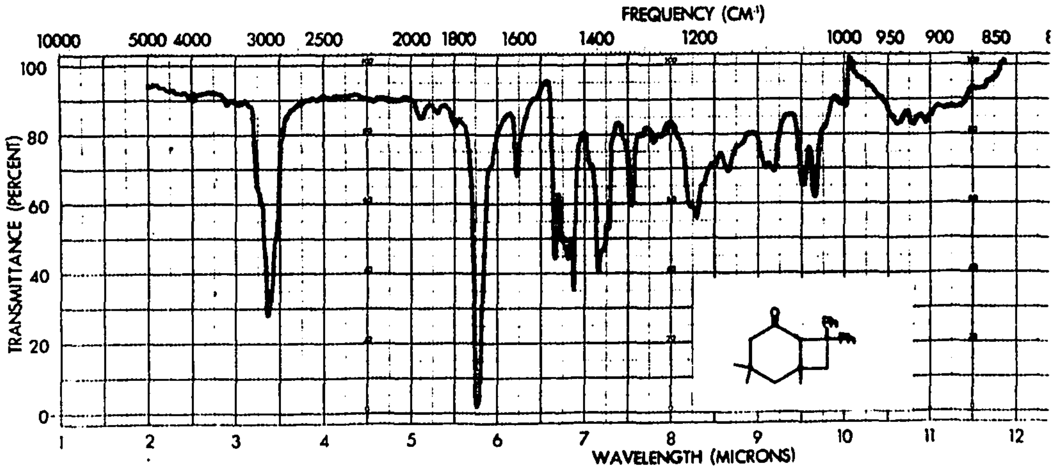
FREQUENCY (CM⁻¹)
10000
5000 4000
3000
2500
2000
1800
1600
1400
1200
1000
950
900
850
TRANSMITTANCE (PERCENT)
100
80
60
40
20
0
1
2
3
4
5
6
7
8
9
10
11
12
WAVELENGTH (MICRONS)

Figure 6. Nuclear magnetic resonance spectra

Top: 3,3,4a-trimethyl-9-phenyl-1,2,3,4,4a,-9,10,10a-octahydro-1-phenanthrone (100 Mc, CCl_4, 74)

Middle: base isomerized 3,3,4a-trimethyl-9-phenyl-1,2,3,4,4a,9,10,10a-octahydro-1-phenanthrone(100 Mc, $CDCl_3$, 77)

Bottom: 3,3,4a-trimethyl-9-phenyl-1,2,3,4,4a,-9,10,10a-octahydro-1-phenanthrone-2,2,10a-d_3 (100 Mc, $CDCl_3$, 78)

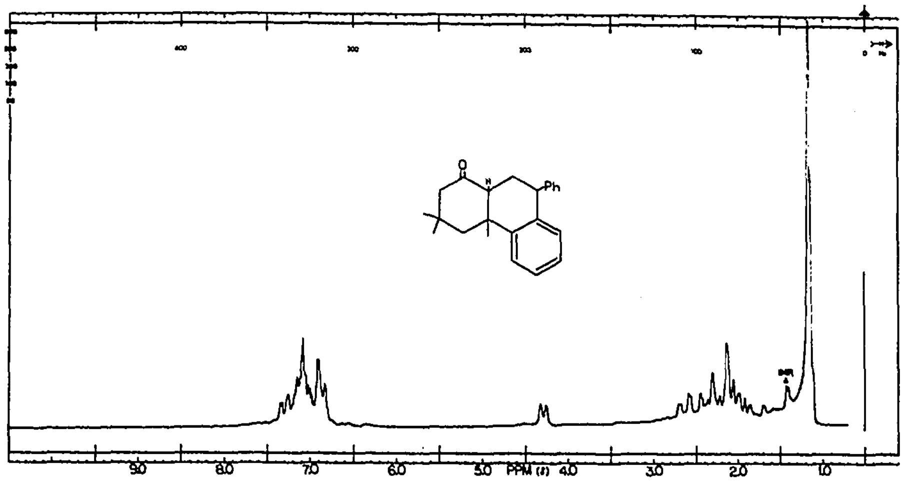

O
H
Ph
400
300
200
100
0
Hz
SHR
9.0
8.0
7.0
6.0
5.0
PPM (δ)
4.0
3.0
2.0
1.0

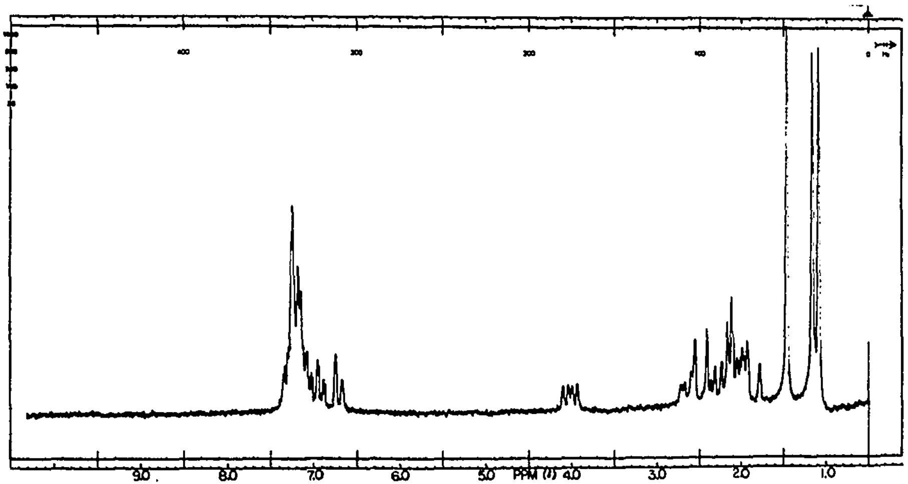

400
300
200
100
0
Hz
9.0
8.0
7.0
6.0
5.0
PPM (δ)
4.0
3.0
2.0
1.0

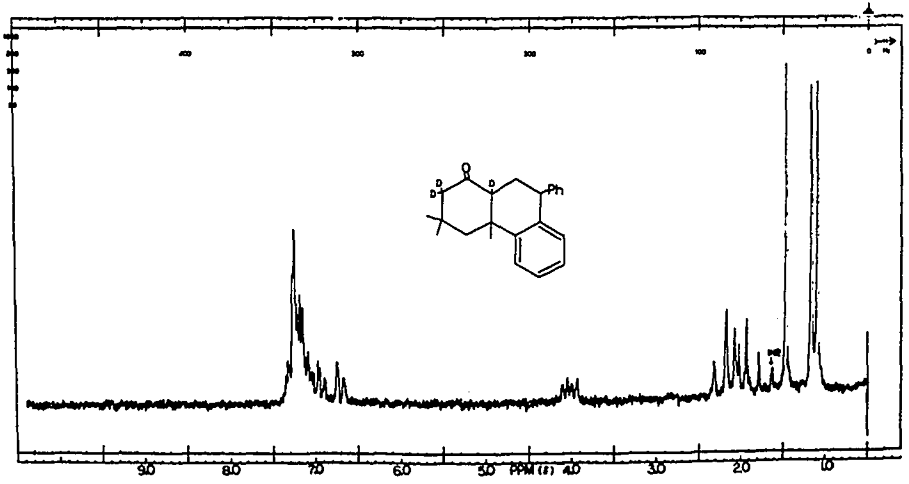

O
D
D
D
Ph
400
300
200
100
0
Hz
SHR
9.0
8.0
7.0
6.0
5.0
PPM (δ)
4.0
3.0
2.0
1.0

Figure 7. Nuclear magnetic resonance spectra

Top: 2,2,10a-trimethyl-9-phenyl-1,2,3,4,4a,-9,10,10a-octahydro-4-phenanthrone (60 Mc, CCl_4, 75)

Middle: 2,2,10a-trimethyl-9-phenyl-1,2,3,4,4a,-9,10,10a-octahydro-4-phenanthrone-3,3,4a-d_3 (60 Mc, CCl_4, 79)

Bottom: 4,4,6-trimethyl-8,8-diphenylbicyclo-[4.2.0]octan-2-one (100 Mc, $CDCl_3$, 76)

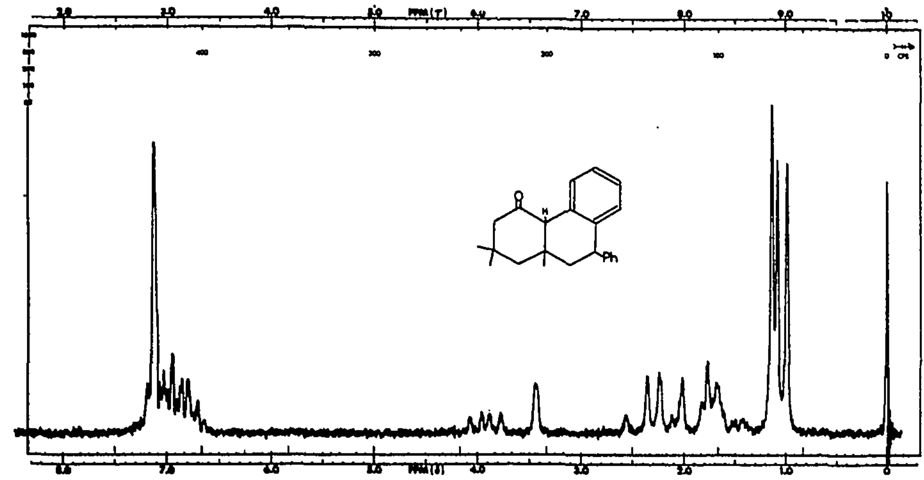
PPM (τ)
PPM (δ)
CPS
H
Ph

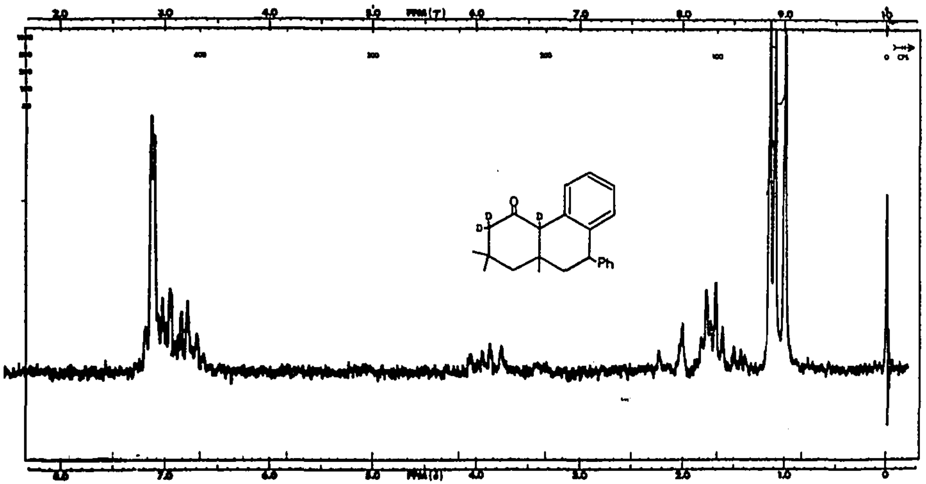
PPM (τ)
PPM (δ)
CPS
D
Ph

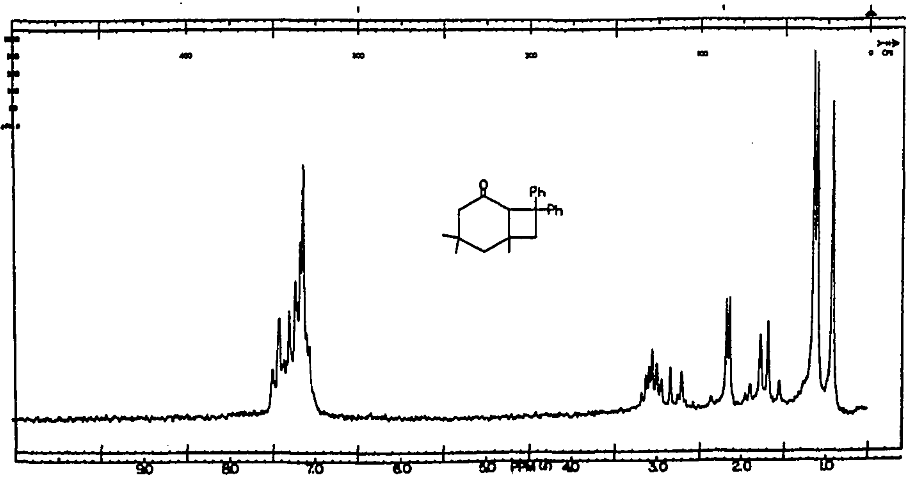
PPM (δ)
CPS
Ph
Ph
9.0
8.0
7.0
6.0
5.0
4.0
3.0
2.0
1.0

Table 2. Mass spectra of adducts 74, 75 and 76

74		75		76	
m/e	rel. int.	m/e	rel. int.	m/e	rel. int.
319	10.4	319	25.3	318	0.2
318	41.7	318	100.0	181	15.7
304	24.5	303	24.8	180	100.0
303	100.0	300	9.4	179	11.3
225	22.3	285	25.3	178	7.4
219	6.5	221	11.0	165	14.0
205	7.8	220	10.6	115	4.0
181	10.9	205	13.3	91	5.4
180	18.3	192	10.8	55	3.8
179	10.4	180	25.5	41	3.1
178	12.2	91	18.2		
142	10.3	83	27.2		
141	8.7	56	8.8		
115	8.7	43	8.4		
91	25.1	41	8.3		
83	12.0				
55	8.2				
41	10.6				

The two absorptions near 13 µ suggest aromatic rings with different substitution.

The mass spectrum (m/e 318, 42%) indicates a 1:1 adduct ($C_{23}H_{26}O$), and the very few peaks of high intensity indicate few favorable cleavage mechanisms. A significant feature is the low intensity of the m/e 180 ion of the diphenylethylene fragment. If the compound were a cyclobutane adduct, this fragment would predominate from a major cleavage mechanism of the cyclobutane ring.

The nmr spectrum (Figure 6) shows several significant features. The first is a multiplet from 6.7 to 7.4δ , which integrates for nine rather than ten aromatic protons. The second feature is a doublet at 4.3δ (J = 6 Hz) integrating for one proton. The position of this proton is too far downfield for a bridgehead α-keto proton on a bicyclo[4.2.0]-octanone, but is in the correct region for a benzylic proton. The balance of the spectrum consists of a multiplet from 1.8 to 2.8δ integrating for 7 protons, and a singlet at 1.15δ for the three methyl groups.

The nmr spectrum could not be completely spin decoupled because of the complexity of the multiplet between 1.8-2.8δ.[1]

---

[1] The author wishes to thank Drs. Hal Wright and Colin McIntosh for running and spin decoupling the 100 Mc nmr spectra.

However, irradiation at 2.34δ caused a partial collapse of one peak of the doublet at 4.3δ, and irradiation at 2.22δ caused a partial collapse of the other peak. In both cases, the doublet also narrowed.

The spectra of the minor adduct show similarities to that of the major adduct. The infrared spectrum of this adduct (75, Figure 5) shows a strong carbonyl absorption at 5.84 μ and aromatic absorption at 6.26 μ (m), 6.71 μ (m), and 6.89 μ (m). The mass spectrum (m/e 318, 100%) and microanalysis are consistent with a 1:1 adduct ($C_{23}H_{26}O$). The mass spectrum is similar to that of the major adduct in that there are very few peaks of major intensity, and the m/e 180 ion for diphenylethylene cleavage is also minor. The nmr spectrum (Figure 7) reveals only nine aromatic protons from 6.6 to 7.2δ , a multiplet from 1.3 to 2.6δ (6H), and three singlets for the methyl groups at 1.14, 1.08, and 0.98δ. The spectrum also indicates a benzylic proton as a doublet of doublets at 3.92δ, and a methine proton at 3.43δ (wide singlet, half-peak width, 3 Hz).

The spectral data of these two compounds clearly eliminate bicyclo[4.2.0]octanone adducts for their structure. Structures that have nine aromatic protons and one benzylic proton could result from closure of a diradical at the *o*-phenyl position rather than at the second atom of the double bond in the olefin. The two possible structures for such a closure are given by 74 and 75. The assignment of these structures to the adducts could be made by isomerization and deuteration of the compounds.

Treatment of the major adduct with alcoholic potassium hydroxide resulted in its isomerization to a compound (77) with a higher melting point (174-175°) and a carbonyl absorption at 5.88 u. In the nmr spectrum of 77 (Figure 6), one methyl group now appears as a singlet at 1.47δ, and two methyl groups (probably the gem-dimethyl) appear as singlets at 1.17 and 1.09δ. The benzylic proton appears as a doublet of doublets between 3.9 and 4.2δ. The mass spectrum (M^+ =318) and microanalysis of 77 are consistent with the empirical formula $C_{23}H_{26}O$. These facts indicate that treatment of the major adduct with base caused its isomerization about the A-B ring junction to an isomer of greater stability. Since the benzylic proton did not exchange, the stereochemistry must remain unchanged at this asymmetric center.

Treatment of the major adduct with sodium methoxide, methanol-OD, and deuterium oxide results in a new product (78) of m.p. 176-177°.[1] The nmr spectrum in $CDCl_3$ (Figure 6) consists of a multiplet, 6.6-7.4δ (9H, aromatic), a quartet centered at 4.0δ (1H, benzylic), a multiplet, 1.7-2.4δ (4H, methylene), and three singlets at 1.47, 1.17 and

---

[1] The deuteration of this adduct was carried out by Dr. P. J. Nelson.

1.10δ (9H, methyls). The melting point and the position of the methyl groups in the nmr spectrum indicate that isomerization to a product of the same stereochemistry as 77 took place under the deuteration conditions. The nmr and mass spectra are consistent with the replacement of the three α-keto protons by deuterium. These protons appear in the nmr spectrum of the undeuterated compound in the 2.5δ region.

In contrast, treatment of the minor photoadduct with alcoholic potassium hydroxide under conditions designed to effect epimerization resulted in no change in the spectral characteristics or the melting point. The adduct could be deuterated with sodium methoxide, methanol-OD, and deuterium oxide to produce a new compound (79) of identical melting point and with the three α-keto protons replaced by deuterium. The nmr spectrum of 79 (figure 7) shows only the following changes: the singlet at 3.43δ disappears completely indicating that it is the α-keto methine proton, and the methylene protons now appear as a narrower multiplet at 1.4-2.3δ integrating for four protons.

The position of the α-keto methine proton in these two structures allows the correct assignment to structures 74 and 75 to be made. In structure 75, the α-keto methine proton is also at a benzylic position which would cause it to be shifted downfield from the normal position near 2.5δ for such a proton. The α-keto methine proton at 4.3δ in the minor adduct is in accord with the assignment of structure 75 for this adduct. This α-keto methine proton appears as a broadened singlet indicating that it is not coupled to any adjacent methylene protons. Double resonance techniques show that the broadened singlet narrows when irradiating at either 1.8δ (α-keto methylene region) or 6.87δ (aromatic region). The coupling of the α-keto proton to both the aromatic region and the α-keto methylene region would be possible only in structure 75 where H_a' and H_b' are in close proximity. The

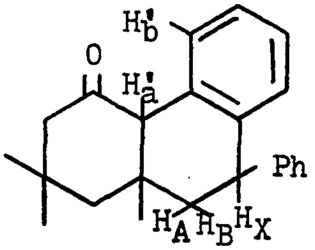

75

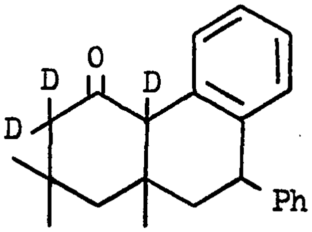

79

doublet of doublets at 3.92δ due to the benzylic proton is the X part of an ABX system formed with the two adjacent methylene protons.

An examination of Dreiding models of compound 75 does not allow an assignment of the stereochemistry of this compound (which has four stereoisomers) to be made. Arguments based on steric interactions affecting thermodynamic stability, or the stereochemistry affecting the coupling of adjacent protons are not conclusive because of the many steric interactions in this molecule and because several isomers could give the observed coupling.

The assignment of structure 74 for the major adduct is consistent with the spectral data for this compound and its derivatives. The α-keto methine proton near 2.5δ is in accord with the location of such a proton in a normal environment. The doublet at 4.3δ in the undeuterated compound is coupled to the adjacent methylene protons as shown by decoupling techniques. In the isomerized compound 77 and in the deuterated analog 78, the benzylic proton appears as the 4-line X part of an ABX system. This analysis was confirmed by spin decoupling techniques. Irradiation at 2.02 and 2.08δ caused each half of the quartet to collapse to a singlet. Conversely, irradiation in the region of the quartet caused collapse of the lines at 2.01 and 2.08δ to a singlet in the spectrum of the deuterated adduct. These lines form a portion of the AB part of the ABX system. Protons H_a and H_b appear as a 4-line AB pattern in the methylene region.

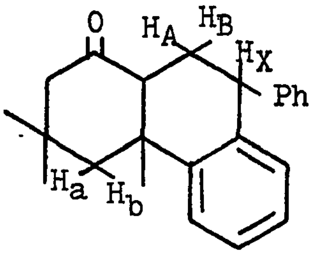

74

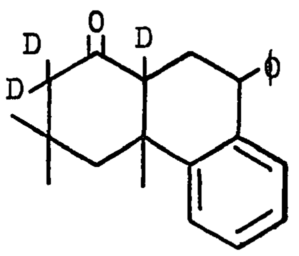

78

In the deuterated sample these lines can be identified as the ones at 1.78, 1.92, 2.17, and 2.31δ ($J_{a\,b}$ = 14 Hz), since they are unchanged in the decoupling procedure.

The stereochemistry of the two isomers of 74 are again a matter of conjecture. It is interesting to note that 74 is formed in the thermodynamically least stable isomeric form, whereas 75 is evidently formed in the more stable isomeric form since it fails to isomerize under basic conditions. In the original isomer of adduct 74, the benzylic proton is not completely coupled to the two adjacent protons, whereas in the isomerized adduct the coupling is complete and therefore appears as the 4-line pattern. This fact may indicate that the original adduct is the <u>trans</u> isomer which is more rigid and could prevent complete coupling. The <u>cis</u> adduct is less rigid and has enough conformational freedom to allow complete coupling of the benzylic proton to the adjacent methylenes. These assignments, however, are not definite.

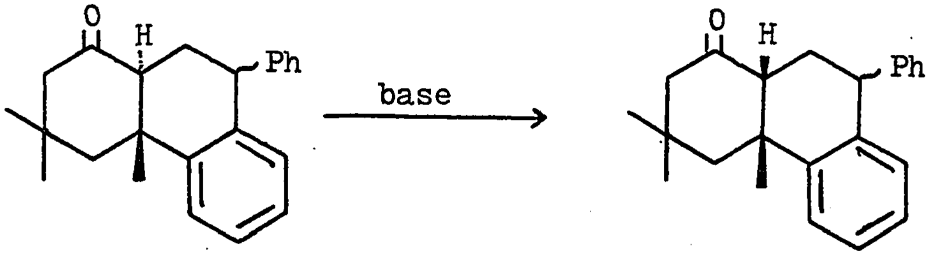

74 77

An attempt at a chemical degradative sequence for the structure proof of 74, involving Baeyer-Villiger oxidation of the adduct, which has been used successfully with bicyclo[4.2.0]octan-2-ones (1, 2, 15) was not successful in this case. The adduct is consumed during the course of the reaction, but unknown oxidation products are obtained rather than the desired lactone. The reason for the failure of this reaction is not known.

The structure of the third adduct rests exclusively on spectral considerations because of the small amount obtained from the preparative reaction. The infrared spectrum of 76 (Figure 5) shows a strong carbonyl absorption at 5.77 μ and medium peaks at 6.22, 6.65, 6.74, 6.81, and 6.87 μ indicative of aromatic substituents. The low value for the carbonyl absorption suggests a trans-fused cyclobutane adduct in analogy with similar structures, but this assignment is not definite.

The mass spectrum of 76 is considerably different from adducts 74 and 75. The parent ion is very weak, and the base peak at m/e 180 results from cleavage to produce the diphenylethylene fragment. The mass spectrum suggests a cyclobutane adduct, and this is confirmed by the presence of 10 aromatic protons and no benzylic proton in the nmr spectrum. The nmr spectrum (Figure 7) supports an 8,8-disubstituted adduct. Three protons adjacent to the carbonyl appear as a complete multiplet at 2.5-3.2δ. The two sets of methylene protons appear as 4-line AB patterns. The high-field set, presumably due to the cyclobutane ring methylenes, has δA = 1.8, δB = 1.6 (J = 12 Hz). The low field set due to the cyclohexane ring methylenes has δA = 2.24, δB = 2.11 (J = 19 Hz). The lack of spin decoupling in these areas to any other part of the spectrum confirms these as AB couplings. Structure 80 is ruled out for this adduct by the lack of coupling of the cyclobutane ring methylene protons to the α-keto methine proton, which would be expected in structure 80.

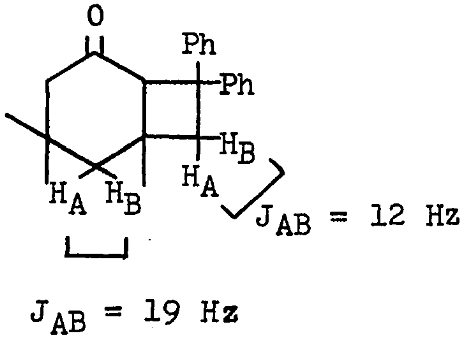

76

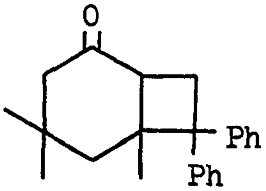

80

The possibility always exists that structural assignments, which are based solely on spectral evidence, can be incorrect. The spectra of these adducts seems to be totally consistent with the structures as assigned, and the possible number of adducts that could result from this reaction is limited. Because of these facts, it is felt that these structures are well established despite the lack of degradative evidence.

The orientation of the products obtained in this cycloaddition reaction is less amenable to explanation by the Corey rule than in many other cycloaddition reactions because of the low charge separation in the olefin. Huckel molecular orbital calculations that were carried out on acrolein show that the β-carbon atom is slightly more electron rich than the α-carbon atom in the n,π^* excited state. This assignment is in agreement with configuration interaction calculations carried out by Zimmerman _et_ _al_. (51) on the enone moiety. Simple H. M. O. calculations also indicate that 1,1-diphenylethylene has no charge separation in either the ground of the π,π^* excited states. The orientation is therefore more subject to control by steric factors rather than electronic as in the addition reactions of other olefins to isophorone. This view is supported by the appearance, for the first time, of two adducts, _75_ and _76_, which result from a head-to-tail orientation of the enone and olefin. If one assumes a mechanism similar to Corey's, with adduct formation proceeding through a π-oriented complex which gives a diradical, then these two products result from orientation _81_ whereas adduct _74_ results from orientation _82_, as shown in the following scheme. Consideration of the steric interactions of the methyl and phenyl groups leads to the prediction that

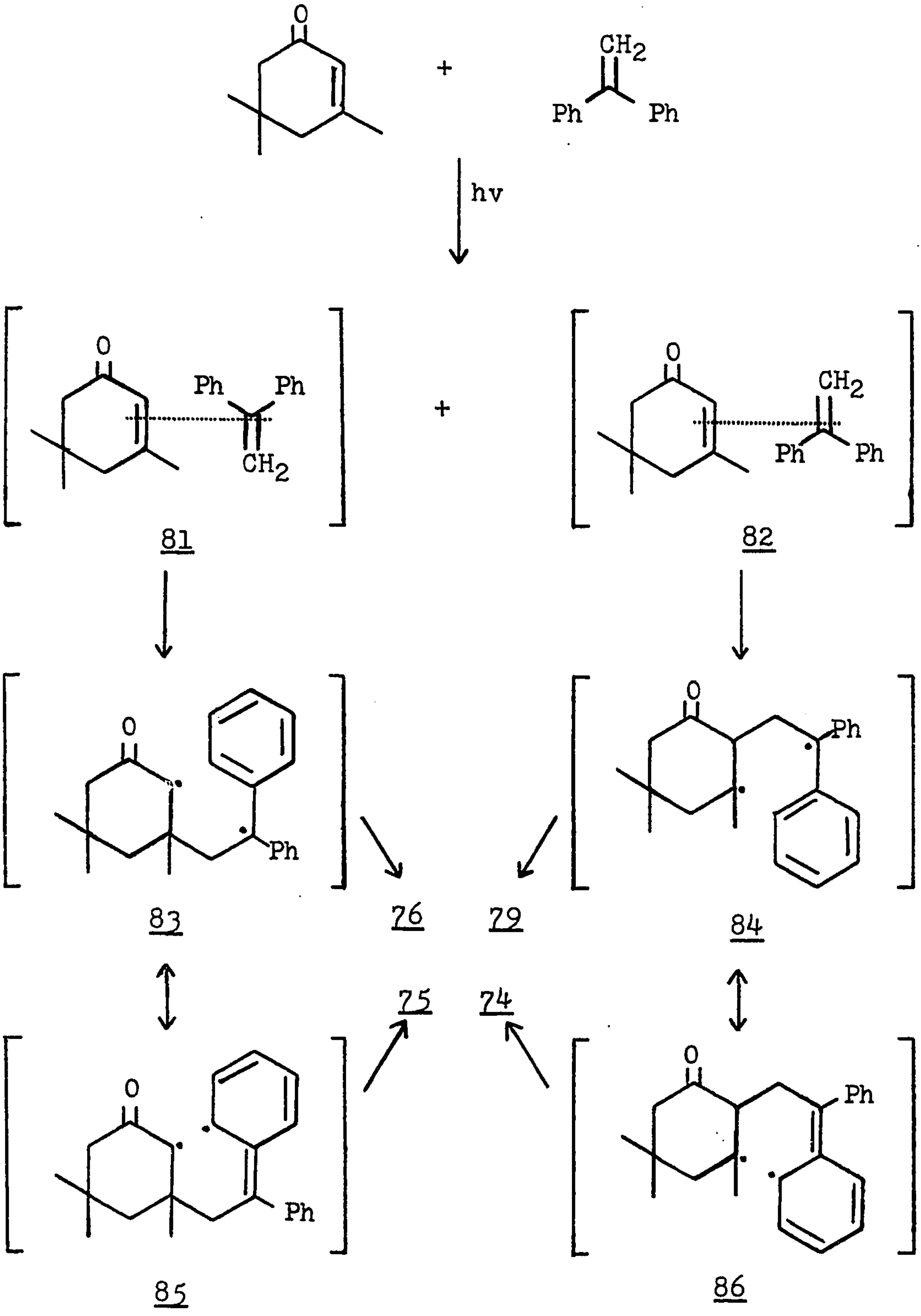
O
CH2
Ph
Ph
+
hv
81
82
83
84
85
86
76
79
75
74

π-complex 81 would be formed more readily than π-complex 82. However, the approach of the methylene carbon of the olefin to the enone to form a bond between the two would be more favorable in the latter case because of the steric hindrance of the methyl group on the β-carbon. It is not surprising therefore that adduct 74 predominates in the reaction because of the more favorable formation of diradical 84.

With the formation of diradicals 83 and 84, the reactions depart from the expected path of product formation. Closure of these diradicals to give 76 and 79 is almost negligible. Instead, closure takes place at the *ortho*-positions of one of the benzene rings to give cyclohexane rather than a cyclobutane adduct. This closure is somewhat unusual for several reasons. The radical centers in 85 and 86 are *secondary* instead of *tertiary*, and these forms are less important resonance contributors. Closure at the *o*-benzene position causes the benzene resonance to be interrupted, and a hydrogen atom migration is necessary to restore it. The migration can be pictured as a [1,3] or [1,7] sigmatropic shift, both of which are allowed photochemically (52), or it could also take place in a non-concerted process.

This cycloaddition reaction is in dramatic contrast to the addition of 1,1-diphenylethylene to 4,4-dimethyl-2-cyclohexenone. The major product of that reaction was a cyclobutane adduct (27). The product resulting from closure at the

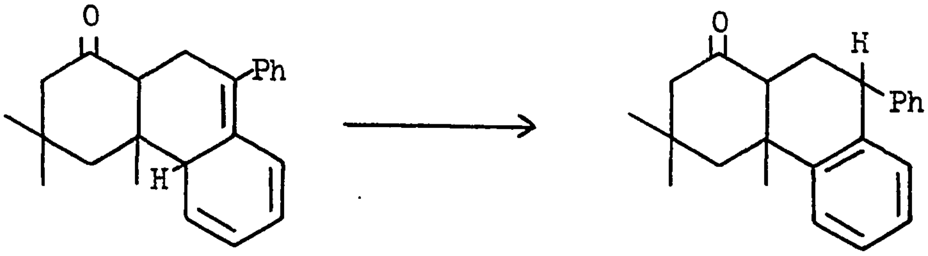

benzene ring (28a) to give an adduct analogous to 74 was formed in very low yield. The formation of adducts 74 and 75 provide strong support for the diradical mechanism in cycloaddition reactions. The factors which occasionally cause these reactions to form less stable isomers and to effect closure at different centers in the resonance system are still not completely known. Clearly, there is presently no suitable explanation which will completely rationalize these observations.

The cycloaddition reaction remains interesting from the standpoint of the excited state or states that are involved in product formation. In analogy with studies of other cycloaddition reactions, it is possible that the formation of the three adducts arise from different excited states, and that the conformations of these excited states are responsible for the differences in their structure, orientation, and stereochemistry, in contrast to the explanation just offered.

The best method of determining the nature and number of excited states involved in the reaction would be a mechanistic study involving the observation of the effect of added quenchers and sensitizers on the reaction efficiency. Unfortunately, this reaction is poorly suited for such a mechanistic study because of its low yield and the difficulty of quantitatively measuring product formation. A more suitable subject of study was the photocycloaddition of 4,4-dimethyl-2-cyclohexenone and 1,1-dimethoxyethylene. Since this enone also photorearranges and photoreduces, a mechanistic study of these reactions was undertaken to determine their relationship to the accompanying cycloaddition reaction.

The Photorearrangement and Photoreduction of 4,4-Dimethyl-2-Cyclohexenone

The photorearrangement of 4,4-dimethyl-2-cyclohexenone in _t_-butyl alcohol has been briefly studied several times (1, 2), and the triplet nature of the reaction has been confirmed. The present study was undertaken to more completely characterize the triplet nature of the reaction by quenching and sensitization studies, and to relate the rearrangement of this molecule to its concurrent photoreduction in isopropyl alcohol and to its photocycloaddition reactions with olefins.

The photorearrangement to products 2 and 3 is a very inefficient reaction. The quantum yields for formation of these two products are 6.5×10^{-3} and 7.7×10^{-3} moles/einstein respectively at 366 nm, 25°. The low quantum efficiency of this rearrangement is characteristic of the photorearrangement reactions of 2-cyclohexenones. The rearrangement of the phenanthrone 11 to product 38 has a quantum yield of 8.4×10^{-3} (5); octalone 42 rearranges to product 48 with a quantum yield of 3.8×10^{-3} (5). The rearrangement of 4,4-diphenyl-2-cyclohexenone to three products has a total quantum yield of only 4.3×10^{-2} (31).

The rearrangement is confirmed to be a unimolecular reaction by a study of the effect of the enone concentration on the quantum yield. The results in Table 8 show that over a concentration range of 0.02 to 1.00 M 4,4-dimethyl-2-cyclohexenone, no appreciable change in the quantum yield for rearrangement occurs. This data rules out any bimolecular mechanism involving excimer formation in the enone.

Rettig (1) determined in 1966 that the rearrangement is a triplet reaction by efficient sensitization with benzophenone (E_t=69) (53). The present results confirm the triplet nature of the reaction. Sensitization with acetophenone (E_t=74)(53) and benzophenone, as shown in Tables 11 and 12 give ϕ_{sens}/ϕ_o ratios near 1.0. Sensitization with lower energy sensitizers, 9-fluorenone (E_t=53) (53) and 2-acetonaphthone (E_t=60) (53) give little or no sensitization, as the results in Table 14 indicate. Sensitization with thioxanthone (E_t=65.5)(53) gave intermediate values for ϕ_{sens}/ϕ_o depending on the sensitizer concentration. The reason for the sensitizer concentration dependence will be discussed later.

The triplet nature of the reaction is also confirmed by quenching with both di-t-butyl nitroxide (E_t=53)(54) and naphthalene (E_t=60.9)(53), as shown in Tables 9 and 10. The triplet nature is reflected by the linear Stern-Volmer plots of $1/\phi$ versus quencher concentration for di-t-butyl nitroxide and naphthalene shown in Figure 8. Non-linear Stern-Volmer plots indicate product formation from two or more excited states of different lifetimes. The single reactive excited state in the rearrangement is a triplet state, and a consistent mechanism and the kinetic relationships derived from it are shown in Figure 9.

Plots of ϕ_o/ϕ_q versus $[Q]$, a modified form of the Stern-Volmer expression, are also linear with intercepts of 1.0 and slopes equal to $k_q\tau$, where τ is the lifetime of the reactive triplet state. Porter and Wilkinson (55) have shown that when the triplet state of a donor molecule is more than 3 kcal/mole above the triplet state energy of the acceptor, then triplet energy transfer between the two will be diffusion controlled. Under such conditions, k_q in equation 11 is assumed equal to the rate of diffusion calculated by the Debye equation (56).

Figure 8. Stern-Volmer plot for quenching rearrangement by di-_t_-butyl nitroxide and naphthalene in _t_-butyl alcohol

□ - di-_t_-butyl nitroxide; slope = 2042 ± 63 l./mole

Δ - naphthalene; slope = 1472 ± 44 l./mole
intercept = 73.5 ± 2.5

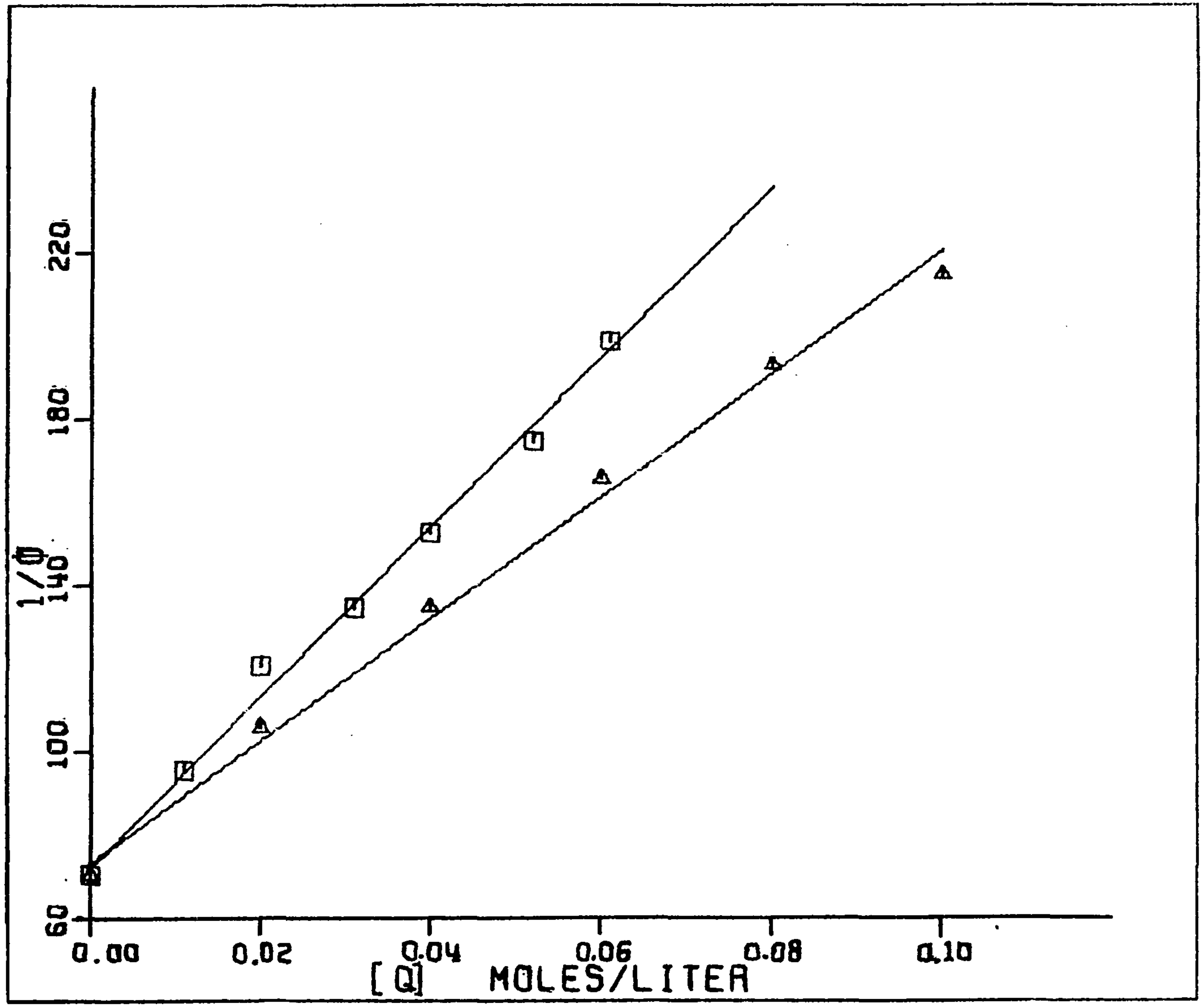
220
180
140
100
60
1/Φ
0.00
0.02
0.04
0.06
0.08
0.10
[Q] MOLES/LITER

$$K \xrightarrow{h\nu} {}^1K$$

$${}^1K \xrightarrow{k_d} K$$

$${}^1K \xrightarrow{k_{ic}} {}^3K$$

$${}^3K \xrightarrow{k_{d'}} K$$

$${}^3K \xrightarrow{k_r} \text{Products}$$

$${}^3K + Q \xrightarrow{k_q} K + {}^3Q$$

$${}^3S + K \xrightarrow{k_s} {}^3K + S$$

$${}^3S \xrightarrow{k_{ds}} S$$

$$\varphi = \frac{k_{ic}}{k_{ic} + k_d} \qquad (9)$$

$$\phi_o = \varphi_{ic} \frac{k_r}{k_r + k_{d'}} \qquad (10)$$

$$\frac{\phi_o}{\phi_q} = 1 + k_q \tau [Q] \qquad (11)$$

$$\frac{1}{\phi_q} = \frac{1}{\varphi_{ic}} \left[\frac{k_r + k_{d'}}{k_r} + \frac{k_q}{k_r} [Q] \right] \qquad (12)$$

Figure 9. A triplet mechanism for the rearrangement of 4,4-dimethyl-2-cyclohexenone

The slopes of the Stern-Volmer plots given by equation 11 are 28.5 ± 1.8 for di-t-butyl nitroxide and 20.9 ± 0.6 for naphthalene quenching. The variation between the two slopes suggests that naphthalene quenching may not be completely diffusion controlled because the energy gap is probably less than 3 kcal/mole between its triplet energy and that of the enone. Using 5.88 centipoises for the viscosity of t-butyl alcohol at 25° (57), the diffusion rate constant calculated by the standard Debye equation is 1.1 x 10^9 M^{-1} sec^{-1}. (The slightly modified Debye equation (58) gives a value of 1.7 x 10^9 M^{-1} sec^{-1} for K_{diff}). From the slopes of the Stern-Volmer plots and the diffusion rate constant calculated from the standard Debye equation, the reactive lifetime of the 4,4-dimethyl-2-cyclohexenone triplet is calculated to be 2.6 x 10^{-8} sec and 1.9 x 10^{-8} sec for di-t-butyl nitroxide and naphthalene quenching, respectively. These values are comparable to the value of 7 x 10^{-9} sec measured by Koch (2) for this compound at 45°.

The reactive lifetime of the triplet is determined by the rates which deactivate the triplet, given by the rate constants k_r and k_d'; that is, $\tau = 1/(k_r + k_d')$. Values for these rate constants can be obtained by plotting the data in the form of a Stern-Volmer expression given by equation 12 and shown in Figure 8. When ϕ_{ic} is equal to 1.0, the slope of the plot is given by k_q/k_r. There is documentation in the literature (2, 5, 40) and later in this thesis that the intersystem crossing efficiencies of 2-cyclohexenones are unity. Using this value for ϕ_{ic} and the slopes of the lines for the two quenchers, and assuming $k_q = k_{diff}$ as before, values of k_r are calculated as 5.5 x 10^5 sec^{-1} and 7.3 x 10^5 sec^{-1} for di-t-butyl nitroxide and naphthalene quenching. Using these values and the intercepts of each plot, values of k_d' are calculated to be 3.9 x 10^7 sec^{-1} and 5.3 x 10^7 sec^{-1} for di-t-butyl nitroxide and naphthalene quenching. These rates are comparable to those measured by Zimmerman, et al. (5) for the rearrangement of phenanthrone 11 in which he found $k_r = 2.9 \times 10^5$ sec^{-1} and $k_d = 3.9 \times 10^7$ sec^{-1}. In that case, di-t-butyl nitroxide and naphthalene quenched the phenanthrone with equal efficiency.

The low efficiency of the rearrangement of 4,4-dimethyl-2-cyclohexenone and that of other 2-cyclohexenones in general seems to be derived from the fact that the unimolecular rate of rearrangement is at least 100 times slower than the rate of decay of the cyclohexenone triplet. Zimmerman (5) has also shown that the efficiency of the rearrangement is increased by 4,4-diaryl substitution and even more by introduction of a $\Delta^{5,6}$ double bond, both of which cause k_r to increase relative to k_d. The increase in k_r is ostensibly due to enhancement of necessary 3,5 bonding in the rearrangement, as mentioned previously. The possibility of a discreet diradical intermediate similar to 57 in the rearrangement reactions which preferentially regenerates starting material in its ground state rather than closing in an alternate manner to give the rearrangement products could account for the unusually high values of k_d leading to inefficient rearrangement (26).

The exact energy of the reactive triplet state of 4,4-dimethyl-2-cyclohexenone is not known since the molecule does not phosphoresce. An energy range for the triplet state can be obtained from the quenching and sensitization data.

On the basis of a comparison with the cyclohexenone systems studied by spectroscopic techniques, the triplet energy of 4,4-dimethyl-2-cyclohexenone should be near 70 kcal/mole. It cannot be this high, however, because of the efficient sensitization obtained with benzophenone, $E_t = 69$. Since thioxanthone can sensitize the rearrangement, and naphthalene can quench it, the triplet energy must lie in the 61-65 kcal/mole region. Naphthalene is less efficient than di-t-butyl nitroxide in quenching the rearrangement. This fact suggests that energy transfer between the enone and naphthalene is less than diffusion controlled, and that the triplet energy of 4,4-dimethyl-2-cyclohexenone is in the 61 kcal/mole range. This low value for the triplet energy of 4,4-dimethyl-2-cyclohexenone is in agreement with the triplet energy of 2-cyclohexenone, $E_t = 61$, measured from Saltiel plots (35). The value is surprisingly low, however, compared to the more rigid cyclohexenone systems. It also appears to be lower than the triplet energy of isophorone, which is at least 63 kcal/mole, since naphthalene is very efficient at quenching the photocycloaddition of isophorone and 1,1-dimethoxyethylene (18).

In his study of the photocycloaddition and photorearrangement reactions of 4,4-dimethyl-2-cyclohexenone, Koch (2) proposed that the rearrangement, trans-adduct, and oxetane products come from one daughter triplet state, and the cis-adduct from another (see Figure 2). Di-t-butyl nitroxide is able to quench the formation of the trans-adduct about twice as efficiently as the photorearrangement products, however. Naphthalene is very inefficient in quenching any of the cycloadducts, but the present results show that it is able to quench the rearrangement. These facts suggest that the rearrangement is not coming from the same daughter triplet that gives the trans-adduct and the oxetane. There are several alternate explanations that can explain these results.

The first possibility involves rearrangement coming from the parent triplet state, $^3K^*$, and photocycloaddition from the daughter triplets. The parent triplet is sufficiently high in energy to be quenched by both di-t-butyl nitroxide and naphthalene, but the daughter triplets would be too low in energy to be quenched by naphthalene. Instead, naphthalene would be quenching the parent triplet state and would not show differential quenching with respect to the cycloadducts. Di-t-butyl nitroxide, on the other hand, is low enough in energy so it could quench the daughter triplets and account for the differential quenching. It must also quench the parent triplet, and the Stern-Volmer plot for cycloadduct quenching should be non-linear, since more than one excited state is being quenched. Although the experimental plot determined by Koch is linear out to 0.05 M quencher, this may merely be the result of not carrying the plot out to the high concentrations necessary to observe the curvature that would result from also quenching the parent triplet state. This is a reasonable assumption and has been observed in a similar system. When the cycloaddition reactions of isophorone and 2-cyclohexenone to 1,1-dimethoxyethylene are quenched with di-_t_-butyl nitroxide, the Stern-Volmer plots show curvature upward between 0.05 and 0.10 M quencher concentrations (18). This curvature could likewise be due to the quenching of a parent triplet state along with the daughter triplets that are responsible for product formation.

A more plausible explanation that accounts for the data is the exciplex mechanism proposed by Koch (2) (see Review of Literature Section). The lack of a concentration dependence of enone on the rearrangement clearly excludes any excimer mechanism for rearrangement, but exciplex formation for cycloaddition could account satisfactorily for the differential quenching of all of the products. Although the rate of exciplex formation must compete efficiently with quenching rates, this is not a serious objection. The rate constant for reaction of 2-cyclopentenone with 1,1-dimethoxyethylene in hexane is 6.0×10^9 M^{-1} sec^{-1} (59) which is sufficiently high to compete with diffusion controlled quenching. Because of the similarity of these two systems, the rates of exciplex formation and quenching could also be competitive in the addition of

4,4-dimethyl-2-cyclohexenone and 1,1-dimethoxyethylene.

In investigating the photorearrangement and photoreduction reactions of 4,4-dimethyl-2-cyclohexenone, it was necessary to relate the studies on each to a common basis by using identical probes of study. Since the probes in this study were quencher and sensitizer molecules, there was a need to choose ones that could be used in both reactions. The quenchers used in studying the rearrangement pose no problems in use for quenching reduction. The sensitizers acetophenone and benzophenone could not be used to study reduction, however, because they are themselves susceptible to photoreduction. It was necessary therefore, to choose some additional compounds that would be suitable for sensitizing both the rearrangement and the reduction.

Sensitizers such as acetophenone and benzophenone, which have n,π^* states, are much more susceptible to photoreduction than aromatic ketones having π,π^* triplet states (60, 61). Extensive investigations have shown that the placement of electron-donating substituents on the aromatic rings of ketones causes a reversal of the n,π^* and π,π^* triplet states and leads to dramatic reductions in the photoreactivity of the molecules in photoreduction and Norrish Type II reactions, where they are possible (62-68). A corresponding increase in the triplet lifetime is noted (see Table 3). Accordingly, the sensitizers m-methoxyacetophenone, p-methoxyacetophenone,

Table 3. Photoreactivity of substituted acetophenones[a]

Compound	ϕ_{red}	E_t(kcal)	τ_{rad}(sec)
Acetophenone	0.68	74.1	0.005
p-Methylacetophenone	0.66	72.8	0.14
3,4-Dimethylacetophenone	0.12	71.5	0.30
p-Methoxyacetophenone	0.04	71.5	0.38
m-Methoxyacetophenone	0.006	72.4	0.71
3,4-Methylenedioxyacetophenone	0.002	65.8	1.20

[a] Data taken from reference (64)

and 3,4-methylenedioxyacetophenone were chosen to study both of the reactions. These compounds are relatively inert to photoreduction, have high triplet energies, and high intersystem crossing efficiencies (vide infra).

Sensitization of the rearrangement with 0.02 M m-methoxyacetophenone gave efficient sensitization as expected (ϕ_{sens}/ϕ_o = 0.96). A repeat of this experiment using 1.0 M sensitizer to ensure complete light absorption gave much less efficient sensitization (ϕ_{sens}/ϕ_o = 0.32). Since the sensitizer was absorbing all or nearly all of the light in both cases, the large variance in these results cannot be explained on the basis of a conventional energy transfer mechanism. To investigate this unusual phenomenon further, a complete concentration dependence study of the sensitizer on the quantum yield was carried out. The results, listed in Table 15, show a definite inverse relationship of ground state sensitizer concentration on quantum yield. (Since the sensitizer is absorbing 100% of the light in all cases, the concentration of the sensitizer triplet state remains constant.)

To verify the generality of the concentration dependence, studies were carried out for other sensitizers using the rearrangement as a test system. p-Methoxyacetophenone (Table 16) shows a slight, but definite, concentration dependence. Thioxanthone and 3,4-methylenedioxyacetophenone (Tables 13 and 17) show greatly enhanced concentration effects. Higher concentrations than those used were not possible because of the solubility limit for these compounds. Both acetophenone and benzophenone (Tables 11 and 12) show very minor concentration dependence. The effect, therefore, seems to be pronounced only among aromatic ketones having low-lying π,π^* triplet states.

The phenomenon that is noted here is essentially a form of self-quenching and should be observable in phosphorescence emission spectra as the concentration of the emitting species is varied. In order to demonstrate the effect more extensively, this possibility was investigated by determining the phosphorescence emission spectrum of m-methoxyacetophenone in EPA glass at 77° K as a function of its concentration.

Unfortunately, it was not possible to determine if the intensity of the emission decreased with increasing concentration. The phosphorescence excitation spectra of many emitting species, including this one, vary greatly over wide concentration ranges due to inner filter effects (69). As a result, at a given wavelength of excitation, the extinction coefficient varies over a concentration range, causing a similar change in the intensity of emission. The phosphorescence emission wavelength maximum, however, did show a gradual shift to longer wavelengths with increasing concentrations (see Figure 10). This shift amounts to a change of 40 nm over a concentration range of 10^{-5} M to 1.0 M. A shift of this type is indicative of a new emitting species at longer wavelengths. It is believed that this new emitting species is not an impurity because of careful purification of the m-methoxyacetophenone and by the absence of any anomalous changes in the excitation spectrum. In analogy with observed phenomena of this type in fluorescence studies (70), it is probable that the species emitting at high concentrations is an excimer; that is, a complex compound of an excited state molecule and a ground state molecule (71, 72, 73). Excimer formation results in a lowering of the excited state energy levels causing emission at a longer wavelength than in the uncomplexed species.

The existence of triplet excimers has been in question for many years, although singlet excimers are well documented (74). There have been no reports of excimer phosphorescence from aromatic ketones, but in recent years there have been several reports of excimer phosphorescence from aromatic hydrocarbons. In 1966, Castro and Hochstrasser (75) reported long wavelength (430-440 nm) phosphorescence emission from rigid glasses of p-dibromobenzene, 1,3,5-tribromobenzene, and 1,3,5-trichlorobenzene at 77° K. They assigned this emission to that of an excimer since normal emission from these compounds occurred at about 385 nm. In a repeat of this work, Lim and Chakrabarti (76) assigned this observed long wavelength emission to photoproducts produced during irradiation of the samples. At the same time, they reported excimer emission from glasses of chlorobenzene, bromobenzene, and iodobenzene in high concentrations. This emission, having an intensity maximum near 495 nm, decayed non-exponentially, appeared at concentrations only greater than 10^{-2} M, and could also be produced by direct excitation upon irradiating at energies corresponding to the $S_0 \rightarrow T_1$ absorption band. Other excimer emissions have been since reported for solutions of naphthalene and phenanthrene (77) and tetrachloro-p-xylene (78). In a conflicting report, Chandross and Dempster (79) note that the phosphorescence of an intramolecular dimer of a naphthalene sandwich pair (88) is identical with the phosphorescence of the starting material 87. The fluorescence of 88, however, is typical of the naphthalene singlet excimer. The investigators conclude that a triplet excimer is not formed and that the interaction between the naphthalene nuclei is much weaker than in the singlet excimer case. At the same time, they concede the possibility that the preferred orientation of a triplet excimer is much different than a single excimer which precludes its formation in this case.

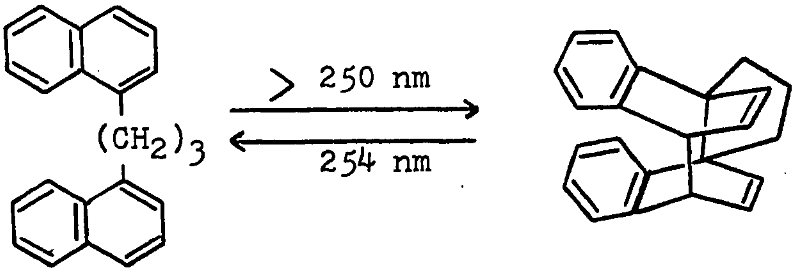

87 88

Cundall and Voss (80) have presented evidence that triplet excimers may be largely responsible for the unusually short lifetimes of some aromatic triplet molecules. From *cis*-*trans* isomerization measurements of *cis*-2-butene by *o*-xylene sensitizations, the lifetime of the *o*-xylene triplet state can be estimated. The results show a decrease in the triplet lifetime with increasing o-xylene concentration, which is consistent with rapid deactivation of the triplet state by an excimer route, according to equation 13.

$$^3X + X \longrightarrow \left[{}^3(X_2)\right] \longrightarrow X + X \qquad (13)$$

Evidence for the intermediacy of triplet excimers has also appeared recently in the photosensitized dimerization of indene (81), the direct photodimerization of thymine and uracil (82), and the photoaddition of benzophenone to furan (83).

The identification of triplet excimers is important to the confirmation of theoretical accounts of intermolecular forces in these species (84, 85, 86) and comparison with molecular orbital calculations of energies and energy differences between the complexed and uncomplexed triplet states (87, 88). The conclusions from molecular orbital calculations on triplet excimer stability are not at present clear cut. Simple H.M.O. calculations indicate reasonable stabilization energies for excimers (88) while more extensive calculations predict that excimer triplet states of most polycyclic hydrocarbons may be unstable with respect to dissociation into a monomer triplet and a monomer ground state (87).

The possibility that the long wavelength emission from m-methoxyacetophenone is due to an excimer is therefore not remote, but it is unprecedented. The possibility of excimer emission from the other sensitizers that showed a concentration dependence was also investigated. Other similar concentration ranges, all the other sensitizers exhibited no shift in the wavelength maximum of their phosphorescence emission, excluding the possibility of excimer formation.

Excimer formation in the sensitizer would provide the inverse dependence of quantum yield on sensitizer concentration required by the experimental data. In view of the tenuous assignment of triplet excimer formation, an alternate, but equally acceptable, explanation would be concentration dependent triplet quenching by ground state sensitizers to two vibrationally excited ground state molecules. These two possibilities are expressed in equations 14 and 15 below.

$$^{3}S + S_o \xrightarrow{k_t} {}^{3}(S_2) \longrightarrow 2\ S_o \qquad (14)$$

$$^{3}S + S_o \xrightarrow{k_t} 2\ S_o \qquad (15)$$

Either possibility is, in essence, simply a mechanism for self-quenching and either one provides the necessary kinetic explanation of the data. Inclusion of either expression in the basic mechanism of Figure 9 leads to the kinetic expressions shown in equations 16 and 17. The relationship

$$\phi_{sens} = \varphi' \quad \frac{k_s k_r [K]}{(k_d' + k_r)(k_{ds} + k_s[K] + k_t[S]} \qquad (16)$$

$$\frac{\phi_o}{\phi_{sens}} = \frac{\varphi}{\varphi'} \quad \frac{k_{ds} + k_s[K] + k_t[S]}{k_s[K]} \qquad (17)$$

φ= intersystem crossing efficiency of 4,4-dimethyl-2-cyclohexenone

φ'= intersystem crossing efficiency of the sensitizer

in equation 17 predicts that a plot of ϕ_o/ϕ_{sens} versus sensitizer concentration should be linear. Plots of this type for thioxanthone, 3,4-methylenedioxyacetophenone, m-methoxyacetophenone, and p-methoxyacetophenone are shown in Figure 11 and give a consistent fit to this mechanism. Acetophenone and benzophenone show a very minor concentration dependence over a similar range. This variation lies within the range of experimental error and may not be a real effect. The assumption is made, therefore, that the concentration effects are pronounced when the aromatic ketones have lowest triplet states which are predominantly π,π^* in nature. While there is no published evidence that the triplet state of thioxanthone is π,π^*, the phosphorescence emission spectrum in EPA is structureless and the molecule is unreactive in

Figure 10. Phosphorescence emission spectra of m-methoxyacetophenone as a function of concentration (EPA glass, 77° K)

— — — — 10^{-5} M

———————— 10^{-4} M

——·····——·——·· 10^{-3} M

------------ 10^{-2} M

······························ 10^{-1} M

—·—·—·—·— 1 M

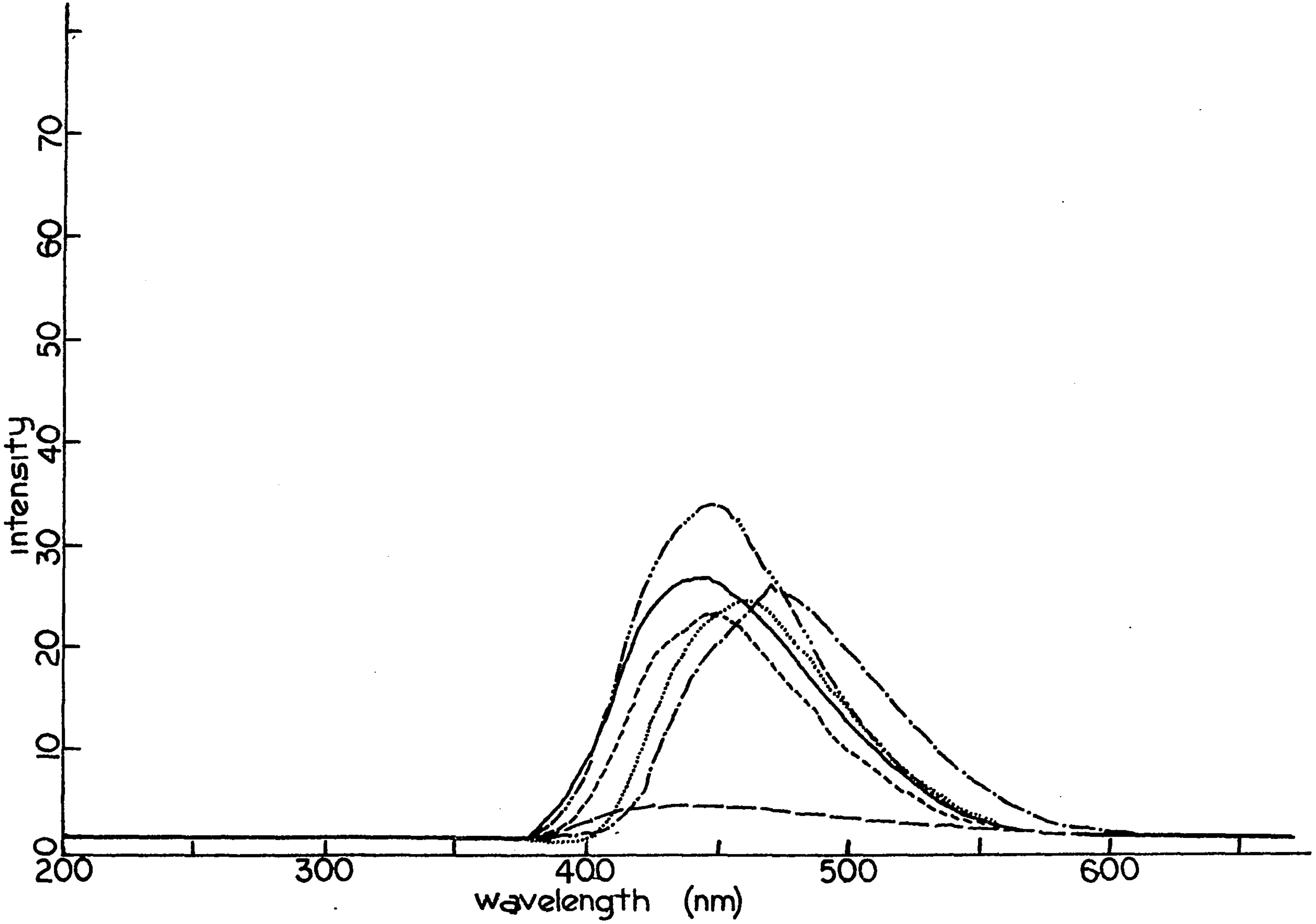
intensity
0
10
20
30
40
50
60
70
200
300
400
500
600
wavelength (nm)

Figure 11. Plot of ϕ_o/ϕ_{sens} versus sensitizer concentration for thioxanthone, 3,4-methylenedioxyacetophenone, *m*-methoxyacetophenone, and *p*-methoxyacetophenone sensitization of rearrangement

□ - *p*-methoxyacetophenone; slope = 0.30 ± 0.05 l./mole
intercept = 0.97 ± 0.04

Δ - *m*-methoxyacetophenone; slope = 2.11 ± 0.03 l./mole
intercept = 0.98 ± 0.02

◇ - 3,4-methylenedioxyacetophenone; slope = 9.45 ± 0.90 l./mole
intercept = 1.15 ± 0.10

* - thioxanthone; slope = 220 ± 2.3 l./mole
intercept = 0.99 ± 0.01

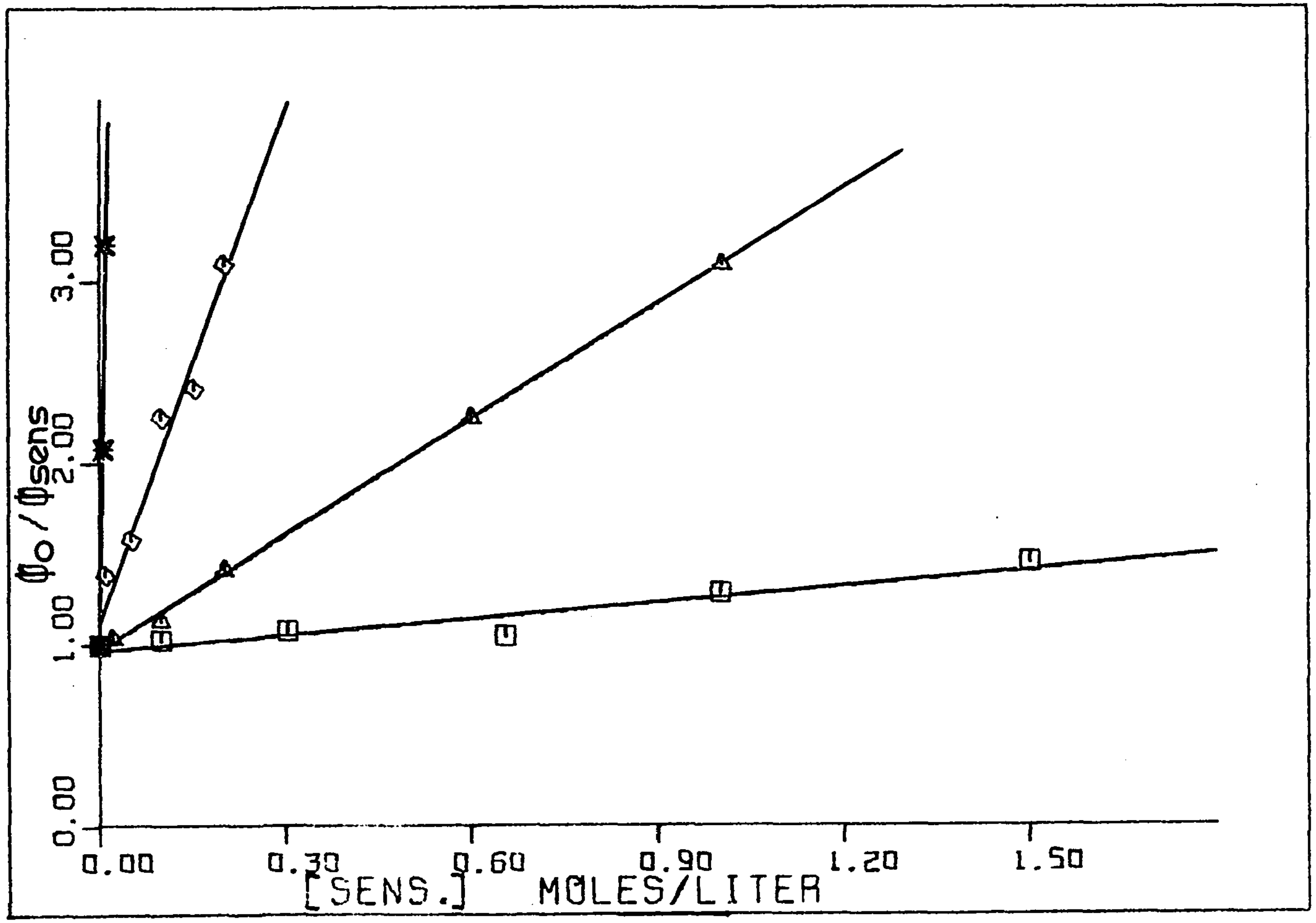

ϕo / ϕsens
0.00
1.00
2.00
3.00
0.00
0.30
0.60
0.90
1.20
1.50
[SENS.] MOLES/LITER

photoreduction, both of which are characteristic of $^3(\pi,\pi^*)$ states. The maximum quantum yield for the photoreduction of thioxanthone in isopropyl alcohol is 0.005 which is comparable to the value for other compounds having π,π^* states.

If one assumes that the ratio of the intersystem crossing efficiencies of 4,4-dimethyl-2-cyclohexenone and sensitizer is unity, then the slope of the plots in Figure 11 is given by $k_t/k_s[K]$. From the measured intersystem crossing efficiencies (vide infra), this assumption is plausible and introduces little error. Assuming a diffusion controlled rate constant for k_s for energy transfer from the sensitizer to the enone, it is possible to obtain approximate values for k_t, the rate constant for reaction of the ground state and triplet state sensitizer. Using a value of 1.91 centipoises for the viscosity of t-butyl alcohol at 43° (57), a value of 3.7×10^9 l./mole/sec is calculated for k_s from the standard Debye equation. Using this value and the slopes of the plots in Figure 11, values for k_t were calculated and are shown in Table 4. The intercepts of the plots in Figure 11 are given by $(1 + k_{ds}/k_s[K])$. The fact that the intercepts of the plots are very nearly 1.0 indicates that k_{ds}, the rate constant for decay of the triplet sensitizer, is almost negligible compared to k_s, the rate constant for energy transfer to the enone. Alternatively, the small variance from 1.0 could result from the ratio of intersystem crossing

Table 4. Approximate values of k_t

Sensitizer	k_t $M^{-1}sec^{-1}$
p-Methoxyacetophenone	1.1×10^8
m-Methoxyacetophenone	7.7×10^8
3,4-Methylenedioxyacetophenone	3.5×10^9
Thioxanthone	8.1×10^{10}

efficiencies not being exactly unity.

The concentration dependence of energy transfer is seen from Table 4 to be due to competition between the ground state sensitizer and the enone triplet for the sensitizer triplet. When the rate constant k_t is large, there is a large concentration effect due to this self-quenching effect which competes with energy transfer to the enone. If an excimer is actually formed as an intermediate, it does not transfer energy to the enone, probably because its triplet energy is lowered. For example, the 40 nm shift observed for m-methoxyacetophenone results in a decrease in the triplet energy of almost 6 kcal/mole. If a lowering of similar magnitude occurs in the triplet energy of thioxanthone and 3,4-methylenedioxyacetophenone, this could cause energy transfer from these sensitizers to become endothermic.

It is interesting to note two correlations which these results present. The first is that the degree of concentration dependence of each sensitizer (as measured by the slopes of the plots in Figure 11 or by the values of k_t in Table 4) follows the trend of decreasing reactivity in photoreduction and increasing triplet lifetime, as shown in Table 3. It is possible that excimer formation or sensitizer self-quenching could also be a factor in both reactivity and lifetime of ketone triplet states. The second correlation is that the degree of concentration dependence of each sensitizer increases as the triplet energy gap between the sensitizer and the enone decreases. This observation lends some support to an excimer mechanism in which the triplet energy of the sensitizer is lowered sufficiently by complex formation to cause energy transfer to approach endothermic conditions, resulting in the observed concentration dependence.

A third mechanism must be considered that can explain the observed concentration dependence of sensitization. If ground state sensitizer can act to quench triplet state sensitizer by either excimer formation or triplet annihilation, it is not unreasonable to consider also the possibility of ground state sensitizer quenching the triplet state cyclohexenone. There are two mechanisms by which the sensitizer might accomplish this. The first mechanism, shown in equation 18, is reversible energy transfer between the

$$^3K + S \xrightarrow{k_{-s}} K + {}^3S \tag{18}$$

sensitizer and the cyclohexenone and would be expected to occur only if the triplet energy gap between the sensitizer and the cyclohexenone was reasonably small. Sandross has shown that triplet energy transfer can be reversible if the excitation energies of donor and acceptor are similar (89). Such a situation is unlikely in this case since the recipient triplet state of the cyclohexenone is located near 61 kcal/mole. The above mechanism would obtain if the recipient triplet state were higher in energy, near 70 kcal/mole. In such a case, energy transfer from the sensitizers that have been studied to 4,4-dimethyl-2-cyclohexenone would be nearly isothermal, and reversible energy transfer would be possible. Although the detection of triplet states near 70 kcal/mole in rigid cyclohexenone systems (see Review of Literature) lends credence to this possibility, it is unlikely that simple cyclohexenones, such as 4,4-dimethyl-2-cyclohexenone, have a triplet state lying at this higher energy which is the recipient state in energy transfer experiments, but is undetected by spectroscopic or quenching studies because of the lower triplet state which is involved in such processes.

The second possible mechanism is shown in equation 19.

$$^3K + S \xrightarrow{k_{-S}} K^v + S^v \qquad (19)$$

This process involves quenching of the triplet state by the ground state sensitizer to give vibrationally excited ground states of the sensitizer and the ketone. A singlet-state reaction analogous to equation 19 which involves the possibility of a singlet exciplex intermediate has recently been reported (90). This quenching mechanism is very similar to the earlier proposed sensitizer self-quenching mechanism; the variation in the two is the proposed exciplex rather than excimer intermediate.

The triplet mechanism for rearrangement of Figure 9 that is inclusive of either process shown in equation 18 or 19 gives a rather complex expression for the sensitized quantum yield. The expressions for the two are listed below in equation 20 for the reversible energy transfer mechanism and in equation 21 for the sensitizer ground state quenching mechanism. The important feature of these two relationships, which are quite

$$\frac{\Phi_o}{\Phi_{sens}} = \frac{\varphi_{ic}}{\varphi_{ic'}}\left[1 + \frac{k_d'k_{ds} + k_r k_{ds} + k_{ds}k_{-s}[S]}{k_r k_s[K] + k_d'k_s[K]}\right] \tag{20}$$

$$\frac{\Phi_o}{\Phi_{sens}} \quad \frac{\varphi_{ic}}{\varphi_{ic'}}\left[1 + \frac{k_d'k_{ds} + k_r k_{ds} + k_{ds}k_{-s}[S] + k_s k_{-s}[S][K]}{k_r k_s[K] + k_d'k_s[K]}\right] \tag{21}$$

similar, is the appearance of the sensitizer concentration dependence term in each expression which satisfies the observed linear relation. Unfortunately, because of the complexity of these equations, it is impossible to obtain any rate constants from analysis of the plots in Figure 11 according to either mechanism.

Although either mechanism appears to account kinetically for the observed concentration dependence, they both have factors which decrease their importance in the present system. The reversible energy transfer mechanism shows the correct trend in the correlation between the triplet energy of the sensitizer and the extent of the concentration dependence, a relationship that was discussed earlier. As the triplet energy of the sensitizer decreases, reversible energy transfer is able to become more predominant, and the extent of effective energy transfer to the substrate decreases, thus lowering the quantum yield. However, because of the low triplet energy of 4,4-dimethyl-2-cyclohexenone, reversible energy transfer from all of the sensitizers that were used is relatively unimportant. The reversible energy transfer step would be 5-10 kcal/mole endothermic and the rates for such a transfer are 10^6 times slower than diffusion controlled (55). Despite the unimportance of this mechanism in the present system, reversible energy transfer has been postulated in several other photochemical studies (81, 82, 83, 91). It appears that this mechanism may be a common phenomenon in photochemical systems where the energy requirements can be met.

The mechanism expressed by equation 19 in which the ground state sensitizer quenches the triplet enone also fails to explain the correlation noted above. This mechanism would predict that all sensitizers, including those with $^3(n,\pi^*)$ states, should have equal efficiencies in quenching the reaction, unless a certain spatial overlap or interaction is required in the quenching process. Because of the rapid rates of energy transfer, such an interaction is unlikely. The more reasonable explanation of the sensitizer concentration effects remains the sensitizer self-quenching mechanism proposed first.

The possibility of sensitizer concentration effects have been rather generally neglected in studies of photosensitization. Since sensitizer concentrations are usually chosen on the basis of light absorption considerations, there are numerous cases of sensitization with high concentrations of the sensitizer being used, which may have led to erroneous conclusions when little or no sensitization was observed.

Several other studies have noted sensitizer concentration effects. In his studies of the sensitization of the photocyclization of α-(N-methylanilino)styrene to 1-methyl-2-phenyl-2,3-dihydroindole, Eian (92) noted sensitizer concentration effects with xanthone and Michler's Ketone. In both cases, increasing the sensitizer concentration caused a decrease in the quantum yield of cyclization. The effect was attributed to self-quenching of the sensitizer triplet state.

In his studies of the photosensitized dimerization of indene, DeBoer (81) noted that the quantum yield of dimer formation decreased with increasing concentrations of sensitizers when they had triplet energies lower than that of indene (59 kcal/mole). With sensitizers of greater energy than this, the quantum yield of dimerization was invariant with sensitizer concentration. These results were explained on the basis of a reversible energy transfer mechanism as expressed by equation 18.

In 1964, Hammond and coworkers (93) studied the sensitized *cis*-*trans* isomerization of a number of olefins in solution. Large sensitizer concentration effects were noted on the photostationary state ratios, which Hammond attributed to reversible energy transfer between the sensitizer and the olefin. In at least one case, increasing the concentration of the sensitizer caused a decrease in the quantum yield of isomerization. The variation was attributed to small variations in the efficiency of the intersystem crossing efficiency of the sensitizer. In general, the concentration of the sensitizer was believed to have no effect on the efficiency of energy transfer or on any other photophysical processes, and the effect was not investigated further.

In view of the fact that sensitizer concentration effects have not been extensively studied, yet appear to be evident in several photochemical systems, this phenomenon was subjected to further study. The system chosen for a test model in this case was the sensitized isomerization of olefins. There were several reasons for this selection. First, it involved a substrate other than a ketone, which could show that the effect is not peculiar to the interaction of only ketones with one another. Second, sensitizer concentration effects have been shown to occur in this reaction, but have not been fully pursued. Since the mechanism of *cis*-*trans* olefin isomerization has been investigated in detail, this eliminated the disadvantage of working with a test reaction whose mechanistic steps are unclear. An important reason for choosing this reaction as a test system however, is that it is a common method of measuring intersystem crossing inefficiencies of sensitizers (94). It was thought that if sensitizer concentration effects were noted, they may have effected the determination of valid values for intersystem crossing efficiencies in the past.

The basic mechanism of the sensitized isomerization of olefins (94) is shown in Figure 12 for the case in which the reaction is carried out with the pure *trans* isomer and no *cis* isomer is present.

$$S \xrightarrow{h\nu} {}^1S$$

$${}^1S \xrightarrow{k_2} S$$

$${}^1S \xrightarrow{k_3} {}^3S$$

$${}^3S \xrightarrow{k_4} S$$

$${}^3S + O_t \xrightarrow{k_5} S + {}^3O$$

$${}^3O \xrightarrow{k_6} O_c$$

$${}^3O \xrightarrow{k_7} O_t$$

S = sensitizer
O_t = *trans*-olefin
O_c = *cis*-olefin

Figure 12. A mechanism for the sensitized *cis*-*trans* isomerization of olefins

Assuming a steady-state concentration for all excited states, the following expression is derived for the quantum yield of *trans* to *cis* isomerization:

$$\phi_{t\rightarrow c} = \varphi_{ic}\,\frac{k_6}{k_6 + k_7}\quad\frac{k_5[O_t]}{k_4 + k_5[O_t]} \tag{22}$$

Equation 22 can be simplified further by using a sufficiently high concentration of olefin substrate to render nonradiative decay of the sensitizer triplets negligible (*i.e.*, $k_4 \ll k_5$). Experimentally, the presumption that k_4 is negligible can be demonstrated by showing that the quantum yield is independent of the olefin concentration in the region of use. Under such conditions equation 22 simplifies to equation 23 and the intersystem crossing efficiency is given by equation 24, where $\underline{x} = k_7/k_6$. The value of $\underline{x}$ can be determined

$$\phi_{t\rightarrow c} = \varphi_{ic} \frac{k_6}{k_6 + k_7} \qquad (23)$$

$$\varphi_{ic} = \phi_{t\rightarrow c} \; (1 + \underline{x}) \qquad (24)$$

experimentally. If sensitizers of very high energies are used, then the rate of energy transfer to the trans-olefin and to any cis-olefin that forms during the irradiation are both diffusion controlled and therefore equal. The composition of the olefin after the photostationary state has been reached is thus dependent only on the decay ratios k_6 and k_7. That is, at the photostationary state, $[\underline{\text{trans}}]_{ss}/[\underline{\text{cis}}]_{ss} = k_7/k_6$. The measurement of this substrate decay ratio can be determined simply by measuring the photostationary state ratio using a high energy sensitizer.

In order to achieve good analytical accuracy, it is necessary to effect conversions to a high enough percentage so that some energy transfer does occur to the cis-olefin molecules that are formed. This results in a lowering of the quantum yield which is proportional to the percent conversion. Correction of the raw data to obtain values of initial quantum yields are therefore made by using a form of the integrated rate law for approach of a system to the stationary state. This correction is given by equation 25, where β is conversion (trans $\longrightarrow$ cis) without back reaction, α is the conversion at the photostationary state, and β' is

$$\beta = 2.30\alpha \log\left[\alpha/(\alpha-\beta')\right] \qquad (25)$$

the conversion measured experimentally. Using this technique and starting with a pure isomer of one of several olefins, Lamola and Hammond measured intersystem crossing efficiencies of a number of compounds, several of which are listed in column 1 of Table 5. In all cases, Hammond used the lowest concentrations of sensitizer necessary to give complete absorption of light, and no sensitizer concentration effects were studied.

The olefin chosen for the present studies was β-methylstyrene, E_t (trans) = 59.8 (94). The pure trans isomer was obtained by preparative v.p.c., and all analyses were performed starting with this isomer. Sensitization of a 1:1 isomer mixture of cis- and trans-β-methylstyrene with two high energy sensitizers (acetophenone and p-methoxyacetophenone) to the photostationary state gave an average value of $[\text{trans}]_{ss}/[\text{cis}]_{ss}$ of 0.93 which is in agreement with the

Table 5. Intersystem crossing efficiencies

Compound	φ_{ic}[a]	φ_{ic}[b]
Acetophenone	1.00	1.00
2-Acetonaphthone	0.84	
Benzophenone	1.00	1.00
Fluorenone	0.93	
3,4-Methylenedioxyacetophenone		0.84
m-Methoxyacetophenone		0.84
Michler's Ketone	1.00	1.00
Naphthalene	0.39	0.39
Thioxanthone		0.98

[a] Data taken from reference (94)

[b] Data taken from the Experimental section at lowest sensitizer concentrations

value of 0.96 measured by Lamola and Hammond (94).

An initial measurement was made using 0.10 M olefin and 0.05 M benzophenone. The measured quantum yield for the isomerization was 0.51. Using equation 24 and a value of 0.96 for x, φ_{ic} for benzophenone was calculated to be 1.00, in agreement with determinations by others. A value of 0.10 M β-methylstyrene is therefore sufficiently high to trap all sensitizer triplets and k_4 can be considered negligible.

Intersystem crossing efficiencies were measured for a number of sensitizers as a function of their concentration. The results of these studies are tabulated in Tables 19 to 25. In all cases, the values that were measured at lowest sensitizer concentrations were in complete agreement with previously measured values of the compounds that had been studied. The values of the intersystem crossing efficiencies obtained at the lowest concentration for each compound studied are shown in column 2 of Table 5.

Acetophenone, Michler's Ketone, m-methoxyacetophenone, thioxanthone, and benzophenone all exhibited definite concentration effects of the type exhibited previously; that is, an increase in their concentration caused a decrease in the quantum yield of isomerization. Within experimental error, naphthalene showed no concentration dependence over a tenfold concentration range. The results with 3,4-methylenedioxyacetophenone are not at all obvious. The variations noted in the quantum yield with increasing concentration are small and almost within experimental error of each other.

The results show that concentration effects are not limited to aromatic ketones having $^3(\pi,\pi^*)$ states, since both acetophenone and benzophenone, having $^3(n,\pi^*)$ states show rather extensive concentration dependence. On the basis of these experiments, it is not possible to report that aromatic hydrocarbons do not show sensitizer concentration effects.

It has recently been demonstrated that olefins at high concentrations efficiently quench the singlet states of aromatic hydrocarbons (95). If the olefin is quenching the singlet state of naphthalene before it can intersystem cross, no concentration effects would be noted. While that effect is probably not occurring here because of the low olefin concentration used, it does place a question of the validity of intersystem crossing efficiencies of aromatic hydrocarbons measured by this method. Several other methods of measuring intersystem crossing efficiencies have resulted in different values for naphthalene, centered about 0.7 (96, 97, 98).

The observed concentration dependence can be accounted for by the self-quenching mechanism proposed earlier. Inclusion of either equation 14 or 15 in the basic mechanism of Figure 12 gives an expression for the quantum yield of isomerization which includes a sensitizer concentration dependence:

$$\phi = \varphi_{ic} \frac{k_6}{k_6 + k_7} \quad \frac{k_s[O_t]}{k_s[O_t] + k_t[S]} \tag{26}$$

This expression can be rewritten to show a linear dependence of $1/\phi$ and $[S]$,

$$\frac{1}{\phi} = \frac{(1 + \underline{x})}{\varphi_{ic}} \left(1 + \frac{k_t[S]}{k_s[O_t]} \right) \tag{27}$$

Linear plots of $1/\phi$ versus $[S]$ are shown for acetophenone and m-methoxyacetophenone in Figure 13, for Michler's Ketone in Figure 14, and for benzophenone in Figure 15. The plot for Michler's Ketone is expressed in a log-log manner because of the wide range of sensitizer concentrations used. A more extensive plot of the benzophenone concentration shown in Figure 16 exhibits a strange deviation from linearity at high concentrations. The reason for this curvature is not known.

According to equation 27, the intercept of these plots in Figures 13-15 is given by $(1 + \underline{x})/\varphi_{ic}$. From the intercepts of the plots and a value of 0.96 for $\underline{x}$, φ_{ic} is determined to be 0.98 for acetophenone, 0.85 for m-methoxyacetophenone, 0.94 for Michler's Ketone, and 1.01 for benzophenone. These values are in reasonable accord with those in Table 5, in support of the mechanism.

Values for k_t can be obtained from the slopes of these plots. The slope, as given by equation 27 is equal to $\left|(1 + \underline{x})/\varphi_{ic}\right|\left|k_t/k_5[O_t]\right|$. If k_5 is taken as a diffusion controlled rate constant ($\eta = 0.60$ centipoise, $k_{diff} = 1.1 \times 10^{10}$ M^{-1} sec^{-1} at 25° in benzene), the values of k_t calculated from the slopes are: 1.5×10^{8} M^{-1} sec^{-1} for acetophenone, 2.7×10^{8} M^{-1} sec^{-1} for m-methoxyacetophenone, 6.6×10^{8} M^{-1} sec^{-1} for Michler's Ketone, and 4.9×10^{8} M^{-1} sec^{-1} for benzophenone. These values are comparable to those measured for k_t in the rearrangement reaction.

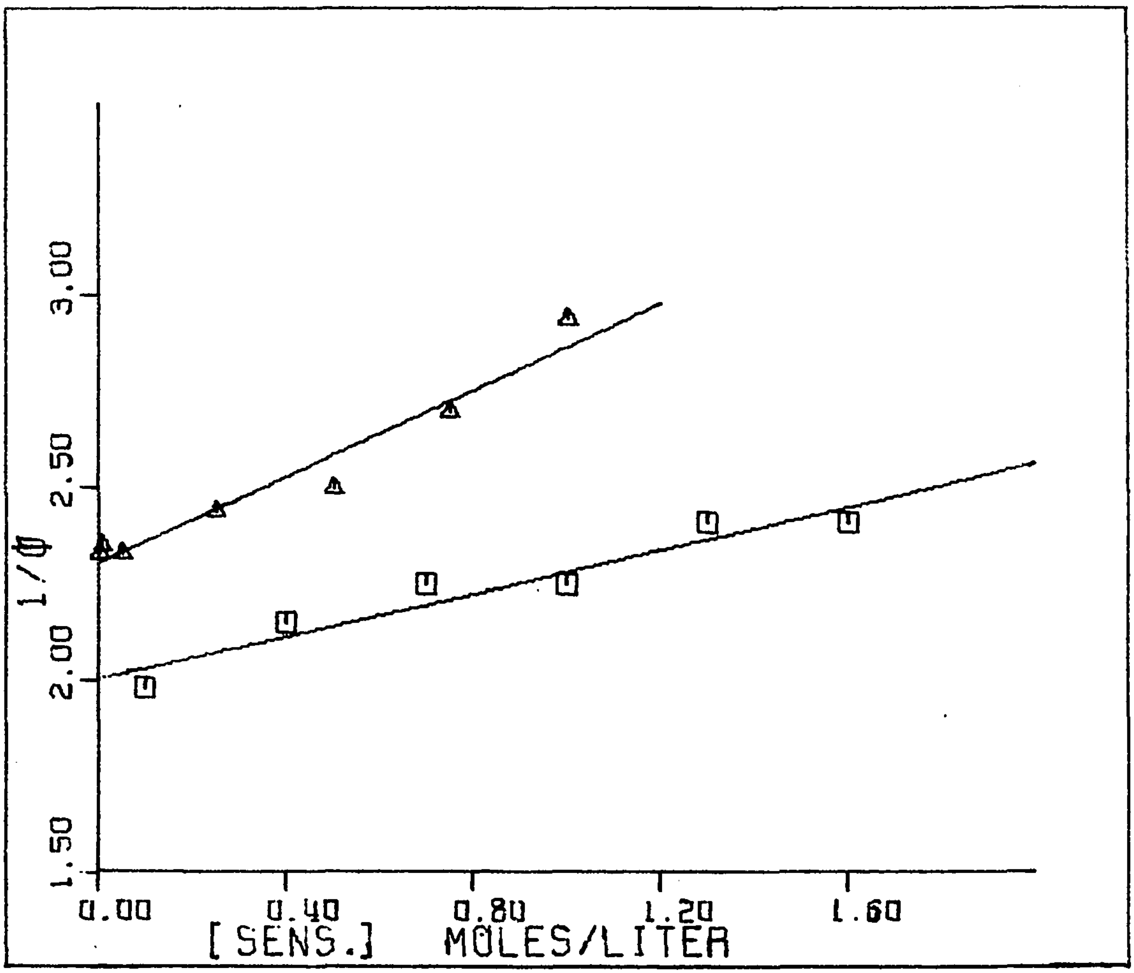

Figure 13. Plot of reciprocal of quantum yield of isomerization of trans-β-methylstyrene versus sensitizer concentration for acetophenone and m-methoxyacetophenone

□ - acetophenone; slope = 0.28 ± 0.04 l./mole
intercept = 2.00 ± 0.04

Δ - m-methoxyacetophenone; slope = 0.56 ± 0.06 l./mole
intercept = 2.30 ± 0.03

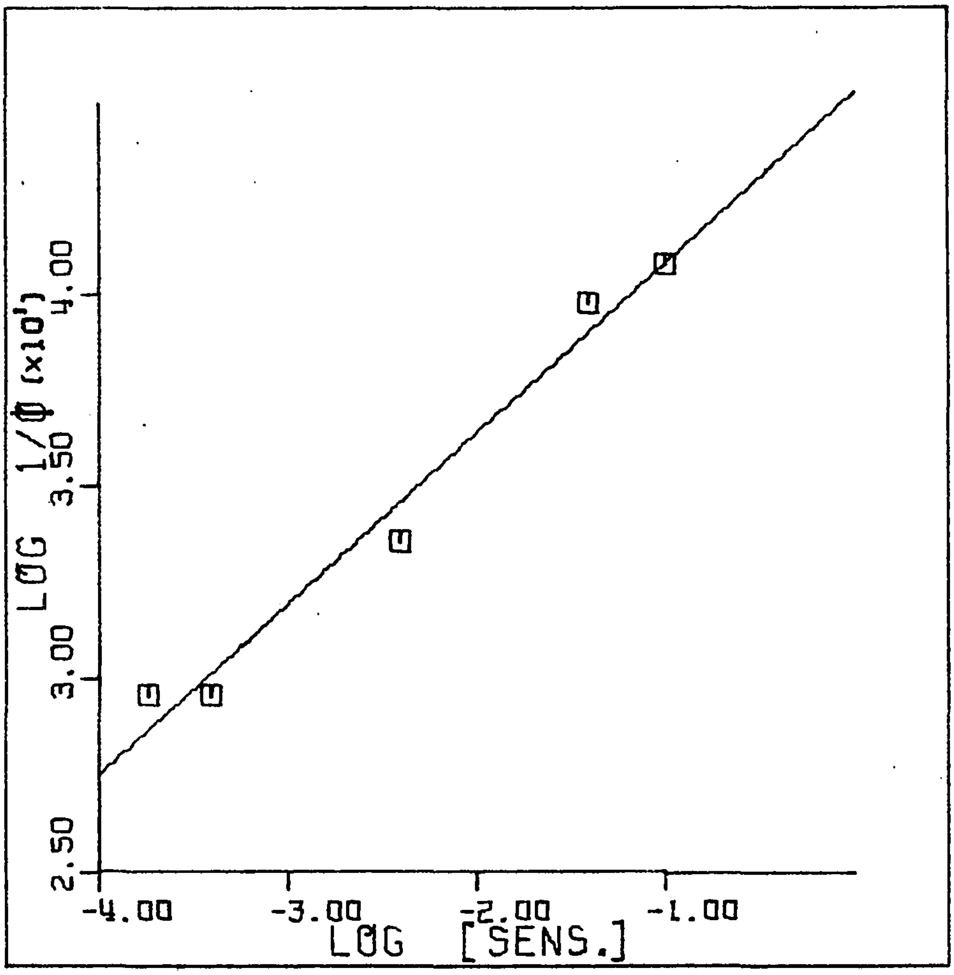

Figure 14. Plot of logarithm of reciprocal of quantum yield of isomerization of <u>trans</u>-β-methylstyrene versus logarithm of sensitizer concentration for Michler's Ketone

slope = 0.044 ± 0.004
intercept = 0.45 ± 0.01

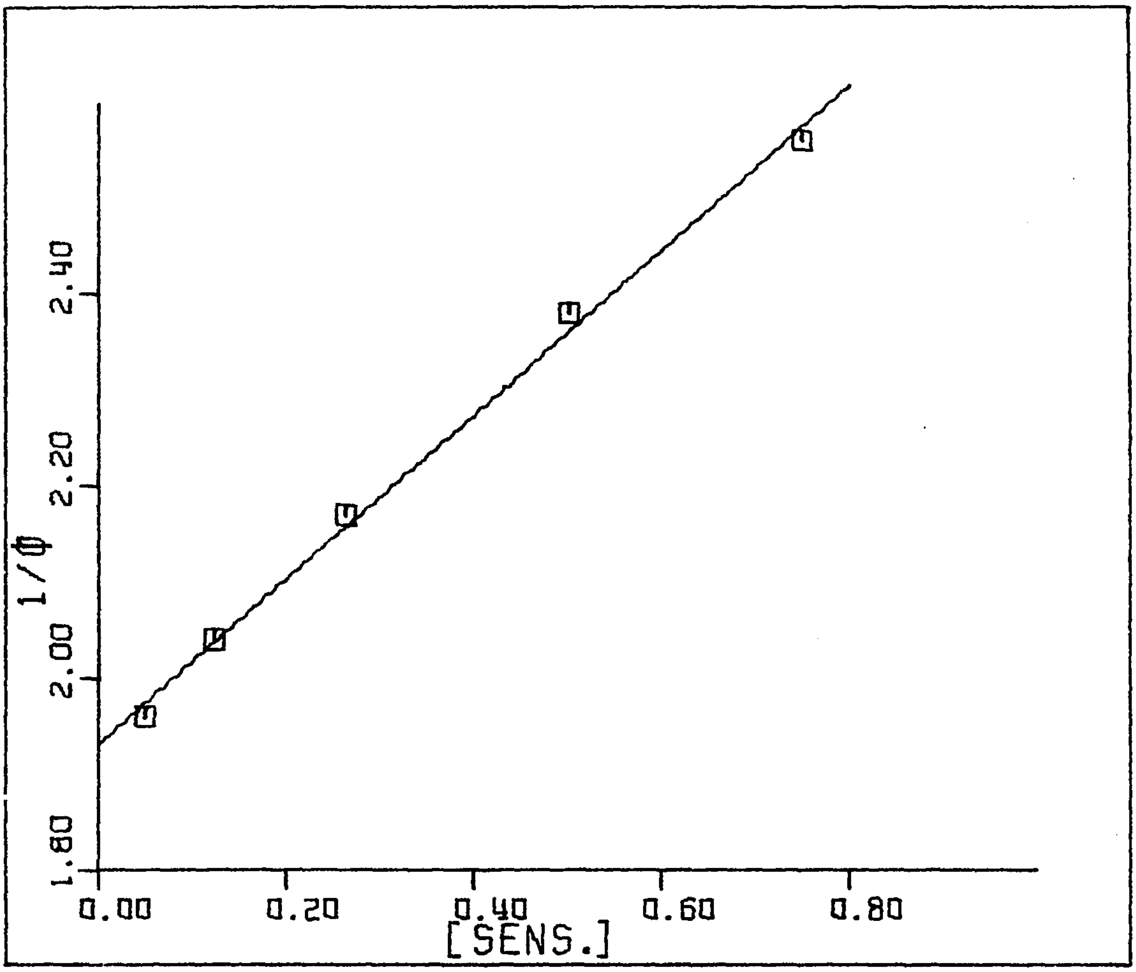

Figure 15. Plot of reciprocal of quantum yield of isomerization of trans-β-methylstyrene versus sensitizer concentration for benzophenone at low concentrations

slope = 0.86 ± 0.03 l./mole
intercept = 1.93 ± 0.01

Figure 16. Plot of reciprocal of quantum yield of isomerization of trans-β-methylstyrene versus sensitizer concentration for benzophenone at high concentrations

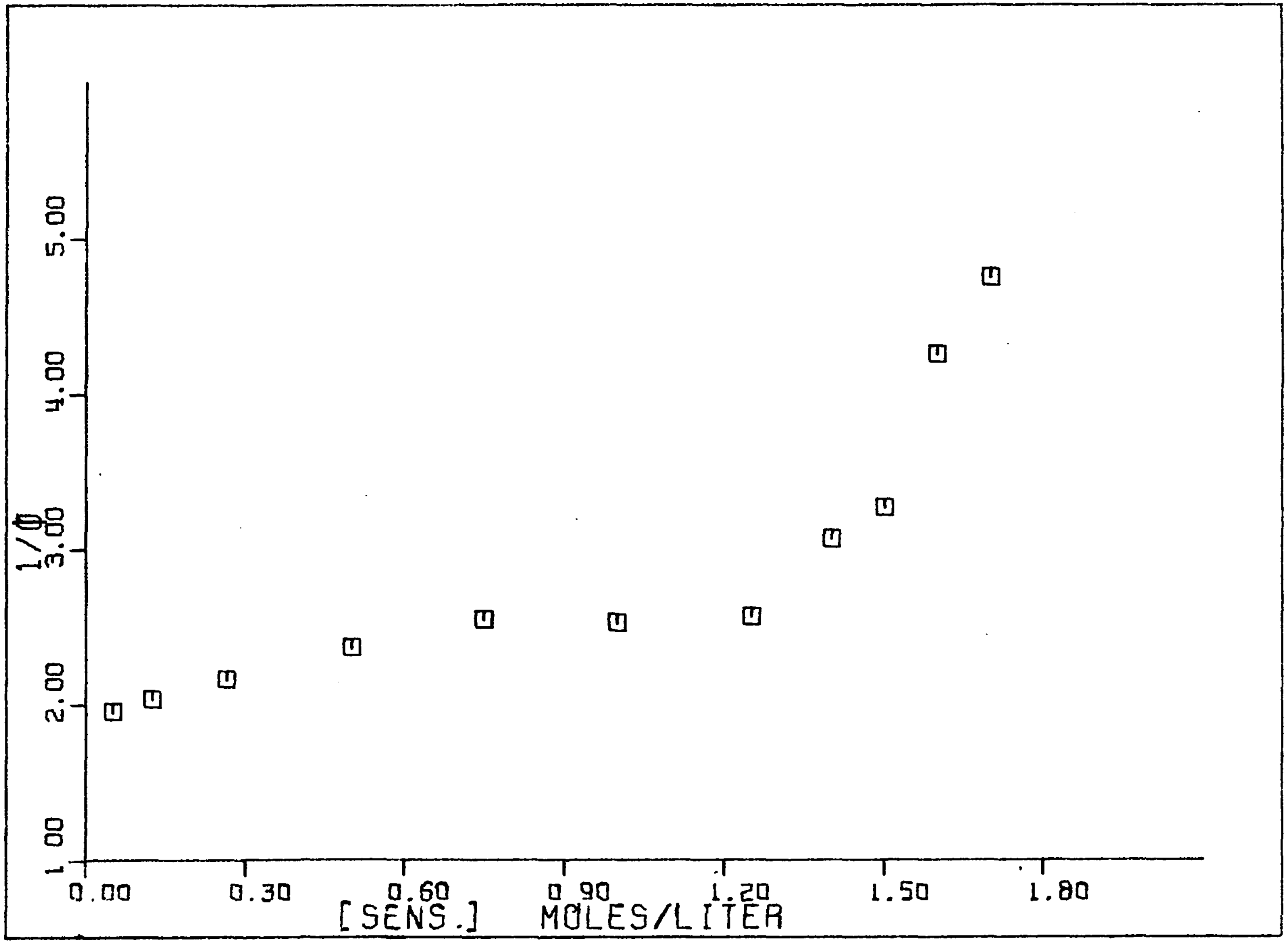
1.00
2.00
3.00
4.00
5.00
1/Φ
0.00
0.30
0.60
0.90
1.20
1.50
1.80
[SENS.] MOLES/LITER

This mechanism predicts that in the absence of a sensitizer concentration effect, the quantum yield of isomerization should be independent of olefin concentration as long as the concentration is high enough to render triplet decay (k_4) negligible. This prediction was confirmed by varying the olefin concentration from 0.10 M to 0.50 using benzophenone sensitization. The olefin concentration is sufficiently high in this case to ensure no triplet decay. A benzophenone concentration of 0.05 M was used, since at this concentration benzophenone exhibits no self-quenching effects. As the data in Table 26 indicates, the quantum yield of isomerization is constant (0.51 ± 0.01) over this range of olefin concentration.

In the presence of sensitizer self-quenching, equation 27 predicts that there should be a linear relationship between $1/\phi$ and $1/[O]$. This relationship was confirmed by varying the olefin concentration over the range previously used (0.10 to 0.50) at a benzophenone concentration of 0.50 M. At such a concentration, benzophenone exhibits self-quenching effects as shown in the plot of Figure 15. The linear plot of the data is shown in Figure 17. According to equation 27, the intercept of this line is given by $(1 + \underline{x})/\phi_{ic}$. The value obtained for the intercept of this plot (1.87) is in good agreement with the value obtained from the benzophenone plot in Figure 15 (1.93). The slope of the plot in Figure 15 is given by $\left((1 + \underline{x})/\varphi_{ic}\right)\left(k_t[S]/k_5\right)$. Assuming that k_5 is the same diffusion controlled rate constant as used previously, the slope of this line gives a value of 6.0×10^8 M^{-1} sec^{-1} for k_t, comparable to 4.9×10^8 M^{-1} sec^{-1} for k_t obtained from the benzophenone plot in Figure 15.

From a comparison of the rate constants k_t for the various quenchers in the two test systems, it appears that the rate of self-quenching of a sensitizer is independent of the system in which it is employed and dependent on the structure of the sensitizer. The high rate constants measured for this effect show the importance of this phenomenon in limiting energy transfer to a substrate when self-quenching competes. In cases where the substrate concentration is low and the sensitizer concentration is high, inefficient sensitization may appear as a manifestation of this effect, and the results should be interpreted accordingly.

The observed concentration dependence cannot be accounted for by either reversible energy transfer between the sensitizer and olefin or by quenching of the olefin triplet by the sensitizer ground state in this case. Both mechanisms must be represented by two equations since the olefin triplet can return to either the cis or the trans ground states. Inclusion of either set of reactions in equations 28 or 29 into the basic mechanism of Figure 12 leads to complex expressions for the quantum yield of isomerization. Both

$$\begin{aligned} {}^3O + S &\xrightarrow{k_8} O_t + S^3 \\ {}^3O + S &\xrightarrow{k_8} O_c + S^3 \end{aligned} \tag{28}$$

reversible energy transfer

$$\begin{aligned} {}^3O + S &\xrightarrow{k_8} O_t^v + S^v \\ {}^3O + S &\xrightarrow{k_8} O_c^v + S^v \end{aligned} \tag{29}$$

sensitizer quenching

expressions contain terms for sensitizer concentration in the numerator and the denominator since the sensitizer is directly involved in a product forming step. It is clear that neither expression will yield the experimentally observed linear relationship between $1/\phi$ and $[S]$. The complex expressions can be simplified considerably by assuming that k_4 is negligible compared to k_5, as done previously. This assumption was shown to be tenable by the absence of an increase in the quantum yield of isomerization as the olefin concentration was increased, showing that all or nearly all of the sensitizer triplets were being captured by the olefin. Although this experimental verification was carried out at low sensitizer concentration, it will hold also at higher concentrations. The rate of deactivation of the triplet state sensitizer does not depend on ground state sensitizer concentration as long as all of the light is being absorbed. Assuming that $k_4 << k_5$, the expression for the reversible energy transfer mechanism reduces to that given in equation 30 and for the sensitizer quenching mechanism to that given in equation 31. Equation 30 predicts a relationship between

$$\phi = \varphi_{ic} \frac{k_6 + k_8 [S]}{k_6 + k_7} \qquad (30)$$

$$\phi = \varphi_{ic} \left(1 + \frac{k_7 + k_8 [S]}{k_6 + k_8 [S]} \right) \qquad (31)$$

the quantum yield and the sensitizer concentration which is the inverse of that noted experimentally, and this mechanism fails to account for the experimental data. Equation 31 predicts a non-linear relationship between the quantum yield and the sensitizer concentration, and the experimental data also fails to account for the observed relationship. Actually, equation 31 can be reduced even further. From photostationary state measurements, $k_7 \cong k_6$; equation 31, to a first approximation, reduces to $\phi = 2\varphi_{ic}$, and indicates no sensitizer concentration dependence.

Of the mechanisms that have been considered to account for sensitizer concentration effects in this thesis, only the sensitizer self-quenching mechanism involving interaction of ground state and excited state sensitizer molecules is consistent with both systems studied. The mechanisms involving reversible energy transfer between substrate and sensitizer or sensitizer quenching of substrate excited states are not totally successful in explaining inefficient sensitization. In other systems where these mechanisms have been postulated, the sensitizer self-quenching mechanism often also explains the data, and at this point, it seems to be the more reliable explanation for inefficiencies in energy transfer.

In addition to the sensitizer concentration effects noted here, several other unusual effects have been observed in sensitized olefin isomerization studies, which complicate the measurement of quantum yields of isomerization. It has been recently reported that the use of high concentrations (1 M to 10 M) of piperylene in triplet counting experiments causes an increase of almost two-fold in the quantum yield of isomerization (99). The plot of ϕ versus [*cis*-piperylene] is linear up to 10 M olefin. The basic mechanism of Figure 12 satisfactorily accounts for the data at olefin concentrations below 1.0 M. A new process is postulated to be taking over at olefin concentrations greater than 1.0 M which involves reaction of the triplet piperylene with its ground state by two possible mechanisms (equations 32 and 33). Both of these reactions result in isomerization enhancement involving a triplet state and a ground state molecule of the olefin. However, these two reactions do not account kinetically for the experimental data. The investigators state that inclusion of equations 32 and 33 into the mechanistic scheme of Figure 12 (except for a change in this case to *cis* → *trans*

$$^3P + \underline{cis}\text{-}P \xrightarrow{k_a} \underline{trans}\text{-}P + {}^3P \tag{32}$$

$$^3P + \underline{cis}\text{-}P \xrightarrow{k_b} \begin{bmatrix}\text{diradical addition to} \\ \text{ground state}\end{bmatrix} \longrightarrow \begin{matrix}\alpha\ \underline{cis}\text{-}P\ + \\ (2-\alpha)\underline{trans}\text{-}P \\ (\alpha < 1)\end{matrix} \tag{33}$$

isomerization) leads to the relationship shown in equation 34. The details of their derivation of this expression are not known. However, the usual kinetic development using Steady-State concentrations for all excited states leads to the

$$\phi = \varphi_{ic}\left(\frac{k_7 + (k_a + k_b)\left[O_c\right]}{k_7}\right) \tag{34}$$

$$\phi = \varphi_{ic}\left(\frac{k_7 + (k_a + k_b)\left[O_c\right]}{k_6 + k_7 + k_b\left[O_c\right]}\right) \tag{35}$$

relationship shown in equation 35. This expression does not show the linear relationship between ϕ and $\left[O_c\right]$ that was found experimentally. Contrary to the investigator's conclusion, equations 32 and 33 together cannot explain the enhancement of isomerization at high olefin concentrations. Equation 33 alone also fails in this respect, giving an expression for the quantum yield of isomerization similar to that in equation 35. If only equation 32 is included in the mechanism, the expression in equation 36 is derived. The desired linear relationship is present in this expression,

$$\phi = \varphi_{ic} \left(\frac{k_7 + k_a [O_c]}{k_6 + k_7} \right) \qquad (36)$$

and it appears that the reaction of a triplet olefin molecule with its ground state given by equation 32 may be an important step in solution at high concentrations.

These results reveal there is a real disadvantage in carrying out triplet counting experiments by using very high concentrations of the substrate. These observations are also pertinent to the present work in that evidence is presented for the reaction of a ground state molecule with its triplet state in solution to provide complicating and unexpected effects in the reaction. Although the kinetic analysis rules out a reaction of the type shown in equation 33, there is recent evidence that points to a similar diradical or Schenck type (100) intermediate in the sensitized isomerization of nonaromatic olefins (101). The use of simple alkenes in triplet counting experiments could thus lead to further complicating effects and incorrect values for φ_{ic}.

The use of olefins that contain small amounts of impurities in isomerization experiments may lead to abnormally high quantum yields for isomerization. An investigation by Hammond and coworkers (102) of the benzophenone sensitized isomerization of 2,4-hexadiene was carried out in an attempt to infer if the preferred configuration of the lowest lying triplet state of the diene is in the form of a 1,4-radical or an allyl-methylene system. Measurement of the quantum yields of isomerization with increasing concentrations of the diene (0.005 M to 1.00 M) resulted in large increases in the total quantum yield of isomerization (up to ~72) which were indicative of a quantum-chain mechanism. Hammond believed that the chain-carrying species was an electronically excited state of the diene. A reinvestigation of this experiment has shown, however, that the chain-carrier is actually an impurity in the diene (103). When carefully purified diene was used, the previously observed concentration dependence disappeared.

Results that are similar to this have been observed in this work in the triplet counting experiments using trans-β-methylstyrene that was not purified prior to use. A chromatographic analysis of this impure sample of olefin indicated that several impurities in less than 1% total were present. When this impure sample was used in triplet counting experiments with benzophenone sensitization, the results shown in Table 27 were obtained. An increase in the olefin concentration from 0.10 M to 1.50 M caused an increase in the quantum yield from 0.37 to 3.13, clearly evident of a quantum chain process. Previous experiments have shown that the use of the pure olefin in the concentration range of 0.10 M to 0.50 M results in only a slight increase in the quantum yield (Table 26). The effect can be attributed to an impurity chain-carrier in the olefin sample, and may be illustrated by a reaction of the type shown in equation 37, where I is the impurity chain carrier. The exact nature of the chain

$$I + O_t \xrightarrow{k_i} I + O_c \qquad (37)$$

carrier is not known. It may be generated photochemically and be an excited state species, or it may be a ground state radical system which can effect isomerization by adding to the olefin and then dissociating after isomerization has occurred.

Inclusion of a reaction of the type shown in equation 37 in the mechanism of Figure 12 leads to the expression given in equation 38, which specifies a concentration dependence on

$$\phi = \frac{\varphi_{ic}}{(1+\underline{x})} + k_i[I][O_t] \qquad (38)$$

both the olefin and the impurity. Since the ratio of the concentrations of these two components is constant in the various samples, the concentration dependence should manifest itself in the form of a linear relationship between the quantum yield and $[O]^2$. A plot of the data in this form bears out this relationship (see Figure 18) and supports the impurity chain-carrier mechanism first noted by Hammond.

It is apparent, therefore, that there are many undesirable side effects that can be encountered in this method of measuring intersystem crossing efficiencies, and that valid results will be obtained only if the problems are recognized and the proper precautions are taken in the experimental procedure to avoid them.

The same method of triplet counting was also used to measure the intersystem crossing efficiences of isophorone and 4,4-dimethyl-2-cyclohexenone. The olefin that was used in these cases was α-methylstilbene since it has a lower triplet energy (E_t (trans) = 50) (94) ensuring exothermic energy transfer from these enones. An initial experiment using 0.05 M olefin and 0.05 M benzophenone gave a value of 0.565 for the quantum yield of isomerization. Using the steady-state ratio of 0.81 for x (94), an intersystem crossing efficiency of 1.0 was determined for benzophenone, indicating that the olefin concentration was high enough to intercept all of the sensitizer triplets.

Using the same procedure, an intersystem crossing efficiency of 0.89 was measured for isophorone. This high value is in accord with those measured for other cycloalkenones (9, 35, 104). With the same olefin concentration, however, a very low intersystem crossing efficiency was measured for 4,4-dimethyl-2-cyclohexenone ($\varphi_{ic} = 0.30$). This low value suggested that the olefin concentration was not sufficiently high enough to capture all of the enone triplets. A problem of this type is not without precedent. deMayo et al. (104) using the same method to measure the intersystem crossing efficiency of 2-cyclohexenone, found that no upper limit of olefin concentration could be found to capture all of the cyclohexenone triplets. Whenever the olefin concentration was increased, a corresponding increase in the quantum yield of isomerization was noted. The same situation was confirmed in this case by raising the olefin concentration. When this was done, the quantum yield for isomerization also increased (see Table 28). In such a case, the only kinetic expression that represents the data is given by equation 22. If this equation is rearranged to the form shown in equation 39, it is apparent that a plot

$$\frac{1}{\phi} = \frac{1 + \underline{x}}{\varphi_{ic}}\left(1 + \frac{k_4}{k_5[O_t]}\right) \tag{39}$$

of $1/\phi$ versus $1/[O]$ should be linear and the intersystem crossing efficiency available from the intercept. The data of Table 28 does give a linear plot as shown in Figure 19. The large units of the ordinate axis make an accurate value of the intercept difficult to measure. The problem is

Figure 17. Plot of reciprocal of quantum yield of isomerization of *trans*-β-methylstyrene versus reciprocal of olefin concentration

slope = 0.051 ± 0.004 M
intercept = 1.87 ± 0.02

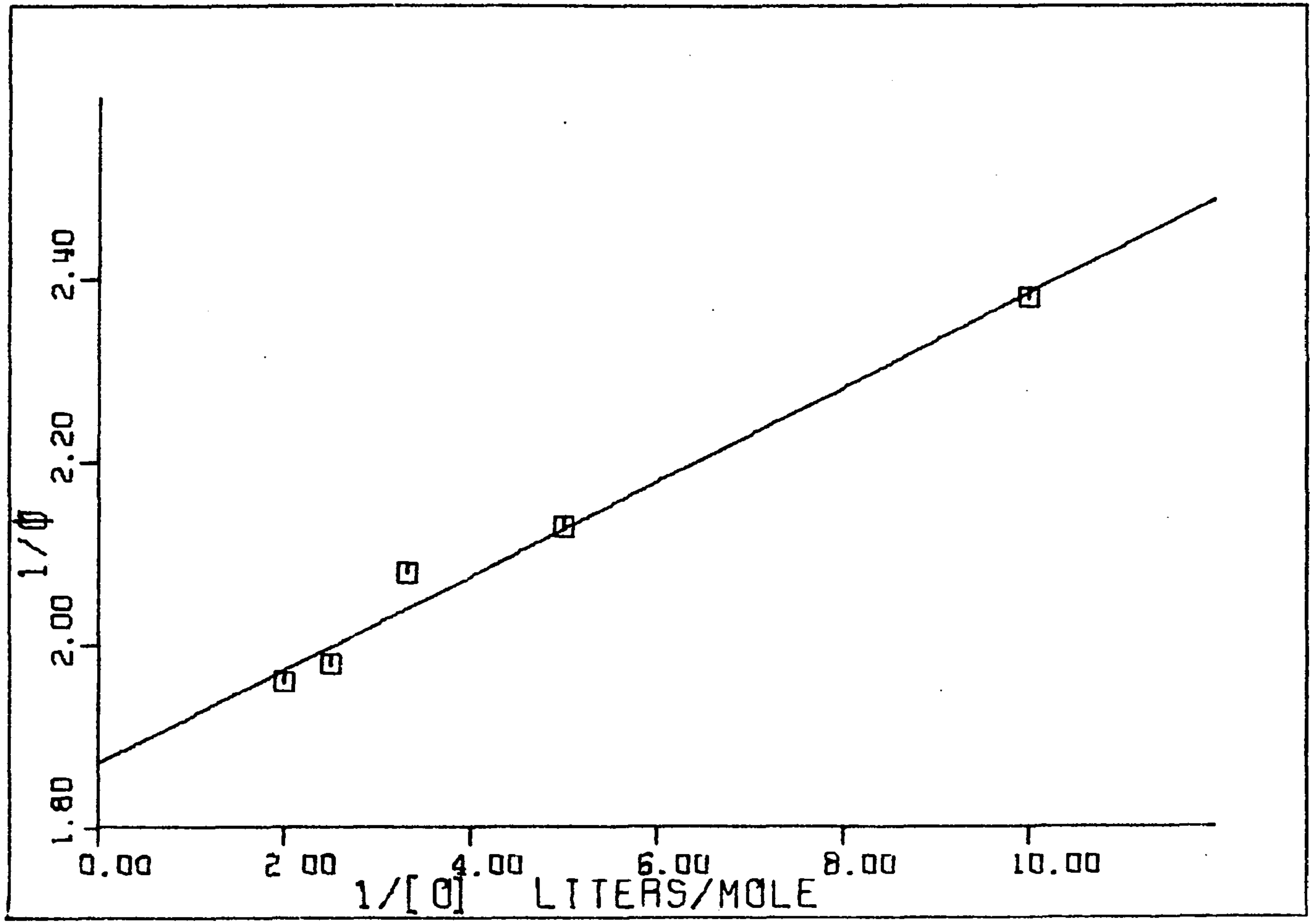
1.80
2.00
2.20
2.40
1/Φ
0.00
2.00
4.00
6.00
8.00
10.00
1/[O] LITERS/MOLE

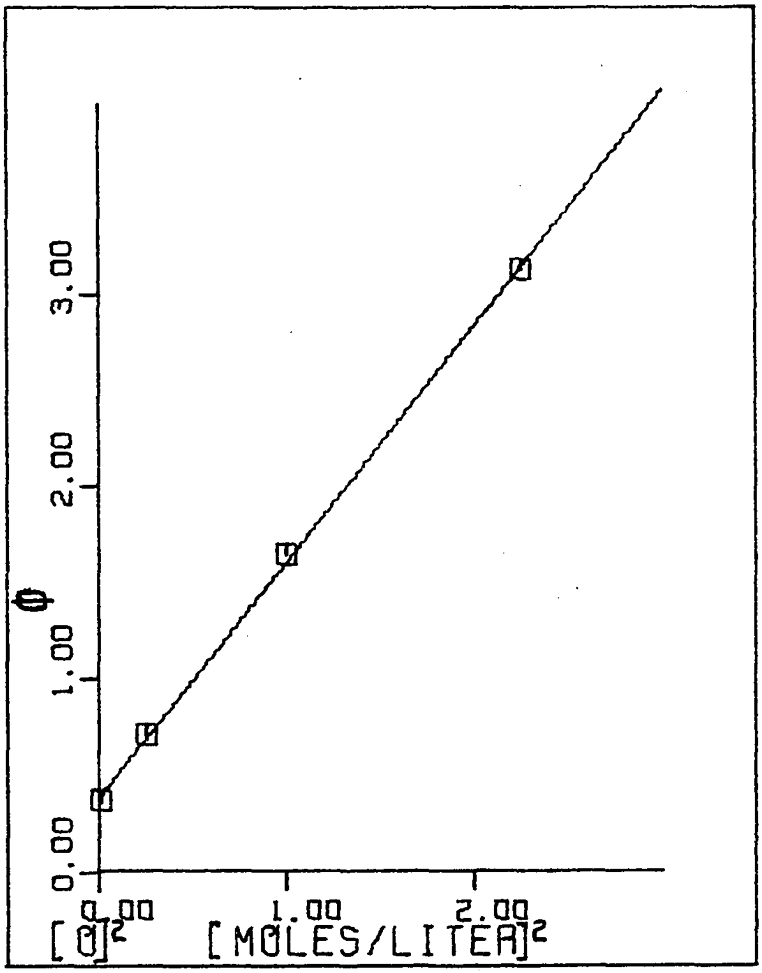

Figure 18. Plot of quantum yield of isomerization of <u>trans</u>-β-methylstyrene versus square of the concentration of impure olefin

slope = 1.23 ± 0.02 (l./mole)^2

Figure 19. Plot of reciprocal of quantum yield of isomerization of *trans*-α-methylstilbene versus reciprocal of concentration of 4,4-dimethyl-2-cyclohexenone

slope = 0.50 ± 0.003 M
intercept = 1.13 ± 0.13

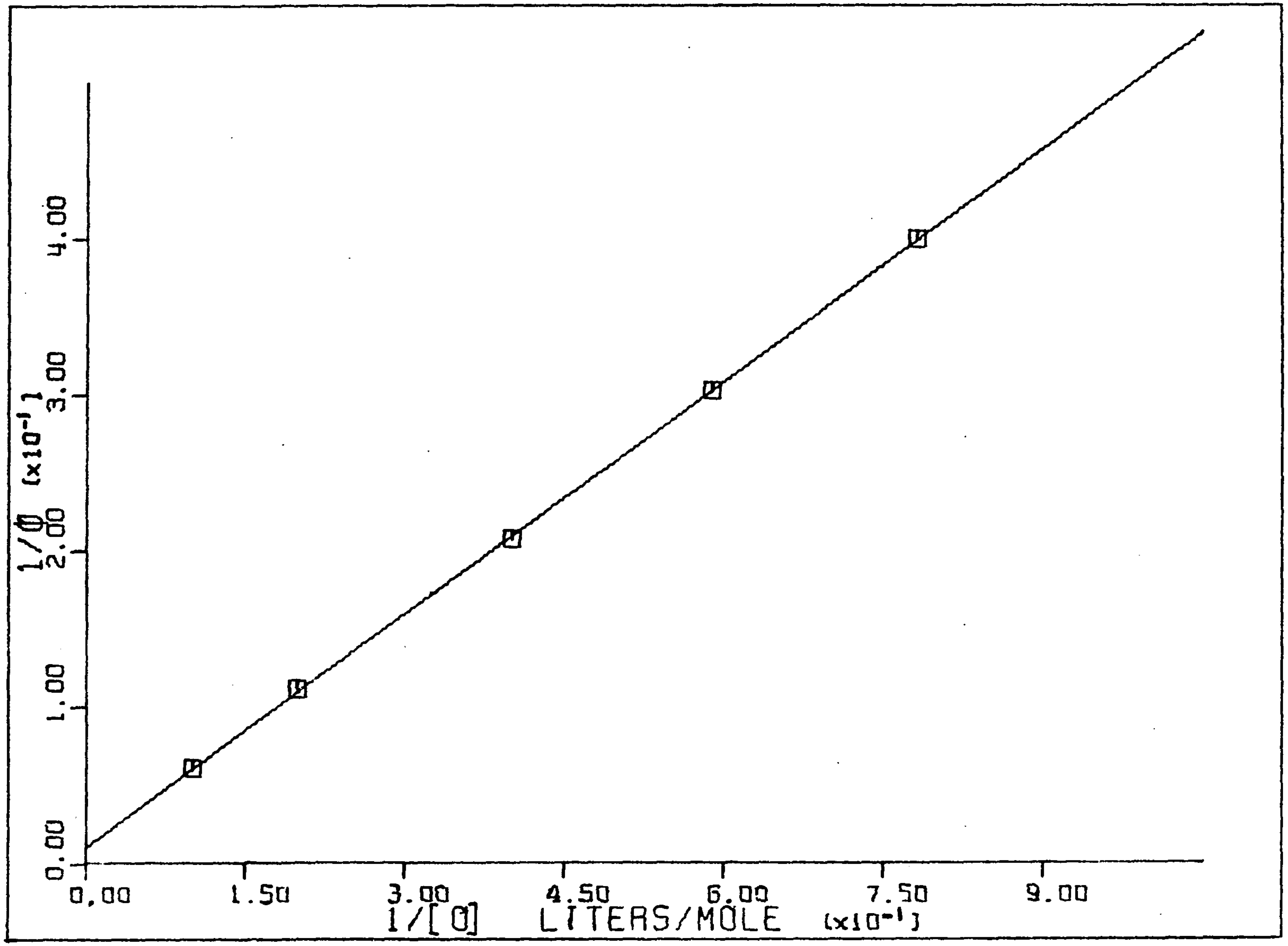
1/Φ (x10⁻¹)
0.00
1.00
2.00
3.00
4.00
0.00
1.50
3.00
4.50
6.00
7.50
9.00
1/[Q] LITERS/MOLE (x10⁻¹)

compounded by the fact that the quantum yields at the higher olefin concentrations must be corrected for light absorption by the olefin, and these corrections have a pronounced effect on the intercept. The corrected plot of Figure 19 has an intercept of 1.13 ± 0.13. Using a value of 0.81 for x, the value calculated for φ_{ic} is 1.62 ± 0.19. The large value obtained is due, in part, to the approximate corrections made to the data. In fact, the uncorrected data gives a value of 1.1 ± 0.1 for φ_{ic}, so the corrections may not be valid. The large value is also due to the wide range of the ordinate axis values, which make a number near 1.0 difficult to determine accurately. In any case, it seems certain that the intersystem crossing efficiency is near unity in accordance with that measured for other cycloalkenones. This means that the observed ineffiencies in the photoreactions of cyclohexenones derives mainly from processes that occur after the triplet state has been reached.

Like the rearrangement, this inefficiency is also demonstrated in the photoreduction of 4,4-dimethyl-2-cyclohexenone. In isopropyl alcohol, the quantum yield for photoreduction is 3.7×10^{-3} and that for rearrangement is 1.5×10^{-2}. Reduction product 4 comprises 20% of the product mixture.

The triplet nature of the photoreduction was established by sensitization using sensitizers whose triplet states are

π,π^* in nature and therefore not susceptible to reduction. Both m-methoxyacetophenone and p-methoxyacetophenone gave ϕ_{sens}/ϕ_o ratios near unity for rearrangement and near 0.75 for reduction (see Table 32). Less efficient sensitization was achieved with 3,4-methylenedioxyacetophenone and thioxanthone. There are no obvious reasons for the lower efficiency of sensitization using the latter two compounds. Both have triplet energies which are reasonably above that of the enone. If the energy levels of the sensitizers and the enone are shifted slightly closer to each other in isopropyl alcohol from that which they were in t-butyl alcohol, then energy transfer could become less exothermic and less efficient, but this should not reduce the efficiency of sensitization to the extent that is found. Both sensitizers have strong concentration effects, but at the concentrations used, self-quenching of these sensitizers should be no more serious than it was in sensitizing the rearrangement.

The mechanism of the photoreduction is best pictured as proceeding through several distinct steps in a short radical chain process, initiated by the $^3(n,\pi^*)$ state of the enone (equation 40). In this excited state, the oxygen atom of the enone moiety is electron deficient and is able to abstract a hydrogen atom from the solvent. The reduction is completed by abstraction of a second hydrogen atom with the concurrent formation of acetone.

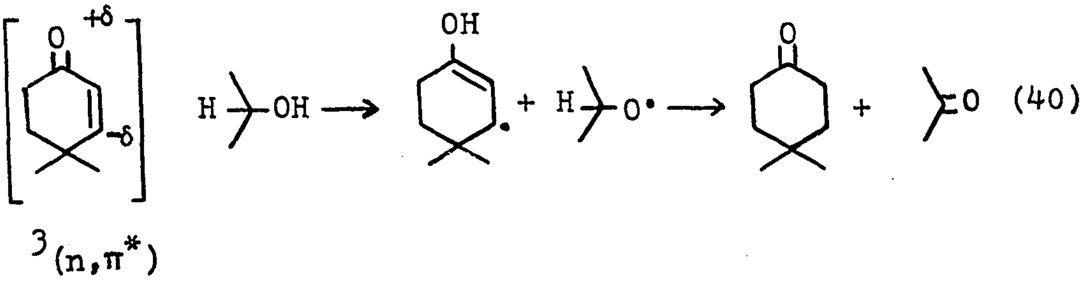

The photoreduction could also take place by the formation of an intermediate pinacol which cleaves to give the reduction product and the starting material, as shown in equation 41.

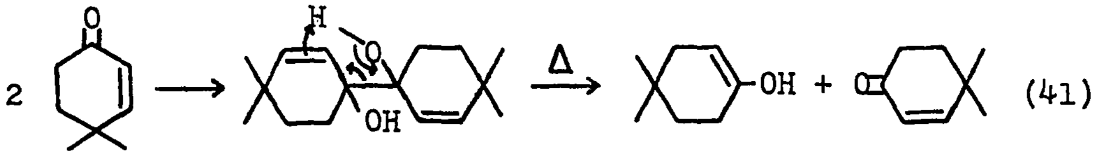

37

A preparative reaction demonstrated that the dl and meso pinacols 37 are formed in the photoreduction reaction, along with dimers of 4,4-dimethyl-2-cyclohexenone. These pinacols are stable under the analytical procedures used for the measurement of quantum yields, and they pass through the column and detector of the gas chromatograph without cleavage to the cyclohexanone. Because the photoreduction reaction was carried to only several percent completion for the measurement of quantum yields, and because the pinacols have very low extinction coefficients, it is not possible that the small amount of pinacols that were formed could absorb enough light to photochemically cleave to the cyclohexanone. This reaction can therefore be dismissed in contributing to the photoreduction process.

Di-t-butyl nitroxide quenches both the rearrangement and the reduction. An unusual effect is noted in the quenching of the reduction, as shown in the Stern-Volmer plot of Figure 20. Up to concentrations of 0.015 M, the nitroxide enhances the quantum yield for photoreduction. Above this concentration, it begins quenching in a Stern-Volmer manner. This observed "sensitization" is not due to a reaction between the excited nitroxide molecules and the enone. If the irradiation is carried out in such a manner that the nitroxide is absorbing all of the light, no reaction of the 4,4-dimethyl-2-cyclohexenone occurs. In the samples containing the low concentrations of nitroxide, which cause the anomalous enhancement of the reaction, the nitroxide is completely destroyed during the course of the irradiation. This finding is in contrast to the reported photostability of di-t-butyl nitroxide in hexane solution (2). A reasonable conclusion is that the nitroxide reacts with and destroys some unknown triplet quencher of the reduction that is present in low concentration in the solution. This unknown triplet quencher must be present in every sample (including those that do not contain the nitroxide) for its absence to cause an enhancement of the quantum yield. The most likely possibility for this unknown quencher is oxygen, which is still present to a small degree in all of the degassed samples. In scavenging the oxygen, the nitroxide is consumed, and the photoreduction is in turn no longer quenched by this trace of oxygen, causing the observed enhancement. At higher concentrations of di-t-butyl nitroxide, the quenching effect of the nitroxide overcomes the enhancement effect caused by the absence of traces of oxygen. The result is a linear Stern-Volmer quenching plot.

This type of oxygen (or unknown quencher) scavenging by di-t-butyl nitroxide has been found in other systems. The phosphorescence emission spectra of acetone, biacetyl, benzil, and benzophenone in carefully degassed solvent are enhanced by the addition of small amounts of di-t-butyl nitroxide, but are quenched at higher concentrations of the nitroxide (105). It was found that the scavenging effect must be initiated photochemically, but that it can proceed in the dark after initiation. The effect is attributed to nitroxide scavenging of oxygen or some other unknown triplet quencher which is still present in the samples in small amounts after degassing.

Di-t-butyl nitroxide has been used in the past as a successful triplet quencher (5, 19, 21, 42). It has also been shown to be an effective singlet quencher (54, 106). The low concentrations of nitroxide used in this study preclude the possibility of any singlet quenching. Little is known about the mechanism by which nitroxides quench excited states. It has been determined that quenching occurs only when the energy transfer is exothermic and that such quenching is diffusion controlled (54). The unpaired spin apparently has little to do with the quenching process.

In view of the radical nature of the photoreduction, several irradiations were carried out in the presence of well known radical trapping agents in order to determine their effect on the reaction. Irradiation in the presence of thiophenol resulted in an enhancement of the quantum yield for photoreduction (4.9×10^{-3}) and in a decrease of the quantum yield for rearrangement (1.1×10^{-2}). Thiophenol probably enhances the photoreduction by acting as a readily available hydrogen atom source and by being a good chain carrier of the radical species; thus, the following steps could be involved in the presence of thiophenol:

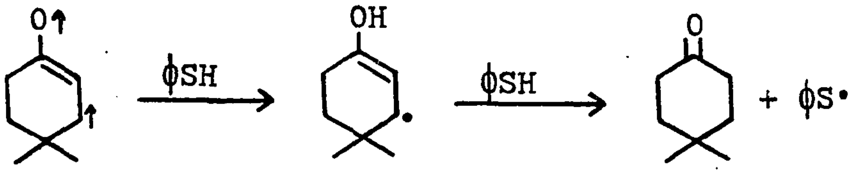

$$\phi S\cdot + \phi S\cdot \longrightarrow \phi SS\phi$$

Since the rearrangement and the reduction probably have a common precursor, they are competitive reactions, and the decrease in the rearrangement may be a result of the enhancement of the reduction. This cannot be the sole cause, however, since the efficiency of rearrangement decreases more than the reduction increases. Thiophenol must therefore either inhibit directly the formation of the diradical species responsible for rearrangement or cause this species to revert to ground state enone instead of rearranging. A more dramatic illustration of this inhibition of rearrangement is shown by hydroquinone. Hydroquinone is an effective radical trapping agent in that it donates a hydrogen atom to the radical and ultimately forms benzoquinone which is stable. When the irradiation is carried out with varying amounts of hydroquinone present, there is a very slight quenching effect on the quantum effect on the rearrangement. The amount of inhibition of the rearrangement is directly proportional to the amount of hydroquinone present, as the plot in Figure 22 illustrates.

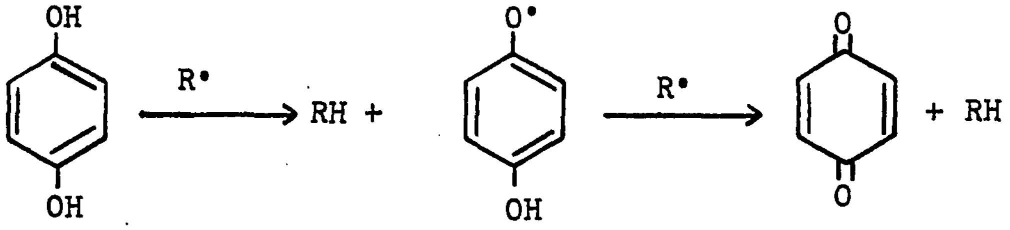

The fact that hydroquinone has little effect on the photoreduction must mean that hydroquinone and isopropyl alcohol have similar efficiencies in donating hydrogen atoms to the enone. Hydroquinone is not an effective chain carrier because of its strong drive to release a second hydrogen atom to give a

Figure 20. Stern-Volmer plot for quenching reduction and rearrangement by di-t-butyl nitroxide in isopropyl alcohol

□ - reduction; slope = 22500 ± 767 l./mole
intercept = 291

Δ - rearrangement; slope = 2194 ± 79 l./mole
intercept = 63.7 ± 3.0

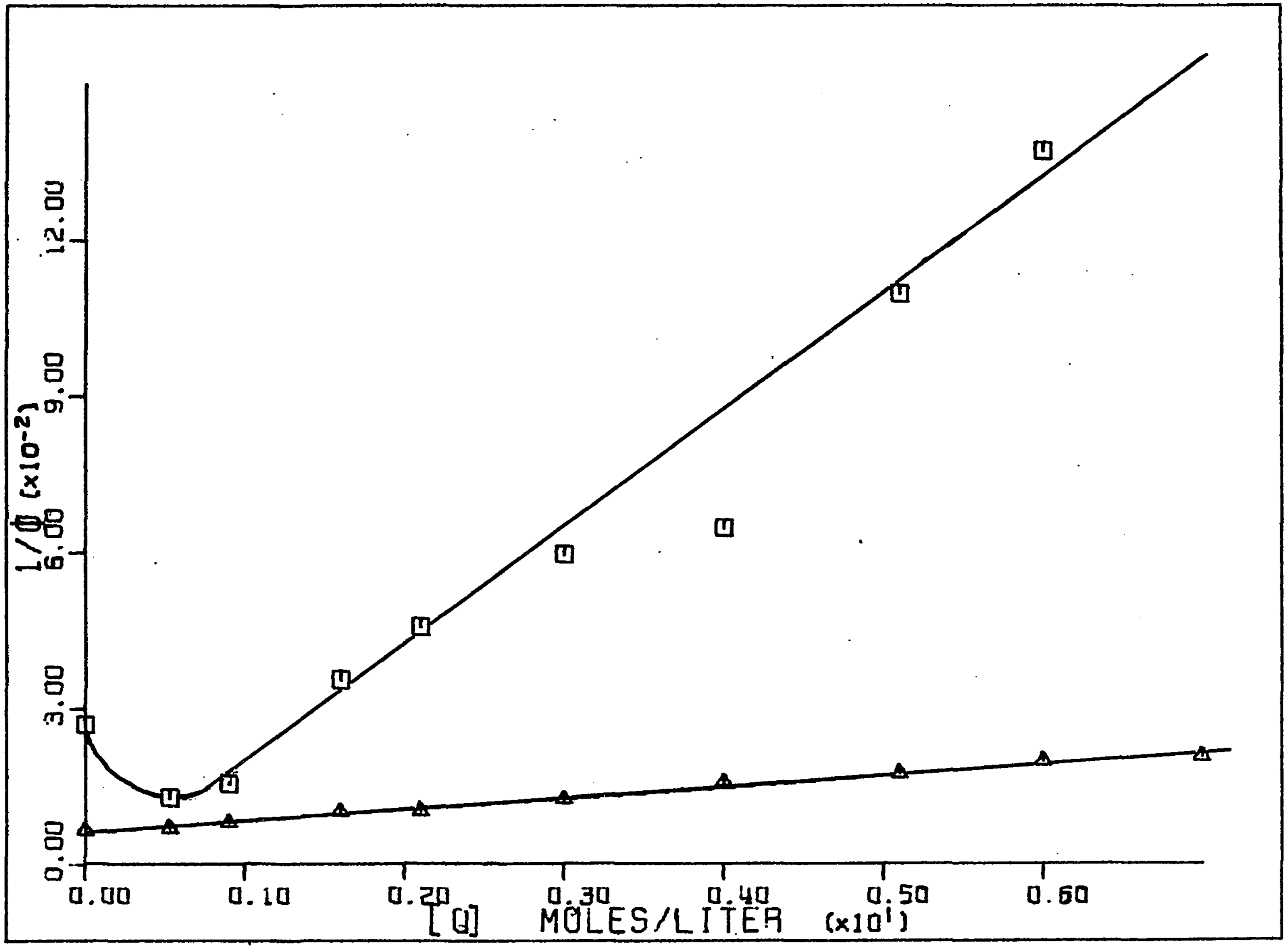
1/Φ (x10⁻²)
12.00
9.00
6.00
3.00
0.00
0.00
0.10
0.20
0.30
0.40
0.50
0.60
[Q] MOLES/LITER (x10¹)

Figure 21. Stern-Volmer plot for quenching reduction and rearrangement by naphthalene in isopropyl alcohol

□ - reduction; slope = 3244 ± 76 l./mole
intercept = 291 ± 12

△ - rearrangement; slope = 1298 ± 18 l./mole
intercept = 72.8 ± 2.9

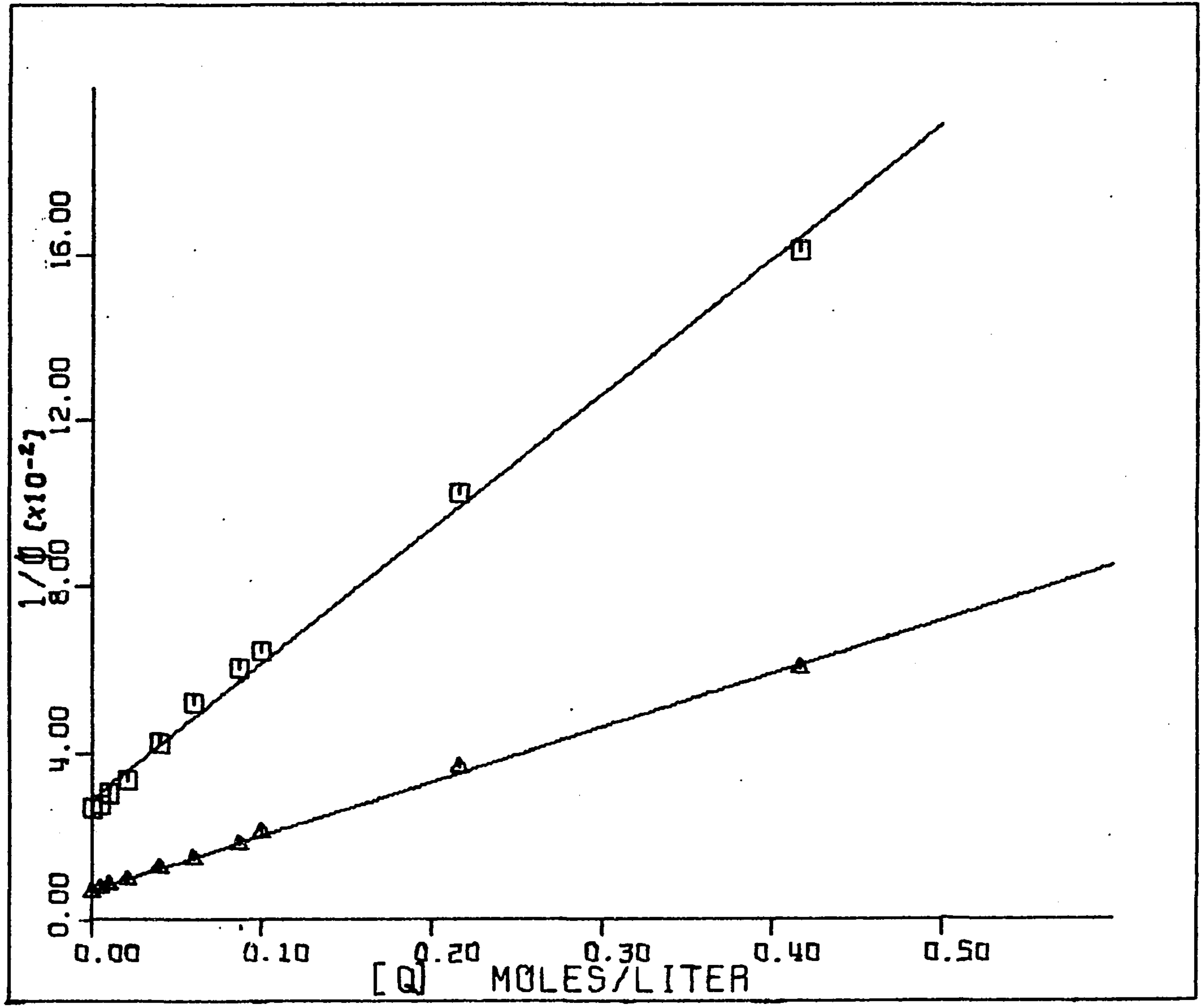
1/Φ (x10-2)
16.00
12.00
8.00
4.00
0.00
0.00
0.10
0.20
0.30
0.40
0.50
[Q] MOLES/LITER

Figure 22. Stern-Volmer plot for quenching reduction and rearrangement by hydroquinone in isopropyl alcohol

□ - reduction; slope = 0.62 ± 0.13 l./mole

Δ - rearrangement; slope = 12.4 ± 0.3 l./mole

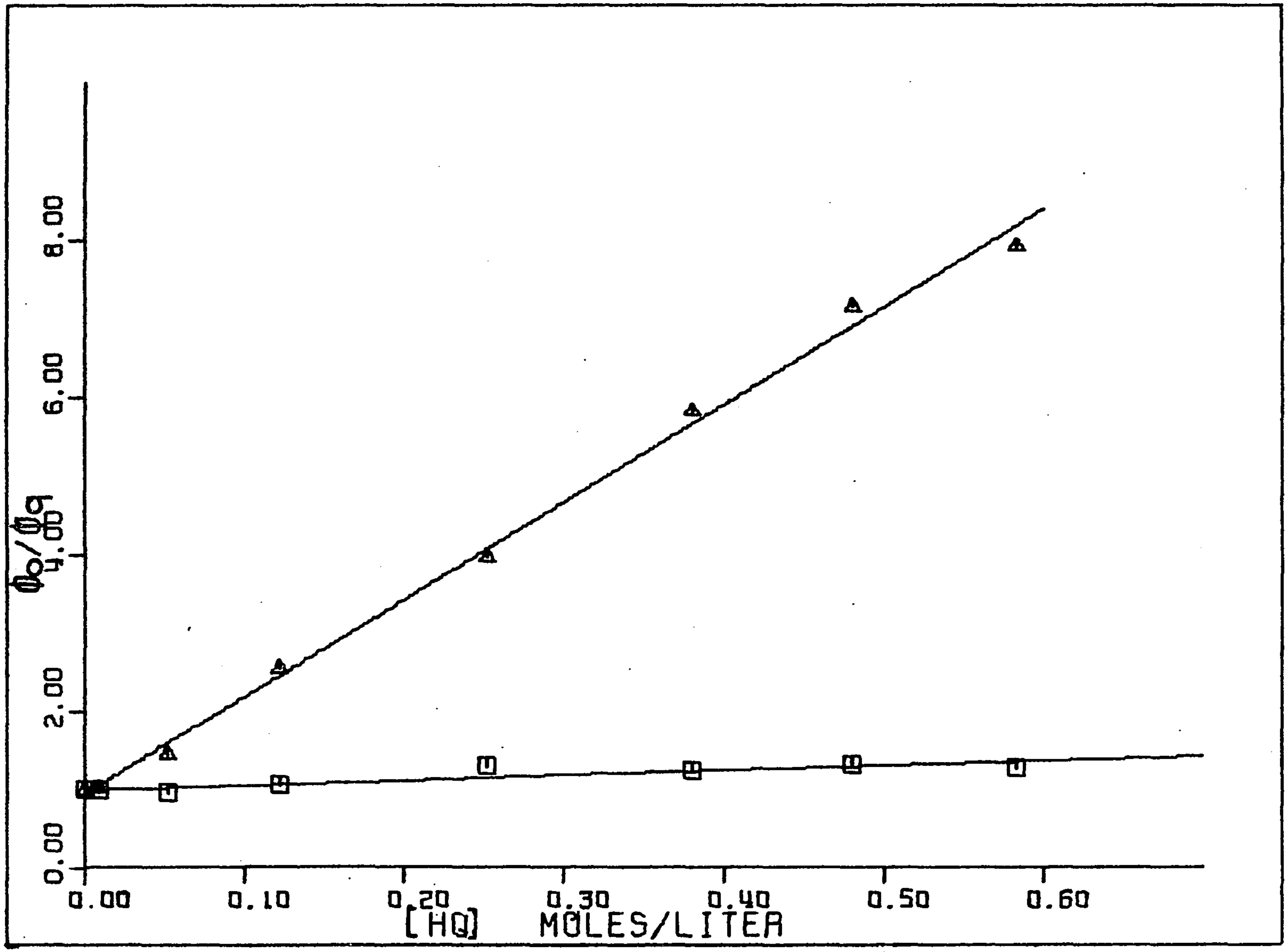
8.00
6.00
4.00
2.00
0.00
φo/φq
0.00
0.10
0.20
0.30
0.40
0.50
0.60
[HQ] MOLES/LITER

non-radical product. Hydroquinone is much more effective than thiophenol is inhibiting the rearrangement. The effect is due to the hydrogen atom donating character of hydroquinone. If the photoreaction is carried out in the presence of a high concentration of hydroquinone dimethyl ether, the quantum yields for photoreduction and photorearrangement are the same as in the absence of this additive. This rules out a mechanism involving energy transfer quenching. In the absence of more extensive studies, it is not possible to elaborate on the mechanism by which hydroquinone inhibits the rearrangement, except to point out that this is a chemical quenching effect which involves reaction of the quencher with the enone to give a species which reverts to ground state enone instead of rearranging. If the rearrangement of 2-cyclohexenones involves a discreet diradical intermediate such as compound 57, for example, radical quenchers such as hydroquinone could capture such a species and prevent its rearrangement. The possibility that during the course of the reaction sufficient benzoquinone (E_t = 50) (107) builds up to quench the reaction is ruled out, since the reduction would then be quenched in addition to the rearrangement.

The Stern-Volmer plot of di-t-butyl nitroxide quenching exhibits a further significant effect. Separate Stern-Volmer plots are obtained for quenching of the reduction and the rearrangement. The slope of the linear portion of the quenching plot for reduction is over ten times that of the slope for rearrangement. Differential quenching of the reduction and rearrangement products is also obtained with naphthalene (Figure 21). In this case, the effect is less pronounced; the slope for quenching of the reduction is about 2½ times that for rearrangement. The quenching ratios (ϕ_o/ϕ_q) of Tables 29 and 30 reveal that di-t-butyl nitroxide quenches the reduction more efficiently than the rearrangement. Naphthalene, in contrast, quenches the rearrangement more efficiently than the reduction. A number of diene quenchers were investigated; Table 31 lists single point ϕ_o/ϕ_q ratios for quenching by 0.10 M 2,5-dimethyl-2,4-hexadiene, 0.10 M isoprene, and 0.10 M trans-piperylene. The quenching effects of these three dienes upon the reduction and rearrangement reactions are also rather erratic. In all cases it is clear, however, that the reduction and the rearrangement reactions are differentially quenched by these dienes. The quencher 2,5-dimethyl-2,4-hexadiene follows the pattern of naphthalene in quenching the rearrangement more efficiently than the reduction. Trans-piperylene and isoprene are similar to di-t-butyl nitroxide in that they quench the reduction more efficiently than the rearrangement. With all of these dienes, small amounts of dimer formation and adduct formation with the cyclohexenone occurred upon irradiation.

The reversal in the quenching efficiencies of reduction and rearrangement when different quenchers are used is unusual. The probable cause is non-diffusion controlled energy transfer from the dienes and naphthalene to the enone. These quenchers have triplet energies ranging from 58 to 61 kcal/mole, while that of the enone is near 61 kcal/mole. In this respect, di-t-butyl nitroxide quenching is the most representative of differential quenching, in that its triplet energy is sufficiently low to ensure diffusion controlled energy transfer. The observed reversal in quenching efficiencies might also be accounted for by a change in the quenching mechanism. The dienes isoprene and trans-piperylene add very rapidly to 4,4-dimethyl-2-cyclohexenone to give cycloadducts. The diene 2,5-dimethyl-2,4-hexadiene, in contrast, reacts extremely slowly to give adducts and naphthalene does not add at all. The ability of the former two dienes to add so rapidly to the enone may enable them to quench the reduction and rearrangement via a Schenck type mechanism (equation 42) rather than an energy transfer mechanism.

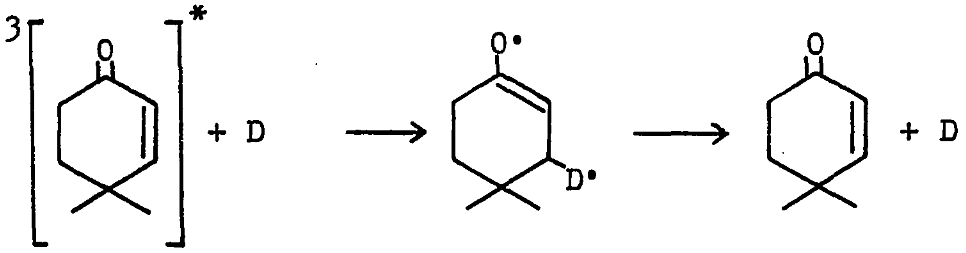

(42)

The Stern-Volmer quenching plots and the differential quenching obtained with the dienes indicate that the reduction and the rearrangement reactions do not come from the same reactive triplet state. Di-*t*-butyl nitroxide clearly differentiates the two triplet states in terms of lifetime, rate of reaction, and rate of deactivation to the ground state. The results from naphthalene quenching are less clearly differentiated for the reasons outlined above. The slopes of the plots in Figures 20 and 21 are given by k_q/k_r. Using a diffusion controlled rate constant for k_q (viscosity of isopropyl alcohol at 25^{o} = 1.95 cp; $k_{diff} = 3.4 \times 10^{9}$ M^{-1} sec^{-1}) values of k_r, k_d' and τ can be obtained from these plots. The results are tabulated in Table 6.

Table 6. Values of τ, k_r, and k_d' for reduction and rearrangement in isopropyl alcohol

	rearrangement			reduction		
Quencher	τ(sec)	k_r (sec^{-1})	k_d' (sec^{-1})	τ(sec)	k_r (sec^{-1})	k_d' (sec^{-1})
Di-*t*-butyl nitroxide	1.0×10^{-8}	1.6×10^{6}	9.7×10^{7}	2.4×10^{-8}	1.5×10^{5}	4.0×10^{7}
Naphthalene	5.3×10^{-9}	2.6×10^{6}	1.9×10^{8}	3.3×10^{-9}	1.1×10^{6}	3.1×10^{8}

As before, the rate constants for deactivation of the triplet states are one to two orders of magnitude larger than the rate constants for reaction of the triplets to give products, and this accounts for the low quantum efficiencies of these two reactions.

The data in Table 6 indicates that the triplet state that gives rearrangement reacts from 2½ to 10 times faster than that giving reduction. Both states have nearly the same rates for deactivation of the triplet to the ground state. The discrepancy observed in the relative order of τ for the two states is probably due to non-diffusion controlled energy transfer in the naphthalene quenching. The data from the nitroxide quenching in Table 6 is more representative of the reactions.

Indirect evidence is available which shows that oxygen can discriminate between the two triplet states. Only the di-t-butyl nitroxide quenching plot for reduction shows the quantum yield enhancement at low nitroxide concentrations which occurs when oxygen is scavenged from the system. The triplet state giving rearrangement is evidently too short-lived to be quenched by trace amounts of oxygen left in the solvent after degassing, whereas the triplet state for reduction must be of sufficiently long lifetime for oxygen to quench it. The quenching data from di-t-butyl nitroxide in Table 6 shows that the reduction triplet state has a lifetime

2½ times longer than that of the rearrangement triplet state, in agreement with this hypothesis.

The most reasonable possibilities for the two excited states involved in these reactions are the n,π* and the π,π* triplet states. The two states could also differ in geometry about the carbon-carbon double bond as well as electron configuration. Since $^3(n,\pi^*)$ states are much more susceptible to reduction than are $^3(\pi,\pi^*)$ states, the former is presumably the one that leads to photoreduction and the latter to rearrangement and ultimately to cycloaddition in the presence of olefins.

This assignment, of course, is tentative. The differential quenching observed here appears similar to that observed with O-acetyl testosterone and 10-methyl-$\Delta^{1,9}$-2-octalone, which were discussed in the Review of Literature section. In that case, however, rearrangement and reduction were assigned to the same $^3(\pi,\pi^*)$ state, whereas the double bond shift was assigned to the $^3(n,\pi^*)$ state (25). Clearly, additional studies are necessary in these systems before the assignments can be made with more certainty.

An assignment of the ordering of the energy levels of these two states is not definite. It appears that most enones have low-lying $^3(\pi,\pi^*)$ states, but the molecules that were studied all have rigid structures which may affect the relative ordering of the states. Structurally non-rigid molecules including 4,4-dimethyl-2-cyclohexenone do not phosphoresce, so there is no direct method for detecting and assigning the energies of the excited states. The sensitization data obtained for these reactions implies that the triplet state leading to photoreduction is of higher energy. Less efficient sensitization is obtained for reduction than for rearrangement. This may be indicative of non-diffusion controlled energy transfer from the sensitizer triplet to a cyclohexenone triplet lying just a little lower in energy (near 70 kcal/mole), which is distinct from the lower π,π^* triplet state near 61 kcal/mole.

Investigation of this possibility was made by carrying out the photoreduction in the presence of biphenyl ($E_t = 66$) (53) which would quench a high energy triplet, but not the lower-lying rearrangement triplet. Biphenyl, at concentrations up to 0.10 M, had no effect on the quantum yields of reduction or rearrangement. This concentration of biphenyl should be sufficiently high to quench a higher energy triplet state, even if it has a very short lifetime. (Alternately, the possibility exists that ground-state biphenyl, being twisted partially, is a nonvertical and slow energy acceptor). However, it appears that the two triplet states both lie below 66 kcal/mole. If they are of very similar energy, they evidently do not equilibrate rapidly at room temperature. Alternately, the n,π^* triplet could be several kcal/mole higher in energy than the π,π^* triplet and still be below 66 kcal/mole.

The assignment of a higher energy n,π^* triplet state is in agreement with the assignment of the triplet state ordering in 10-methyl-$\Delta^{1,9}$-2-octalone (see Figure 3). In that case, the assignment was made on the assumption that the predominant products of the reaction in a specific solvent will be derived from the lower-lying excited state in that solvent. The same reasoning will apply to the present reaction in that the lower-lying $^3(\pi,\pi^*)$ state affords the major products of the reaction, which are due to rearrangement. This assignment also accords with the observations made on the cyclohexenones investigated by spectroscopic techniques, that were discussed in the first part of the Review of Literature section.

The possibility of the involvement of a second excited triplet state in the photochemistry of a 2-cyclohexenone is not a radical departure from the established photochemistry of these molecules. There has been evidence in the past studies for a higher triplet state in such molecules, as discussed in the Review of Literature section. The photoreduction provides direct evidence for reaction from a second triplet state which may be the higher energy state postulated in the reactions of 2-cyclohexenones.

EXPERIMENTAL

The Photocycloaddition of Isophorone and 1,1-Diphenylethylene

Instruments and methods

All melting points were determined on a Fisher-Johns melting point apparatus and are uncorrected. Infrared spectra were recorded on a Perkin-Elmer Model 21 Spectrometer. Nuclear Magnetic Spectra were recorded on a Varian Associates Model A-60 or HA-100 spectrometer and the values are for solutions in carbon tetrachloride or deuteriochloroform as stated. Spin decoupling was carried out on the latter instrument. Mass spectra were measured on an Atlas CH-4 mass spectrometer. Microanalyses were performed by Spang Microanalytical Laboratories, Ann Arbor, Michigan. Irradiations were carried out in a 1200 ml Pyrex vessel surrounding a water-cooled immersion well housing the lamp. The source of irradiation was a Hanovia 550 watt mercury arc lamp. All solutions were thoroughly purged with and irradiated under an atmosphere of pre-purified nitrogen. Petroleum ether refers to the fraction of boiling point 60-80°.

Purification of reagents

Isophorone and 1,1-diphenylethylene were purified by passage through a 50 cm column of Silica Gel (Baker).

t-Butyl alcohol was distilled from calcium hydride through a 30 cm Vigreaux column. Benzene was distilled from P_2O_5 through a 30 cm Vigreaux column.

Preparative photocycloaddition in t-butyl alcohol

A solution of isophorone (6.90 g, 0.05 mole) and 1,1-diphenylethylene (36.0 g, 0.20 mole) in t-butyl alcohol was irradiated for 28 hours. After irradiation, the solvent was removed with a rotary evaporator, and the resulting oil was chromatographed on 400 g of Silica Gel. Successive elution with petroleum ether, 10% ethyl ether-petroleum ether, and 50% ethyl ether-petroleum ether yielded respectively 29.8 g 1,1-diphenylethylene, 10.0 g photolysis products, and 3.8 g isophorone. The solution of photolysis products yielded crystals (2.1 g, 13.2% yield) of the major photoadduct upon cooling. Chromatography of the remaining oils on 200 g of Silica Gel using 10% ethyl ether-petroleum ether as elutant and collection of 100 ml fractions gave 0.60 g (3.8% yield) of crystals of the minor photoadduct in fractions 7-11 and 0.04 (0.3% yield) g of crystals of the third photoadduct in fractions 22-25; all other fractions gave only oils. Final purification of recovered isophorone (3.17 g) by chromatography on Silica Gel gave a reaction yield of 25% based on the amount of isophorone consumed.

The major photoadduct, comprising 76.7% of the product mixture, was recrystallized from benzene-petroleum ether to give crystals, m.p. 118-122°. By the infrared spectrum (Figure 5), nmr spectrum (Figure 6), decoupling analysis, mass spectrum (Table 2), and by its isomerization and deuteration (<u>vide infra</u>), the adduct was identified as 3,3,4a-trimethyl-9-phenyl-1,2,3,4,4a,9,10,10a-octahydro-1-phenanthrone (<u>74</u>).

The minor photoadduct from fractions 7-11 (21.9% of the product mixture) was recrystallized from benzene-petroleum ether to m.p. 131-133°. By the infrared spectrum (Figure 5), nmr spectrum (Figure 7), decoupling analysis, and mass spectrum (Table 2), the adduct was identified as 2,2,10a-trimethyl-9-phenyl-1,2,3,4,4a,9,10,10a-octahydro-4-phenanthrone (<u>75</u>).

<u>Anal</u>. Calcd. for $C_{23}H_{26}O$: C, 86.75; H, 8.23; mol. wt., 318. Found: C, 86.90; H, 8.20; mol. wt. (mass spectrum), 318.

The crystals of the third adduct from fractions 22-25 (1.4% of the product mixture) were recrystallized from benzene-petroleum ether to m.p. 152-153°. On the basis of the infrared spectrum (Figure 5), nmr spectrum (Figure 7), and mass spectrum (Table 2), the adduct was identified as 4,4,6-trimethyl-8,8-diphenylbicyclo[4.2.0] octan-2-one (<u>76</u>).

Preparative photocycloaddition in benzene

A solution of isophorone (6.9 g, 0.05 mole) and 1,1-diphenylethylene (36.0 g, 0.20 mole) in benzene was irradiated for 28 hours. After irradiation, the solvent was removed with a rotary evaporator and the resulting oil was chromatographed on 400 g of Silica Gel. Successive elution with petroleum ether, 10% ethyl ether-petroleum ether, and 50% ethyl ether-petroleum ether yielded respectively 30.22 g 1,1-diphenylethylene, 14.23 g photolysis products, and 1.55 g isophorone. The isophorone was gummy and could not be further purified.

The solution of photolysis products yielded crystals (4.33 g, 27.2% yield) upon cooling, which were a mixture of adducts 74 and 75 and could only be partially separated by selective crystallization from benzene-petroleum ether. The remaining 8.43 g of oils were chromatographed on 200 g of Silica Gel using 10% ethyl ether-petroleum ether collected in 100 ml fractions. Fractions 4-7 gave 0.09 (0.6% yield) g of crystals of adduct 75, while all other fractions gave only oils.

Isomerization of 3,3,4a-trimethyl-9-phenyl-1,2,3,4,4a,9,10,10a-octahydro-1-phenanthrone

A solution of adduct 74 (1.00 g), potassium hydroxide (0.50 g), methanol (15 ml), and water (2 ml) was heated under reflux for 3 hours. The reaction mixture was diluted with water and the solid was filtered off and dried, yielding 0.89 g (89% yield). The crystals were recrystallized from benzene-petroleum ether to m.p. 174-175°: Infrared, 5.88 μ (C=O); nmr ($CDCl_3$), δ6.6-7.4 (multiplet, 9H), 3.9-4.2 (Quartet, 1H), 1.7-2.8 (multiplet, 6H), 1.47 (singlet, 3H), 1.17 (singlet, 3H), 1.09 (singlet, 3H).

Anal. Calcd. for $C_{23}H_{26}O$: C, 86.76; H, 8.23; mol. wt. 318. Found: C, 86.81; H, 8.12; mol. wt. (mass spectrum), 318.

Deuteration of 3,3,4a-trimethyl-9-phenyl-1,2,3,4,4a,9,10,10a-octahydro-1-phenanthrone

A solution of adduct 74 (200 mg), sodium methoxide (300 mg), methanol-OD (6 ml, 98.6% D), and deuterium oxide (2 ml, 99.5%) was heated under reflux for 3 hours. The methanol was removed with a rotary evaporator and the solution was diluted with 5 ml deuterium oxide (99.5%). The solid was filtered off, dried, and recrystallized from benzene-petroleum ether giving colorless needles (176 mg, 88%), m.p. 176-177°, nmr ($CDCl_3$) δ6.6-7.4 (multiplet, 9H), 4.0 (quartet, 1H), 1.7-2.4 (multiplet, 4H), 1.47 (singlet, 3H), 1.17 (singlet, 3H), and 1.10 (singlet, 3H). The mass spectrum indicated the following deuterium incorporation: 3.4% 2D, 96.6% 3D.

Deuteration of 2,2,10a-trimethyl-9-phenyl-1,2,3,4,4a,9,10,10a-octahydro-4-phenanthrone

A solution of adduct 75 (100 mg), sodium methoxide (500 mg), deuterium oxide (2 ml, 99.5%), and methanol-OD (6 ml, 98%) was heated under reflux for 2 hours. The methanol was removed with a rotary evaporator and the solution was diluted with 10 ml deuterium oxide. The solid was filtered off, dried, and recrystallized from benzene-petroleum ether, yielding 0.08 g (80%) of crystals. Nmr, δ6.6-73 (multiplet, 9H), 3.9 (quartet, 1H), 1.4-2.3 (multiplet, 4H), 1.14 (singlet, 3H), 1.09 (singlet, 3H), and 0.98 (singlet, 3H). The mass spectrum indicated the following deuterium incorporation; 9.8% 0 D, 3.7% 1 D, 14.6% 2 D, 69.5% 3 D.

Attempted isomerization of 2,2,10a-trimethyl-9-phenyl-1,2,3,4-4a,9,10,10a-octahydro-4-phenanthrone

A solution of adduct 75 (90 mg), sodium hydroxide (500 mg), methanol (15 ml), and water (2 ml) was heated under reflux for 3 hours. The methanol was removed with a rotary evaporator, and the remaining solution was diluted with water. The solid was filtered off, dried, and recrystallized from benzene-petroleum ether. An nmr spectrum of these crystals was identical to the starting material and indicated that no isomerization had taken place.

Attempted Baeyer-Villiger oxidation of 3,3,4a-trimethyl-9-phenyl-1,2,3,4,4a,9,10,10a-octahydro-1-phenanthrone

A solution of trifluoroacetic anhydride (840 mg) in methylene chloride (3 ml) was cooled to 0° while hydrogen peroxide (150 µl, 90% solution) was added dropwise over a period of 15 minutes. This solution was added dropwise over a period of 30 minutes to a mixture of adduct 74 (500 mg), methylene chloride (3 ml), and disodium hydrogen phosphate (750 mg), which was vigorously stirred and cooled in an icebath during the addition. After addition was complete, the mixture was stirred at 0° for 30 minutes, warmed to room temperature, heated under reflux with stirring for 6 hours, and stirred at room temperature for 12 hours. Water (15 ml) and methylene chloride (15 ml) were added, and the mixture was shaken to dissolve any inorganic material. The organic layer was then washed with two 10-ml portions of 5% sodium bicarbonate solution and once with a 10-ml portion of water. It was then dried (magnesium sulfate) and the solvent was evaporated. The resulting oil was chromatographed on 25 g of Silica Gel. Elution with 50% ethyl ether-petroleum ether and ethyl ether gave only a small amount of white residue (<50 mg) which could not be identified by spectral means.

Similar procedures using m-chloroperoxybenzoic acid in chloroform and permaleic acid in methylene chloride gave similar results. In both cases, starting material was completely consumed, but the products of the reaction were not identified by spectral means to be the desired lactone.

Instruments and Methods for the Measurement of Quantum Yields

Rotating photochemical apparatus

A rotating photochemical apparatus (referred to as the wheel) similar to that described by Moses *et al.* (108) was used for the simultaneous irradiation of samples. Actinometric calibration (*vide infra*) allowed the selection of eight closely matched cell compartments (± 1% in light intensity) from the twenty-four available. The light source was a Pyrex-jacketed Hanovia 550 watt, type A lamp. The lamp was cooled by recirculated distilled water which passed continually through an ion exchange column (Bamstead, Still and Sterilizer Co.) into a 5 gallon reservoir, which was in turn cooled by copper coils carrying tap water. The lamp and wheel were immersed in a tank of distilled water which maintained the temperature at 25-30°. The lamp was connected through a Stabiline voltage regulator (Superior Electric Corp.) Variations in the light intensity with this system were too small to be detected over extended irradiation times. The lamp housing was fitted with four Corning CS7-60 filters, bandpass at base 295-405 nm, λ_{max} 355 nm. From the spectral output of the lamp, the transmission spectrum of the filters and the Pyrex cells used for irradiation, the spectral output of the wheel was calculated to be: 302.5 nm, 0.5%;

313 nm, 5.1%; 334 nm, 5.3%; and 366 nm, 89.1%.

Linear quantum yield apparatus

A linear quantum yield apparatus was used for the irradiation of single samples and for determining absolute quantum yields. The apparatus employed an Osram 200 watt, super pressure, mercury light source (George W. Gates & Co.) powered with a D. C. power supply (Ionics Corp.). The source was attached to a Bausch and Lomb high intensity monochromator with uv-visible grating and variable slits (0-6 mm). The grating was blazed at 220 nm with a dispersion of 7.4 nm/mm. The entire apparatus was mounted on a Cenco optical bench and enclosed in a dry box with an aluminum heat exchanger above the lamp housing. Cooling fans were located inside the dry box near the monochrometer and above the heat exchanger outside the box. The temperature of the water-jacketed cell-holder was controlled by passage of thermostatically-cooled water from an outside source. Irradiations were carried out at either 25 ± 1° when cooling water was passed through the cell holder, or at 45 ± 2°, the equilibration temperature of the apparatus. The entrance slit of the monochromator was set at 6 mm and the exit slit was varied from 3-6 mm depending on the bandpass desired.[1]

---

[1] The band pass is determined by multiplying the exit slit width times the grating dispersion (7.4 nm/mm).

Cells used for quantum yield measurements

For irradiations at 313 nm and above, round cells (5.0 cm long) constructed from 13 x 100 mm Pyrex culture tubes and equipped with standard taper 10/30 joints, were used. For irradiations at 302 nm on the linear apparatus, cells were used consisting of 1.00 cm square quartz uv cells (Fischer & Porter Co.) equipped with threaded Teflon valves and a side arm with a standard taper 10/30 joint.

Actinometry

Potassium ferrioxalate actinometry (109) was used for measuring light intensities. Cells containing 3.0 ml of 0.013 M potassium ferrioxalate solution were irradiated for a measured amount of time. A 1.0 ml aliquot of the irradiated solution was added to a 50 ml volumetric flask containing 8.0 ml of 0.10% 1,10-phenanthroline solution and 1.0 ml of sodium acetate-sulfuric acid buffer. All volumes were measured with Becton Dickinson syringes equipped with Teflon needles. After diluting to 50 ml, the solutions were stored in the dark for one hour. The optical density was measured with a Beckman DU spectrophotometer equipped with a model 205 Gilford power supply, model 220 Gilford optical density converter, and model 209 Gilford automatic absorbance meter. Actinometers were run in duplicate before and after all irradiations for each cell position. For extended irradiations (10 hours or longer), actinometers were also measured several times during the irradiations. The average quantum output of the wheel was about 2.2 x 10^{16} quanta/sec. The quantum output of the linear apparatus was dependent on wavelength, slit width, and lamp age. Representative values were 2.5 x 10^{16} quanta/sec at 313 nm, 44.4 nm bandwidth, and 4.0 x 10^{16} quanta/sec at 366 nm, 44.4 nm bandwidth.

Preparation and irradiation of samples

For all quantum yield measurements, a 3.0 ml sample was used. Samples were prepared from volumetric solutions of the respective components and were measured into the cells using Becton Dickinson syringes equipped with Teflon needles. The solvent for rearrangement studies was t-butyl alcohol, for reduction studies, isopropyl alcohol, and for olefin isomerization studies, benzene. Samples in Pyrex cells were degassed by four freeze-pump-thaw cycles at liquid nitrogen temperature to 10^{-6} mm and were then sealed with a torch under vacuum. Samples in the quartz cells were purged with pre-purified nitrogen for ½ hour and were sealed with the Teflon valves against a positive pressure of nitrogen. Samples were shielded from light during preparation and degassing by wrapping the tubes with aluminum foil, and were kept in the dark before and after irradiation. The degassed samples were irradiated to 5% completion or less in the wheel or linear apparatus. Irradiation times were measured with an electric stopwatch.

Analytical procedure

Analyses of products were performed on an Aerograph model 1520B gas chromatograph using a thermal conductivity detector (W-2 filaments) and a disc integrator for measurement of peak areas. Product ratios were analyzed relative to an external standard added after irradiation and were corrected for differences in thermal conductivity. Acetophenone was used as external standard for photorearrangement and photoreduction studies, dodecane for β-methylstyrene isomerization studies, and methyl cinnamate for α-methylstilbene isomerization studies.

The data reported in the tables is the average of two or three chromatographic analyses which agreed with ± 3% or less. Rearrangement and reduction products were analyzed without evaporation of solvent. Olefin isomerization samples were analyzed after evaporation of about 3/4 of the solvent. Evaporation of the solvent was found to have no effect on the composition of the sample. On-column injection was used for all analyses, and the columns were eluted with helium at 75 cc/minute. The columns referred to in the experimental section are: Column A, 10 ft. x ¼ in., 5% ethylene glycol succinate (LAC-446) on the Chromosorb P, acid-washed, DMCS treated, 60/80 mesh, maintained at 135-145°; Column B, 7.5 ft. x ¼ in., 5% polyalkylene glycol (Ucon water soluble) on Chromosorb W, acid-washed, 80/100 mesh, maintained at 115-125°; Column C, 10 ft. x ¼ in., 20% polyethylene glycol

(Carbowax 20M) on Chromosorb W, acid-washed, 60/80 mesh, maintained at 155°; Column D, 6 ft. x 3/8 in., 20% polyethylene glycol (Carbowax 20M) on Chromosorb W, 60/80 mesh, maintained at 140°.

Correction of data

In cases where the solution did not absorb 100% of the light, the data has been corrected to total absorption by division of the raw data by the average percentage of light absorbed. The percent of light absorbed by a solution was calculated from uv absorption spectra and from the apparatus emission distribution. For the linear apparatus, the correction was applied at the λ_{max} of the bandwidth only. For the wheel, the correction was applied at the four wavelengths at which major emission occurred, using the calculated percent emission at each wavelength. The absorbance of the solution was determined at these same wavelengths. From the absorbances, the fraction of light absorbed at each wavelength was calculated. The sum of the percent emission times the fraction of light absorbed at each wavelength gave the percent light absorbed by the solution.

Quenching plots have been corrected for quencher absorption by the same method by considering the relative absorbances of the substrate and the quencher.

Quantum yields for olefin isomerization were measured by starting with the pure <u>trans</u> isomer and irradiating to 1-5%

isomerization, and are corrected back to 0% conversion using a form of the integrated rate law for approach of the system to the steady-state (equation 25), as explained in the Results and Discussion section.

Plots of quantum yield data

Least-squares plots were drawn by the simplotter from a PROGRAM PLOT computer program which calculated least-squares slopes, intercepts, and error limits in terms of standard deviations.

Phosphorescence equipment

Phosphorescence excitation and emission spectra were recorded on an Aminco-Bowman Spectrophotofluorometer, model 4-8202 (American Instrument Co., Inc.) equipped with a 150 watt Hanovia Xenon lamp source and a RCA R136 photomultiplier tube. The instrument was connected to an Aminco Photomultiplier Microphotometer, model 10-267, and an Aminco X-Y-T recorder, model 1620-838. A series of six slits could be varied from 2 to 42 nm to obtain the desired sensitivity and resolution.

Samples were dissolved in EPA solvent or freshly distilled 2-methyltetrahydrofuran under nitrogen, and then analyzed in a quartz tube, 3 mm in diameter, immersed in a quartz dewar filled with liquid nitrogen. A blank, containing only solvent, was run prior to each sample under identical conditions. The monochrometer was calibrated using a Pen-Ray quartz lamp (Ultraviolet Products, Inc.).

Format and symbols used in the tables of data

The format for the listing of experimental results of quantum yield measurements consists of a statement of cells used, irradiation times, and irradiation conditions. This is followed by a table listing the pertinent experimental details and results. The symbols used in the tables of experimental data refer to the following: $[K]$, concentration of 4,4-dimethyl-2-cyclohexenone in moles/liter; $[Q]$: concentration of quencher in moles/liter; $[\text{sens}]$, concentration of sensitizer in moles/liter ϕ_o/ϕ_q; ratio of the quantum yield in the absence of quencher to the quantum yield in the presence of quencher; ϕ_{sens}/ϕ_o, ratio of the quantum yield in the presence of sensitizer to the quantum yield in the absence of sensitizer.

Preparation and purification of reagents

4,4-Dimethyl-2-cyclohexenone was prepared by the reaction of isobutyraldehyde piperidine enamine and methyl vinyl ketone (1), and was purified by vacuum distillation at 68.8°, 15 mm (literature b.p. 76°, 21 mm) (1). Di-t-butyl nitroxide was prepared by the treatment of t-nitrobutane with sodium (110), and was distilled through a 50 cm Nester-Faust spinning band column, b.p. 54-56° at 9-11 mm (literature b.p. 60°, 11 mm((110). Acetophenone (Matheson, Coleman, & Bell) was distilled through a 50 cm spinning band column. Benzophenone, thioxanthone, 9-fluorenone, naphthalene, biphenyl, and 2-acetonaphthone (all from Baker Sensitizer Kit) and 3,4-methylenedioxyacetophenone (Frinton Labs) were recrystallized twice from suitable solvents or sublimed and had melting points consistent with literature values. Michler's Ketone (4,4'-bis-(dimethylamino)-benzophenone, Baker Sensitizer Kit) was recrystallized twice from ethanol followed by vacuum sublimation, m.p. 171-172° (literature m.p. 172°) (111). m-Methoxyacetophenone (Aldrich) and p-methoxyacetophenone were vacuum distilled. 2-Methyltetrahydrofuran (Eastman) was distilled from lithium aluminum hydride under nitrogen prior to use. Baker reagent grade t-butyl alcohol and isopropyl alcohol were distilled from sodium through a 30 cm helices-packed Vigreaux column. Isophorone was distilled through a 50 cm spinning band column at 70°, 3.2 mm (literature b.p. 89° at 10 mm) (112). Reagent grade benzene was stirred with concentrated sulfuric acid for 24 hours, followed by extraction with water and sodium bicarbonate solution. After drying over anhydrous calcium chloride, it was distilled from sodium through a 30 cm helices-packed Vigreaux column. Thiophenol, (Baker), hydroquinone (Matheson, Coleman, & Bell), and EPA (American Instrument Co.) were used without further purification. Methyl cinnamate (Matheson, Coleman, & Bell) was recrystallized twice from hexane. 2,5-Dimethyl-2,4-hexadiene was distilled, b.p. 124-125°. Isoprene and trans-piperylene were distilled prior to use. Hydroquinone dimethyl ether was prepared by treatment of hydroquinone with dimethyl sulfate and sodium hydroxide (113). Recrystallization of the product twice from ethanol gave crystals, m.p. 55-56° (literature m.p. 55-56°) (114). Trans-β-methylstyrene was purified by preparative v.p.c. collection (column D). Analysis by analytical v.p.c. indicated an isomer purity greater than 99.95% trans. α-Methylstilbene was prepared by reaction of benzyl magnesium chloride and acetophenone. Recrystallization twice from hexane gave crystals, m.p. 79-81° (literature m.p. 82-83°) (115). Analysis by v.p.c. showed the isomer ratio to be greater than 99.95% trans.

The Photorearrangement of 4,4-Dimethyl-2-Cyclohexenone

Absolute quantum yield of rearrangement

Two samples in Pyrex cells were irradiated in the wheel (1670 min) and analyzed on column A. Two additional samples were irradiated in Pyrex cells in the linear apparatus (sample 1, 1097 min; sample 2, 1124 min) at 366 nm, 29.6 nm bandwidth, 25°, and analyzed on column A. The results are recorded in Table 7.

Table 7. Absolute quantum yield of rearrangement

Apparatus	[K]	$\phi_2 x10^3$	$\phi_3 x10^3$	$\phi_{total} x10^2$	% $\underline{2}$	% $\underline{3}$
Wheel	0.30	6.5	7.2	1.37	46	54
Wheel	0.30	6.7	7.2	1.39	46.5	53.5
Linear	0.60	6.5	8.1	1.46	45	55
Linear	0.60	6.5	7.9	1.44	45	55
Average		6.5	7.7	1.42		

Effect of cyclohexenone concentration on the quantum yield of rearrangement

Samples in Pyrex cells were irradiated in the wheel and analyzed on column A. The results recorded in Table 8 have been corrected to 100% absorption of light.

Table 8. Effect of cyclohexenone concentration on the quantum yield of rearrangement

[K]	Irradiation time(min)	% of light absorbed by K	% $\underline{2}$	% $\underline{3}$	ϕ x 10^2
0.02	576	25.6	48	52	1.37
0.05	619	48.3	46.5	53.5	1.58
0.07	619	58.9	46.5	53.5	1.53
0.10	962	71.5	47	53	1.40
0.20	1020	90.9	46	54	1.30
1.00	3239	100.0	48	52	1.47
				Average	1.43 ± 0.15

Quenching rearrangement by di-t-butyl nitroxide

Samples in Pyrex cells were irradiated in the wheel (1800 min) and analyzed on column A. The results are recorded in Table 9 and plotted in Figure 8.

Table 9. Quenching rearrangement by di-t-butyl nitroxide[a]

$[Q] \times 10^2$	% 2	% 3	ϕ_o/ϕ_q	$1/\phi_q$
0.0	45.5	54.5	1.00	70.4
1.1	46	54	1.36	95.8
2.0[b]	46	54	1.72	121
3.1	47	53	1.92	135
4.0[b]	47	53	2.17	153
5.2[b]	47	53	2.48	175
6.1[b]	47.5	52.5	2.82	199

[a] $[K] = 0.30$ M

[b] Data reported is the average of two irradiations

Quenching rearrangement by naphthalene

Samples in Pyrex tubes were irradiated in the wheel (1900 min) and analyzed in column B. The results are presented in Table 10 and plotted in Figure 8.

Table 10. Quenching rearrangement by naphthalene[a]

$[Q] \times 10^2$	% $\underline{2}$	% $\underline{3}$	ϕ_o/ϕ_q	$1/\phi_q$
0.0	45.5	55.5	1.00	70.4
2.0	44	56	1.50	106
4.0	45	55	1.92	136
6.0	44	56	2.36	166
8.0	44	56	2.74	193
10.0	45.5	54.5	3.05	215

[a] $[K] = 0.30$ M

Sensitization of rearrangement by acetophenone

Samples were irradiated in Pyrex cells in the wheel (1200 min) or in the linear (270 min) at 313 nm, 33.3 nm bandwidth, 25°. Samples were analyzed on column A using phenyl butyrate as external standard. The results are presented in Table 11.

Table 11. Sensitization of rearrangement by acetophenone[a]

Apparatus	[sens]	% light absorbed by sensitizer	$\phi_{sens} \times 10^2$	ϕ_{sens}/ϕ_o
Wheel[b]	1.00	89.4	1.43	1.00
Linear[b]	0.20	90.1	1.54	1.08

[a] $[K] = 0.05$ M

[b] Data reported is the average of two irradiations

Sensitization of rearrangement by benzophenone

Samples in Pyrex cells were irradiated in the wheel (1200 min) or in the linear (395 min) at 366 nm, 44.4 nm bandwidth, 25°. Analysis on column A gave the results presented in Table 12.

Table 12. Sensitization of rearrangement by benzophenone[a]

Apparatus	$[\mathrm{sens}]$	% light absorbed by sensitizer	$\phi_{\mathrm{sens}} \times 10^{2}$	$\phi_{\mathrm{sens}}/\phi_{o}$
Wheel[b]	0.10	90.0	1.33	0.94
Linear	1.00	100.0	1.25	0.88

[a] $[K] = 0.10$ M

[b] Results reported are the average of two irradiations

Sensitization of rearrangement by thioxanthone

Samples in Pyrex cells were irradiated in the wheel (sample 1, 1410 min; sample 2, 1200 min) and analyzed on column A to give the results presented in Table 13.

Table 13. Sensitization of rearrangement by thioxanthone[a]

$[\mathrm{sens}]$	% light absorbed by sensitizer	$\phi_{\mathrm{sens}} \times 10^{3}$	$\phi_{\mathrm{sens}}/\phi_{o}$	$\phi_{o}/\phi_{\mathrm{sens}}$
0.005[b]	93.0	6.8	0.48	2.08
0.01[b]	95.5	4.4	0.31	3.20

[a] $[K] = 0.10$ M

[b] Results reported are the average of two irradiations

Sensitization of rearrangement by 9-fluorenone and 2-acetonaphthone

Samples in Pyrex cells were irradiated in the wheel (3330 min) and samples in square quartz cells were irradiated (1080 min) at 302.5 nm, 44.4 nm bandwidth, 43°. Analysis on column A gave the results presented in Table 14.

Table 14. Sensitization of rearrangement by 9-fluorenone and 2-acetonaphthone[a]

Apparatus	Sensitizer	[sens]	% light absorbed by sens.	$\phi_{sens} \times 10^4$	ϕ_{sens}/ϕ_o
Wheel[b]	9-fluorenone	0.05	95.5	2.2	0.016
Linear	2-acetonaphthone	1.00	100	0.0	0.0

[a] $[K] = 0.10$ M

[b] Results reported are the average of two irradiations

Sensitization of rearrangement by *m*-methoxyacetophenone, *p*-methoxyacetophenone, and 3,4-methylenedioxyacetophenone

Samples in square quartz cells were irradiated in the linear apparatus at 302.5 nm, 44.4 nm bandwidth, 45±2°. Analysis on column A gave the results presented in Table 15 for *m*-methoxyacetophenone, Table 16 for *p*-methoxyacetophenone, and Table 17 for 3,4-methylenedioxyacetophenone. The quantum yields for the blanks were 0.0142 ± 0.0002.

Table 15. Sensitization of rearrangement by m-methoxyacetophenone[a]

[sens]	irradiation time (min)	$\phi_{sens} \times 10^2$	ϕ_{sens}/ϕ_o	ϕ_o/ϕ_{sens}
0.02[b]	600	1.37	0.96	1.04
0.10	520	1.24	0.87	1.14
0.20[c]	1025	1.00	0.70	1.42
0.60	1684	0.63	0.44	2.25
1.00	1110	0.46	0.32	3.09
1.50	2198	0.26	0.18	5.46

[a] [K] = 0.10 M

[b] Sensitizer absorbed 95% of the light at this concentration, 100% at all higher concentrations

[c] Data reported is the average of two irradiations

Table 16. Sensitization of rearrangement by p-methoxyacetophenone[a]

[sens][b]	irradiation time (min)	$\phi_{sens} \times 10^2$	ϕ_{sens}/ϕ_o	ϕ_o/ϕ_{sens}
0.10	590	1.38	0.97	1.03
0.30	536	1.31	0.93	1.08
0.66	540	1.35	0.95	1.05
1.00	1120	1.10	0.77	1.29
1.50	540	0.97	0.68	1.46

[a] [K] = 0.10 M

[b] Sensitizer absorbed greater than 99% of the light in all cases

Table 17. Sensitization of rearrangement by 3,4-methylenedioxyacetophenone[a]

$[\text{sens}]^b$	irradiation time (min)	$\phi_{sens} \times 10^3$	ϕ_{sens}/ϕ_o	ϕ_o/ϕ_{sens}
0.01[c]	426	10.2	0.72	1.39
0.05	400	9.0	0.63	1.58
0.10[c]	369	6.3	0.44	2.25
0.15	430	5.9	0.42	2.41
0.20[c]	943	4.6	0.33	3.09

[a] $[K]$ = 0.10 M

[b] Sensitizer absorbed greater than 99% of the light in all cases

[c] Data reported is the average of two or three irradiations

Quantum yield for photoreduction of thioxanthone in isopropyl alcohol

Two samples of thioxanthone (0.0025 M) in isopropyl alcohol were placed in square quartz cells and purged with nitrogen for ½ hour. After measuring the uv absorbance of the two samples at 404 and 406 nm, they were irradiated in the linear apparatus (sample 1, 544 min; sample 2, 184 min). Uv analysis of the two samples after irradiation allowed calculation of the moles of thioxanthone destroyed and measurement of the quantum yield for photoreduction. The average value determined was $(5.4 \pm 1.3) \times 10^{-3}$.

Photoisomerization Studies of *trans*-β-Methylstyrene

Determination of the sensitized photostationary state of β-methylstyrene

Samples consisting of a 2:3 ratio of *cis*- and *trans*-β-methylstyrene in Pyrex cells were irradiated in the linear apparatus (30 min) at 366 nm, 44.4 nm bandwidth, 25°. Analysis of the samples on column C gave the results presented in Table 18.

Table 18. Sensitization of β-methylstyrene to the photostationary state

[β-Methylstyrene]	Sensitizer	[sens]	[trans]/[cis]	% light absorbed by sensitizer
0.05	acetophenone	0.052	0.91	100
0.05	*p*-methoxyacetophenone	0.014	0.95	100

Sensitization of the isomerization of *trans*-β-methylstyrene

Samples in Pyrex cells were irradiated in the linear apparatus at 25°. In all cases, *trans*-β-methylstyrene concentration was 0.10 M, and the sensitizer absorbed greater than 99% of the light. Analysis on column C gave the results presented in Table 19 for acetophenone, Table 20 for naphthalene, Table 21 for Michler's Ketone, Table 22 for *m*-methoxyacetophenone, Table 23 for 3,4-methylenedioxyacetophenone, Table 24 for thioxanthone, and Table 25 for benzophenone. Irradiation times, wavelengths, and bandwidths for the irradiations are reported in each table. All results reported are the average of two irradiations.

Table 19. Sensitization of trans-β-methylstyrene isomerization by acetophenone[a]

[sens]	irradiation time (min)	ϕ	1/ϕ
0.10	10	0.505	1.98
0.40	10	0.465	2.15
0.70	10	0.445	2.25
1.00	10	0.445	2.25
1.30	10	0.415	2.41
1.60	10	0.415	2.41

[a] Irradiation conditions: 313 nm, 29.6 nm bandwidth

Table 20. Sensitization of trans-β-methylstyrene isomerization by naphthalene[a]

[sens]	irradiation time (min)	ϕ
0.05	20	0.18
0.20	17	0.18
0.52	60	0.20

[a] Irradiation conditions: 313 nm, 29.6 nm bandwidth

Table 21. Sensitization of trans-β-methylstyrene isomerization by Michler's Ketone[a]

[sens]	log[sens]	irradiation time (min)	ϕ	1/ϕ	log 1/ϕ
1.80×10^{-4}	-3.745	7.5	0.505	1.98	0.296
3.90×10^{-4}	-3.409	7.5	0.505	1.98	0.296
3.90×10^{-3}	-2.409	7.5	0.46	2.17	0.336
3.90×10^{-2}	-1.409	7.5	0.40	2.50	0.398
1.00×10^{-1}	-1.000	8.5	0.39	2.56	0.408

[a] Irradiation conditions: 366 nm, 22.2 nm bandwidth

Table 22. Sensitization of trans-β-methylstyrene isomerization by m-methoxyacetophenone[a]

[sens]	irradiation time (min)	ϕ	1/ϕ
0.004	10.5	0.43	2.33
0.10	9.0	0.425	2.35
0.05	8.5	0.43	2.33
0.25	9.0	0.41	2.44
0.50	11.5	0.40	2.50
0.75	10.0	0.37	2.70
1.00	10.0	0.34	2.94

[a] Irradiation conditions: 313 nm, 44.4 nm bandwidth

Table 23. Sensitization of trans-β-methylstyrene isomerization by 3,4-methylenedioxyacetophenone[a]

[sens]	irradiation time (min)	ϕ
0.002	10.0	0.425
0.02	9.0	0.38
0.21	10.5	0.40

[a] Irradiation conditions: 313 nm, 44.4 nm bandwidth

Table 24. Sensitization of trans-β-methylstyrene isomerization by thioxanthone[a]

[sens]	irradiation time (min)	ϕ
6.6×10^{-4}	8.5	0.495
6.6×10^{-3}	8.5	0.435

[a] Irradiation conditions: 366 nm, 29.6 nm bandwidth

Table 25. Sensitization of trans-β-methylstyrene isomerization by benzophenone[a]

[sens]	irradiation time (min)	ϕ	1/ϕ
0.05	7.5	0.51	1.96
0.125	5.0	0.49	2.04
0.265	8.5	0.46	2.17
0.50	9.0	0.42	2.38
0.75	9.0	0.39	2.56
1.00	5.5	0.39	2.56
1.00	10.0	0.395	2.53
1.25	10.0	0.38	2.63
1.25	10.0	0.39	2.56
1.40	10.0	0.325	3.08
1.50	10.0	0.305	3.28
1.60	8.0	0.235	4.26
1.70	10.5	0.21	4.76

[a] Irradiation conditions: 366 nm, 29.4 or 44.4 nm bandwidth

Effect of olefin concentration on the quantum yield of isomerization of trans-β-methylstyrene

Samples in Pyrex cells were irradiated in the linear at 366 nm, 22.2 nm bandwidth, 25°. Analysis of the samples on column C gave the results presented in Table 26. Samples that were greater than 0.20 M in olefin exhibited two new peaks (~1-2%) in the v.p.c. at long retention time which are attributed to dimers. The benzophenone absorbed greater than 99% of the light.

Table 26. Effect of olefin concentration on the quantum yield of isomerization of trans-β-methylstyrene

[benzophenone]	[trans-β-methylstyrene]	irradiation time (min)	ϕ	$1/\phi$	$1/[O]^{a}$
0.05	0.10	4.0	0.50	2.00	10.0
0.05	0.50	8.0	0.52	1.92	2.00
0.50	0.10	9.0	0.42	2.38	10.0
0.50	0.20	5.0	0.47	2.13	5.00
0.50	0.30	7.5	0.48	2.08	3.33
0.50	0.40	6.5	0.505	1.98	2.50
0.50	0.50	8.0	0.51	1.96	2.00

[a] Reciprocal of trans-β-methylstyrene concentration

Effect of impure olefin on the quantum yield of isomerization of trans-β-methylstyrene

Samples made from unpurified trans-β-methylstyrene were irradiated in Pyrex cells in the linear at 366 nm, 22.2 nm bandwidth, 25°. Analysis of the samples on column C gave the results presented in Table 27. Dimer formation was noted at higher olefin concentration (>0.2 M). The benzophenone absorbed greater than 99% of the light.

Table 27. Effect of impure olefin on the quantum yield of isomerization of *trans*-β-methylstyrene

[Benzophenone]	[*trans*-β-methylstyrene]	$[O]^{2}$[a]	irradiation time (min)	ϕ
0.50	0.10	0.01	6.0	0.37
0.50	0.50	0.25	8.0	0.71
0.50	1.00	1.00	3.0	1.65
0.50	1.50	2.25	2.0	3.13

[a] Square of *trans*-β-methylstyrene concentration

Photoisomerization Studies of *trans*-α-Methylstilbene

Samples in Pyrex cells were irradiated in the linear at 366 nm, 22.2 nm bandwidth, 25°. Analysis of the samples on column B at 200° gave the results reported in Table 28 for benzophenone, isophorone, and 4,4-dimethyl-2-cyclohexenone sensitization. The results have been corrected to 100% absorption of light by the sensitizers.

Table 28. Sensitization of the isomerization of <u>trans</u>-α-methylstilbene

Sensitizer	[sens]	[O]	1/[O]	irrad time (min)	% light absorbed by sens.	ϕ	1/ϕ
Benzophenone	0.05	0.05		3.0	100	0.565[a]	
Isophorone	0.40	0.05		3.0	100	0.49[a]	
4,4-Dimethyl-2-cyclohexenone	0.30	0.10	10.0	3.0	94.2	0.165[a]	6.06
"	0.30	0.05	20.0	13.0	97.0	0.089	11.24
"	0.30	0.025	40.0	24.0	98.6	0.048	20.83
"	0.30	0.017	58.8	22.0	99.1	0.033	30.3
"	0.30	0.013	78.1	22.0	100	0.025	40.0
"	0.30	0.009	106.2	22.0	100	0.020	50.0

[a] Results reported are the average of two irradiations

The Photoreduction and Photorearrangement of 4,4-Dimethyl-2-Cyclohexenone in Isopropyl Alcohol

<u>Absolute quantum yield of reduction and rearrangement</u>

Four samples in Pyrex cells, 0.30 M in 4,4-dimethyl-2-cyclohexenone were irradiated in the wheel (samples 1 and 2, 1804 min; samples 3 and 4, 850 min). Analysis of the samples on column A gave: reduction $\phi = 3.7 \times 10^{-3}$, rearrangement $\phi = 1.5 \times 10^{-2}$, and total $\phi = 1.87 \times 10^{-2}$. The results of all four irradiations were within ± 1% of each other. The product composition was 35% 2, 45% 3, and 20% 4.

Preparative photoreduction in isopropyl alcohol

A solution of 4,4-dimethyl-2-cyclohexenone (5.96 g, 0.30 M) in isopropyl alcohol was purged with nitrogen and irradiated for 3 hours to 28% completion. The solvent was removed on a rotary evaporator leaving 5.1 g of a yellow oil. Analysis of the oil by v.p.c. ($\frac{1}{4}$ in. x 9 ft., 7% Dow Corning FS-1265, 0.5% Polyterg J-200 on 60/80 mesh Diatoport S, 155°) indicated the usual reduction and rearrangement products as well as several new products of longer retention time. The oil was chromatographed on 200 g of Silica Gel (Baker) packed in petroleum ether. Elution with 10% ethyl ether-petroleum ether gave 2.4 g of starting material, rearrangement products, and reduction product. The later fractions also contained small amounts of the new products. Elution with 30% ethyl ether-petroleum ether gave fractions totaling 1.0 g consisting of mixtures of the new compounds. Several of the fractions contained a crystalline white compound, several contained a yellow liquid, and others were a mixture of the two. The infrared and n.m.r. spectra of one of the fractions of liquid components allowed identification of these compounds as the dl and meso pinacols 37 by comparison to authentic spectra. The pinacols were found to be thermally stable on column A under conditions used for the measurement of quantum yields, and they did not rearrange on the column to 4,4-dimethylcyclohexanone.

The crystalline product was a dimer of 4,4-dimethyl-2-cyclohexenone. The infrared and n.m.r. spectra indicated a saturated ketone. The mass spectrum (parent ion, m/e 248) is consistent with a dimeric structure.

Quenching reduction and rearrangement by di-*t*-butyl nitroxide

Samples in Pyrex cells were irradiated in the wheel (samples 1 to 5, 1200 min; samples 6 to 10, 2400 min). Analysis of the samples on column A gave the results presented in Table 29 and plotted in Figure 20.

Table 29. Quenching reduction and rearrangement by di-*t*-butyl nitroxide[a]

$[Q] \times 10^2$	% 4	% 2	% 3	reduction		rearrangement		total
				ϕ_o/ϕ_q	$1/\phi_q$	ϕ_o/ϕ_q	$1/\phi_q$	ϕ_o/ϕ_q
0.00	20	35	45	1.00	270	1.00	66.7	1.00
0.53	36	28	36	0.48	130	1.07	71.3	0.85
0.90	34	27	39	0.58	157	1.22	81.3	1.00
1.60	22	33	45	1.32	357	1.54	103	1.49
2.10	19	32	49	1.70	459	1.56	104	1.59
3.00	18	33	49	2.21	597	1.90	127	1.96
4.00	12	36	48	2.40	647	2.40	160	2.44
5.10	14	38	48	4.06	1097	2.66	177	2.86
6.00	13	38	49	5.07	1370	3.01	201	3.28
7.00	16	36	48	-[b]	-[b]	3.13	209	3.30

[a] [K] = 0.30 M

[b] Conversion was too small for an analytical measurement

Irradiation in the presence of di-t-butyl nitroxide at 446 nm

A sample in a Pyrex cell containing 4,4-dimethyl-2-cyclohexenone (0.30 M) and di-*t*-butyl nitroxide(0.78 M) in isopropyl alcohol was irradiated in the linear at 446 nm, 44.4 nm bandwidth, 25° for 1465 min. The nitroxide absorbed all of the light under these conditions. Analysis of the sample on column A indicated that only a trace of rearrangement and reduction products had formed. The irradiation resulted in the formation of a new product of long retention time on the v.p.c. This material was not investigated further.

Determination of the photostability of di-t-butyl nitroxide in isopropyl alcohol

A sample in a Pyrex cell containing 4,4-dimethyl-2-cyclohexenone (0.30 M) and di-*t*-butyl nitroxide(0.011 M) in isopropyl alcohol was irradiated in the wheel for 1201 min. An identical sample was stored in the dark for an equivalent amount of time. Analysis by uv at 446 nm before and after irradiation showed that the di-*t*-butyl nitroxide was completely destroyed in the irradiated sample, but was unchanged in the dark sample.

Quenching reduction and rearrangement by naphthalene

Samples in Pyrex cells were irradiated in the wheel (1200 min.). Light output was not monitored, and ϕ_o/ϕ_q ratios are relative to blanks which were irradiated simultaneously. Analysis of the samples on column A gave the results recorded in Table 30 and plotted in Figure 21. Sample composition for the blanks were within ± 1% of each other.

Table 30. Quenching reduction and rearrangement by naphthalene[a]

$[Q] \times 10^2$	% 4	% 2	% 3	reduction ϕ_o/ϕ_q	reduction $1/\phi_q$	rearrangement ϕ_o/ϕ_q	rearrangement $1/\phi_q$	total ϕ_o/ϕ_q
0.00	20	34	46	1.00	270	1.00	66.7	1.00
0.50	21	36	43	1.02	276	1.15	76.7	1.12
1.00	21	36	43	1.13	305	1.29	86.0	1.26
2.10	21.5	34.5	44	1.25	338	1.47	98.0	1.42
4.00	22	35	43	1.57	424	1.88	125	1.81
6.00	21	35	44	1.92	519	2.22	148	2.17
8.70	22	35	43	2.23	603	2.76	184	2.64
10.0	24	34	42	2.38	643	3.18	212	2.98
21.6	28	34	38	3.79	1024	5.50	367	5.04
41.6	29	35	36	5.95	1608	9.06	604	8.17

[a] $[K] = 0.30$ M

Quenching reduction and rearrangement by dienes

Samples in Pyrex cells were irradiated in the wheel. Light output was not monitored and ϕ_o/ϕ_q ratios are relative to blanks irradiated simultaneously. The amount of product formation could not be measured by comparison to an internal standard because the dimers and adducts that were formed in small amounts had retention times identical to the standard.

Quenching ratios were therefore determined by injecting equal volumes of the blank and quenched samples and comparing the product areas. Control injections revealed that the variation between equal volume injections was no more than 2%. Analysis of the samples on column A gave the results recorded in Table 31.

Table 31. Quenching reduction and rearrangement by dienes[a]

Quencher	[Q]	% 4	% 2	% 3	E_t ($\frac{\text{kcal}}{\text{mole}}$)	(ref.)	reduct. ϕ_o/ϕ_q	rear. ϕ_o/ϕ_q	total ϕ_o/ϕ_q
2,5-Dimethyl-2,4-hexadiene	0.10	30	29	41	58	(116)	4.17	6.50	5.79
trans-piperylene	0.10	10	41	49	59	(117)	3.79	1.29	1.55
isoprene	0.10	7	42	51	60	(117)	7.19	1.59	1.98

[a] [K] = 0.30 M

Effect of thiophenol on reduction and rearrangement

A sample in a Pyrex cell consisting of 4,4-dimethyl-2-cyclohexenone (0.30 M) and thiophenol (0.006 M) in isopropyl alcohol was irradiated in the wheel for 1200 min. Analysis of the sample on column A gave the following results: reduction $\phi = 4.9 \times 10^{-3}$, rearrangement $\phi = 1.1 \times 10^{-2}$, total $\phi = 1.59 \times 10^{-2}$, % 4 = 31, % 2 = 31, % 3 = 38.

Sensitization of reduction and rearrangement

Samples in Pyrex cells were irradiated in the linear apparatus as follows: m-methoxyacetophenone, p-methoxyacetophenone, and 3,4-methylenedioxyacetophenone at 313 nm, 44.4 nm bandwidth, 25°; thioxanthone at 366 nm, 44.4 nm bandwidth, 25°. Analysis of the samples on column A gave the results presented in Table 32.

Table 32. Sensitization of reduction and rearrangement

	Sensitizer			
	m-methoxyacetophenone	p-methoxyacetophenone	3,4-methylenedioxyacetophenone	thioxanthone[a]
[sens]	0.07	0.30	0.01	0.01
[K]	0.30	0.30	0.10	0.10
irradiation time(min)	1167	1208	1202	1923
% light absorbed by sensitizer	95.0	91.9	95.7	99.1
reduction ϕ_{sens}	0.0027	0.0029	0.0016	0.0011
reduction ϕ_{sens}/ϕ_o	0.73	0.78	0.43	0.30
rearrangement ϕ_{sens}	0.0145	0.0149	0.0070	0.0009
rearrangement ϕ_{sens}/ϕ_o	0.97	0.99	0.47	0.06
total ϕ_{sens}/ϕ_o	0.92	0.95	0.46	0.11

[a] Results reported are the average of two irradiations

Effect of hydroquinone on reduction and rearrangement

Samples in Pyrex cells were irradiated in the wheel (1200 min.). Light output was not monitored, and quenching ratios are relative to blanks irradiated simultaneously. Analysis of the samples on column A gave the results recorded in Table 33 and plotted in Figure 22. Sample composition for the blanks was (± 1%) 21% 4, 35% 2, 44% 3.

Table 33. Effect of hydroquinone on reduction and rearrangement[a]

$[Q] \times 10^2$	% 4	% 2	% 3	reduction ϕ_o/ϕ_q	rearrangement ϕ_o/ϕ_q	total ϕ_o/ϕ_q
0.90	21	36	43	1.00	1.03	1.02
5.20	29	32	39	0.97	1.46	1.32
12.2	39	27	34	1.06	2.56	1.97
25.2	44	24	32	1.31	3.98	2.81
38.0	54	20	26	1.25	5.83	3.33
48.0	61	17	22	1.32	7.16	3.62
58.3	63	17	20	1.29	7.93	3.71

[a] $[K] = 0.30$ M

Effect of hydroquinone dimethyl ether on reduction and rearrangement

Two samples in Pyrex cells were irradiated in the wheel (1242 min) without monitoring light output. Sample 1 was 0.30 M in 4,4-dimethyl-2-cyclohexenone and sample 2 was 0.30 M in 4,4-dimethyl-2-cyclohexenone and 0.31 in hydroquinone dimethyl ether. Analysis of the samples on column A gave the following results, reported as quenching ratios relative to the blank: reduction $\phi_o/\phi_q = 1.06$, rearrangement $\phi_o/\phi_q = 1.02$, total $\phi_o/\phi_q = 1.03$. Product ratios were within ± 1% of that obtained in previous irradiations.

Effect of biphenyl on reduction and rearrangement

Samples in Pyrex cells were irradiated in the wheel (1729 min.). Light output was not monitored and quenching ratios are relative to a blank irradiated simultaneously. Analysis of the samples on column A gave the results recorded in Table 34. Sample composition of the blank was within ± 1% of that obtained previously.

Table 34. Effect of biphenyl on reduction and rearrangement[a]

[biphenyl]	% 4	% 2	% 3	reduction ϕ_o/ϕ_q	rearrangement ϕ_o/ϕ_q	total ϕ_o/ϕ_q
0.05	23	34	43	0.90	0.96	0.94
0.10	22	34	44	0.98	0.96	0.96

[a] [K] = 0.30 M

SUMMARY

The photocycloaddition reaction of isophorone and 1,1-diphenylethylene in *t*-butyl alcohol results in three products: 3,3,4a-trimethyl-9-phenyl-1,2,3,4,4a,9,10,10a-octahydro-1-phenanthrone (74), 2,2,10a-trimethyl-9-phenyl-1,2,3,4,4a,9,10,10a-octahydro-4-phenanthrone (75), and 4,4,6-trimethyl-8,8-diphenylbicyclo[4.2.0]octan-2-one (76). Formation of 74 (76.7%), 75 (21.9%), and 76 (1.4%) accounts for 25% of the reaction. In benzene, irradiation gives only 74 and 75, in a combined yield of 28%.

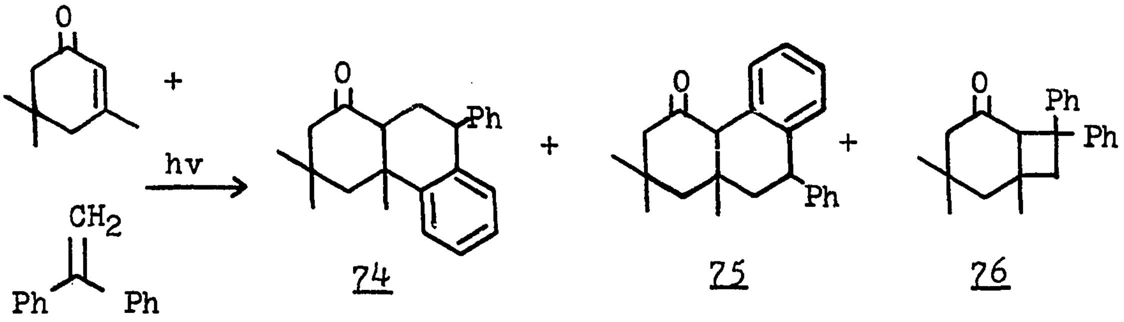

74 75 76

The rearrangement of 4,4-dimethyl-2-cyclohexenone in *t*-butyl alcohol and the accompanying photoreduction in isopropyl alcohol are both very low quantum efficiency reactions. The triplet nature of both reactions is established by efficient sensitization with a variety of triplet sensitizers and by Stern-Volmer type quenching with di-*t*-butyl nitroxide and naphthalene. The low efficiencies of both reactions derive from the rapid deactivation of the reactive

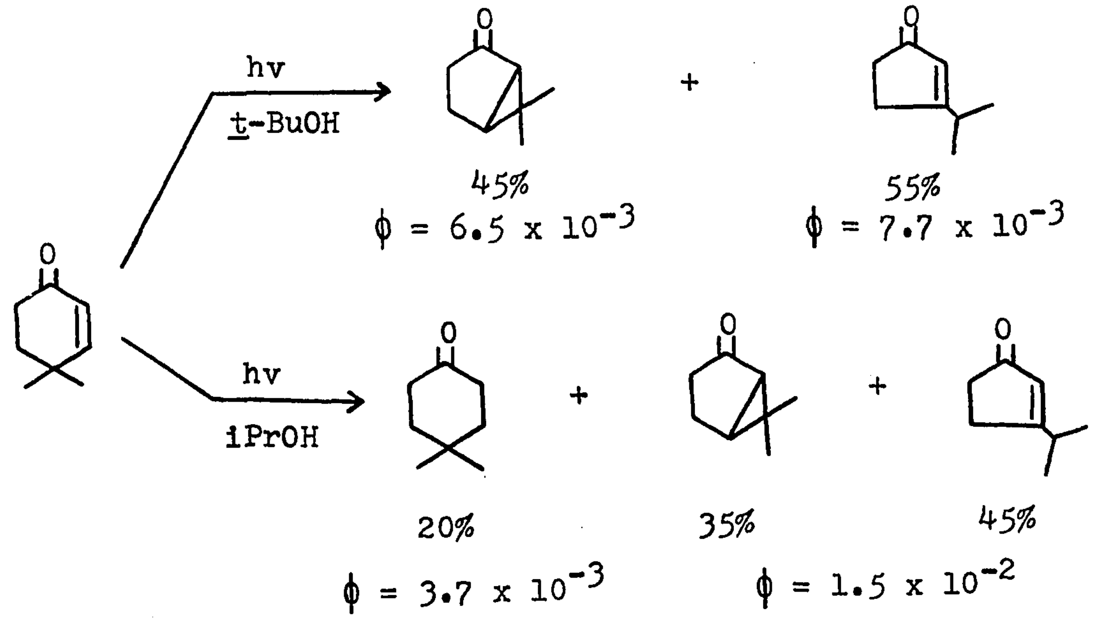

triplet states to ground state which are several orders of magnitude faster than reaction of the triplets to give products. Di-t-butyl nitroxide in concentrations of up to 0.015 M enhances photoreduction by scavenging oxygen or some unknown material which quenches the reaction, but the nitroxide quenches efficiently at higher concentrations. A variety of quenchers differentially quench the photoreduction and photorearrangement products. It is postulated that photoreduction occurs from a $^3(n,\pi^*)$ state and photorearrangement from a $^3(\pi,\pi^*)$ state, with the former state lying somewhat higher in energy.

The efficiency of energy transfer from several sensitizers to 4,4-dimethyl-2-cyclohexenone is concentration dependent. The quantum yield for rearrangement decreases monotonically as the concentration of the sensitizers *m*-methoxyacetophenone, *p*-methoxyacetophenone, 3,4-methylenedioxyacetophenone, and thioxanthone is increased. This effect is believed to be due to sensitizer self-quenching at high concentrations. The generality of this effect is confirmed by observing similar results with aromatic ketone sensitizers in studies of the sensitized *cis*-*trans* isomerization of olefins. The observation of this limitation of energy transfer from sensitizers to substrates is of experimental importance in the design and interpretation of photochemical sensitization experiments.

BIBLIOGRAPHY

1. T. A. Rettig, The Photochemistry of Some 2-Cyclohexenones, Unpublished Ph.D. thesis, Ames, Iowa, Library, Iowa State University of Science and Technology, 1966.

2. T. H. Koch, A Mechanistic Investigation of the Photochemistry of 4,4-Dimethyl-2-cyclohexenone, Unpublished Ph.D. thesis, Ames, Iowa, Library, Iowa State University of Science and Technology, 1968.

3. G. Marsh, D. R. Kearns, and K. Schaffner, Helv. Chim. Acta, 51, 1890 (1968).

4. D. R. Kearns and G. Marsh, J. Chem. Phys., 49, 3316 (1968).

5. H. E. Zimmerman, R. G. Lewis, J. J. McCullough, A. Padwa, S. W. Staley, and M. Semmelhack, J. Amer. Chem. Soc., 88, 1965 (1966).

6. G. Rämme, R. L. Strong, and H. H. Richtol, J. Amer. Chem. Soc., 91, 5711 (1969).

7. G. Marsh, D. R. Kearns, and M. Fisch, J. Amer. Chem. Soc., 92, 2252 (1970).

8. M. H. Fisch and J. H. Richards, J. Amer. Chem. Soc., 90, 1547 (1968).

9. R. L. Cargill, A. C. Miller, D. M. Pond, P. deMayo, M. F. Tchir, K. R. Neuberger, and J. Saltiel, Mol. Photochem., 1, 301 (1969).

10. W. Herz and M. G. Nair, J. Amer. Chem. Soc., 89, 5474 (1969).

11. J. J. McCullough, H. Ohorodnyk, and D. P. Santry, Chem. Commun., 570 (1969).

12. N. C. Baird, Chem. Commun., 199 (1970).

13. E. J. Corey, J. D. Bass, R. LeMahieu, and R. B. Mitra, J. Amer. Chem. Soc., 86, 5570 (1964).

14. T. S. Cantrell, W. S. Haller, and J. C. Williams, J. Org. Chem., 34, 509 (1969).

15. P. J. Nelson, Iowa State University of Science and Technology, Private Communication, 1966.

16. T. H. Koch, Iowa State University of Science and Technology, Private Communication, 1968.

17. O. L. Chapman, P. J. Nelson, and D. Ostrem, Iowa State University of Science and Technology, Private Communication, 1968.

18. F. Klein, Iowa State University of Science and Technology, Private Communication, 1968.

19. O. L. Chapman, T. H. Koch, F. Klein, P. J. Nelson, and E. L. Brown, J. Amer. Chem. Soc., 90, 1657 (1968).

20. O. L. Chapman, T. A. Rettig, A. A. Griswold, A. I. Dutton, P. Fitton, Tetrahedron Lett., 2049 (1963).

21. H. E. Zimmerman, R. G. Lewis, J. J. McCullough, A. Padwa, S. Staley, and M. Semmelhack, J. Amer. Chem. Soc., 88, 159 (1966).

22. O. L. Chapman, J. B. Sieja, and W. J. Welstead, Jr., J. Amer. Chem. Soc., 88, 161 (1966).

23. P. H. Carapellucci, H. H. Richtol, and R. L. Strong, J. Amer. Chem. Soc., 89, 1742 (1967).

24. B. Nann, D. Gravel, R. Schorta, H. Wehrli, K. Schaffner, and O. Jeger, Helv. Chim. Acta, 46, 2473 (1963).

25. D. Bellus, D. R. Kearns, and K. Schaffner, Helv. Chim. Acta, 52, 971 (1969).

26. D. I. Schuster and D. F. Brizzolara, J. Amer. Chem. Soc., 92, 4357 (1970).

27. H. E. Zimmerman and D. I. Schuster, J. Amer. Chem. Soc., 84, 4527 (1962).

28. H. E. Zimmerman and J. S. Swenton, J. Amer. Chem. Soc., 89, 906 (1967).

29. H. E. Zimmerman and J. W. Wilson, J. Amer. Chem. Soc., 86, 4036 (1964).

30. H. E. Zimmerman and K. G. Hancock, Abstracts, American Chemical Society, 153, O-130 (1967).

31. H. E. Zimmerman and K. G. Hancock, J. Amer. Chem. Soc., 90, 3749 (1968).

32. H. E. Zimmerman, R. D. Rieke, and J. R. Scheffer, J. Amer. Chem. Soc., 89, 2033 (1967).

33. D. I. Schuster and V. Y. Abraitys, Chem. Commun., 419 (1969).

34. G. A. Zimmerman, Characterization of the Electronic Excited States of Unsaturated Ketones Through Phosphorescence Analysis, Madison, Wisconsin, Library, University of Wisconsin, 1965.

35. E. Y. Y. Lam, D. Valentine, and G. S. Hammond, J. Amer. Chem. Soc., 89, 3482 (1967).

36. R. Hoffman, International Symposium on Organic Photochemistry, Strasbourg, France, July 20-24, 1964, as cited by H. E. Zimmerman and K. G. Hancock, J. Amer. Chem. Soc., 90, 3749 (1968).

37. K. Ogura and T. Matsuura, Tetrahedron, 26, 445 (1970).

38. T. Matsuura and K. Ogura, J. Amer. Chem. Soc., 89, 3846 (1967).

39. D. I. Schuster and D. H. Sussman, Tetrahedron Lett., 1657 (1970).

40. P. deMayo, J.-P. Pete, and M. Tchir, Can. J. Chem., 46, 2535 (1968).

41. P. deMayo, J.-P. Pete, and M. Tchir, J. Amer. Chem. Soc., 89, 5712 (1967).

42. N. C. Yang, R. Loeschen, and D. Mitchell, J. Amer. Chem. Soc., 89, 5465 (1967).

43. N. C. Yang and R. Loeschen, Tetrahedron Lett., 2571 (1968).

44. R. S. H. Liu and J. R. Edman, J. Amer. Chem. Soc., 90, 213 (1968).

45. R. S. H. Liu and D. M. Gale, J. Amer. Chem. Soc., 90, 1897 (1968).

46. R. S. H. Liu, J. Amer. Chem. Soc., 90, 1899 (1968).

47. D. R. Kearns, R. A. Hollins, A. U. Khan, R. W. Chambers, and P. Radlick, J. Amer. Chem. Soc., 89, 5455 (1967).

48. D. R. Kearns, R. A. Hollins, A. U. Khan, and P. Radlick, J. Amer. Chem. Soc., 89, 5456 (1967).

49. O. L. Chapman, P. J. Nelson, R. W. King, D. J. Trecker, and A. A. Griswold, Rec. Chem. Progr., 28, 167 (1967).

50. J. Michl and J. Kole, J. Amer. Chem. Soc., 92, 4148 (1970).

51. H. E. Zimmerman, R. W. Binkley, J. J. McCullough, and G. A. Zimmerman, J. Amer. Chem. Soc., 89, 6589 (1967).

52. R. B. Woodward and R. Hoffman, Angew. Chem. Intern. Ed. Engl., 8, 781 (1969).

53. W. G. Herkstroeter, A. A. Lamola, and G. S. Hammond, J. Amer. Chem. Soc., 86, 4537 (1964).

54. A. L. Buchachenko, M. S. Khlopyankima, and S. N. Dobryakou, Opt. Spektrosk., 22, 554 (1967).

55. G. Porter and F. Wilkinson, Proc. Roy. Soc., Ser. A, 264, 1 (1961).

56. P. Debye, Trans. Electrochem. Soc., 82, 265 (1942).

57. National Research Council of the United States of America, International Critical Tables of Numerical Data, Physics, Chemistry and Technology, 7, 211 (1930).

58. P. J. Wagner and I. Kochevar, J. Amer. Chem. Soc., 90, 2232 (1968).

59. Y. Izawa, Iowa State University of Science and Technology, Private Communication, 1969.

60. G. S. Hammond and P. A. Leermakers, J. Amer. Chem. Soc., 84, 207 (1962).

61. E. J. Baum, J. K. S. Wan, and J. N. Pitts, Jr., J. Amer. Chem. Soc., 88, 2652 (1966).

62. G. Porter and P. Suppan, Trans. Faraday Soc., 61, 1664 (1965).

63. N. C. Yang and R. L. Dusenbery, Mol. Photochem., 1, 519 (1969).

64. N. C. Yang, D. S. McClure, S. L. Murov, J. J. Houser and R. L. Dusenbery, J. Amer. Chem. Soc., 89, 5466 (1967)

65. P. J. Wagner and A. E. Kamppainen, J. Amer. Chem. Soc., 90, 5898 (1968).

66. J. N. Pitts, Jr., D. R. Burley, J. C. Mani, and A. D. Broadbent, J. Amer. Chem. Soc., 90, 5902 (1968).

67. N. C. Yang and R. L. Dusenbery, J. Amer. Chem. Soc., 90, 5899 (1968).

68. G. Porter and P. Suppan, Pure Appl. Chem., 9, 499 (1965).

69. C. A. Parker, Photoluminescence of Solutions, Amsterdam, Netherlands, Elsevier Publishing Company, 1968.

70. Th. Förster, Angew. Chem. Intern. Ed. Engl., 8, 333 (1969).

71. Th. Förster and K. Kasper, Z. Phys. Chem., N.F., 1, 19 (1954).

72. Th. Förster and K. Kasper, Ber. Bunsenges. Phys. Chem., 59, 976 (1955).

73. B. Stevens and E. Hutton, Nature, 186, 1045 (1960).

74. R. M. Hochstrasser, Annual Review of Physical Chemistry, 17, 466 (1966).

75. G. Castro and R. M. Hochstrasser, J. Chem. Phys., 45, 4352 (1966).

76. E. C. Lim and S. K. Chakrabarti, Mol. Phys., 13, 293 (1967).

77. J. Langelaar, R. P. H. Rettschnick, A. M. F. Lambooy, and G. J. Hoytink, Chem. Phys. Lett., 1, 609 (1969).

78. S. K. Chakrabarti, Mol. Phys., 16, 417 (1969).

79. E. A. Chandross and C. J. Dempster, J. Amer. Chem. Soc., 92, 704 (1970).

80. R. B. Cundall and A. J. R. Voss, Chem. Commun., 116 (1969).

81. C. DeBoer, J. Amer. Chem. Soc., 91, 1855 (1969).

82. P. J. Wagner and D. J. Bucheck, J. Amer. Chem. Soc., 90, 6530 (1968).

83. S. Toki and H. Sakuri, Bull. Chem. Soc. Japan, 40, 2885 (1967).

84. I. H. Hillier, L. Glass, and S. A. Rice, J. Chem. Phys. 45, 3015 (1966).

85. S. I. Choi, J. Jortner, S. A. Rice, and R. Silbey, J. Chem. Phys., 41, 3294 (1964).

86. J. N. Murrell and J. Tanaka, Mol. Phys., 4, 363 (1964).

87. A. K. Chandra and E. C. Lim, J. Chem. Phys., 48, 2589 (1968); 49, 5066 (1968).

88. J. R. Christie and B. K. Selinger, Photochem. Photobiol., 9, 471 (1969).

89. K. Sandros, Acta Chem. Scand., 18, 2355 (1964).

90. R. S. Cooke and G. S. Hammond, J. Amer. Chem. Soc., 90, 2958 (1968).

91. P. J. Wagner, Mol. Photochem., 1, 71 (1969).

92. G. L. Eian, Photochemical Synthesis of 2,3-Dihydroindoles from N-Aryl Enamines, Unpublished Ph.D. thesis, Ames, Iowa, Library, Iowa State University of Science and Technology, 1969.

93. G. S. Hammond, J. Saltiel, A. A. Lamola, N. J. Turro, J. S. Bradshaw, D. O. Cowan, R. C. Counsell, V. Vogt, and C. Dalton, J. Amer. Chem. Soc., 86, 3197 (1964).

94. A. A. Lamola and G. S. Hammond, J. Chem. Phys., 43, 2129 (1965).

95. L. M. Stephenson, D. G. Whitten, G. F. Vesley, and G. S. Hammond, J. Amer. Chem. Soc., 88, 3665 (1966).

96. K. Sandros, Acta Chem. Scand., 23, 2815 (1969).

97. C. A. Parker and T. A. Joyce, Chem. Commun., 234 (1966).

98. T. Medinger and F. Wilkinson, Trans. Faraday Soc., 61, 620 (1965).

99. R. Hurley and A. C. Testa, J. Amer. Chem. Soc., 92, 211 (1970).

100. G. O. Schenck and R. Steinmetz, Bull. Soc. Chim. Belges., 71, 781 (1962).

101. J. Saltiel, K. R. Neuberger, M. Wrighton, J. Amer. Chem. Soc., 91, 3658 (1969).

102. H. L. Hyndman, B. M. Monroe, and G. S. Hammond, J. Amer. Chem. Soc., 91, 2852 (1969).

103. J. Saltiel, L. Metts, and M. Wrighton, J. Amer. Chem. Soc., 91, 5684 (1969).

104. P. deMayo, A. A. Nicholson, and M. F. Tchir, Can. J. Chem., 48, 225 (1970).

105. D. S. Weiss, Iowa State University of Science and Technology, Private Communication, 1970.

106. L. A. Singer, G. A. Davis, and V. P. Muralidharan, J. Amer. Chem. Soc., 91, 897 (1969).

107. H. Berg and K. Kramarczyk, Ber. Bunsen. Phys. Chem., 68, 296 (1964).

108. F. G. Moses, R. S. H. Liu, and B. M. Monroe, Mol. Photochem., 1, 245 (1969).

109. C. G. Hatchard and C. A. Parker, Proc. Roy. Soc., Ser. A, 235, 518 (1956).

110. A. K. Hoffman, A. M. Feldman, E. Gelblum, and W. G. Hodgson, J. Amer. Chem. Soc., 86, 639 (1964).

111. W. Tadros, A. B. Sakla, and M. S. Ishak, J. Chem. Soc., 2631 (1958).

112. J. Bredt, Justus Liebig's Ann. Chem., 299, 131 (1898).

113. G. N. Vyas and N. M. Shah, Org. Syn. Coll. Vol., 4, 836 (1963).

114. H. Hlasiwetz and J. Haberman, Justus Liebig's Ann. Chem., 177, 334 (1875).

115. D. Vorländer and M. Schroedter, Chem. Ber., 36, 1490 (1903).

116. R. E. Kelley and W. T. Simpson, J. Amer. Chem. Soc., 87, 4230 (1965).

117. D. F. Evans, J. Chem. Soc., 1735 (1960).

ACKNOWLEDGEMENTS

The author wishes to thank his parents for their encouragement and patience shown throughout the course of his education. Their support made the completion of this work possible.

The author is grateful to Professor Floyd Krause and other faculty members during his years as an undergraduate student for their advice and encouragement to continue his education.

The author expresses his gratitude and appreciation to Professor O. L. Chapman for the advice, guidance, and encouragement given him during the course of this work and his graduate study. Special thanks are also due to Drs. W. C. Wildman and T. H. Kinstle for helpful advice and letters of recommendation and to members of the Chapman group for their friendship, counsel and experimental assistance.

Financial support from the National Aeronautics and Space Administration and the Petroleum Research Fund is gratefully acknowledged.

A publication originating in part from the research presented here is:

O. L. Chapman and G. L. Wampfler, J. Amer. Chem. Soc., 91, 5390 (1969).